PALAEOCLIMATIC CONDITIONS DURING THE LATE QUATERNARY - A MULTIPROXY APPROACH FROM THE SEDIMENTS OF ARABIAN SEA

Thesis submitted to Goa University
Department of Marine Sciences
for the degree of Ph. D

By

Kamlesh Verma

Under the Guidance of

Dr. M. Sudhakar

National Centre for Antarctic and Ocean Research, Headland Sada

Vasco-da-Gama, Goa

February, 2008

PALAEOCLIMATIC CONDITION DURING LATE QUATERNARY- A MULTIPROXY APPROACH FROM THE SEDIMENTS OF ARABIAN SEA

SYNOPSIS

THESIS

SUBMITTED TO THE GOA UNIVERSITY

FOR THE DEGREE OF DOCTOR OF PHILOSOPHY

IN

MARINE SCIENCE

By

Kamlesh Verma

Under the Guidance of

Dr. M. Sudhakar

(Scientist "G")

National Centre for Antarctic and Ocean Research (NCAOR)

Ministry of Earth Sciences (MoES)

Headland Sada, Vasco-da-Gama

Goa 403 804- India

February- 2008

STATEMENT

As required under the university ordinance O. 19.8(vi), I state that the present thesis entitled "Palaeoclimatic conditions during the Late Quaternary- A multiproxy approach from the sediments of Arabian Sea" is my original contribution and the same has not been submitted on any previous occasion.

The literature related to the problems analyzed and investigated has been cited. Due acknowledgements have been made wherever facilities and suggestions have been availed of.

Place: Goa, India

Date: 14.08.08

Kamlesh Verma

CERTIFICATE

This is to certify that the thesis entitled "Palaeoclimatic conditions during the Late Quaternary- A multiproxy approach from the sediments of Arabian Sea" submitted by Mr. Kamlesh Verma for the award of the Degree of Doctor of Philosophy in Marine Science is based on his original studies carried out by him under our supervision. The thesis or any part thereof has not been previously submitted for any other degree or diploma in any University or institutions.

Place: Goa, India

Date: 14th August, 2008.

Dr. M. Sudhakar
(Research Guide)
Scientist "G"
National Centre for
Antarctic and Ocean Research
Headland Sada
Vasco-da-Gama
Goa-403 804
India.

All the corrections suggested by the Examiners have been incorporated.

(Prof. A.C. Narayana)

CONTENTS

Acknowledgements

A journey is easier when you travel together. Interdependence is certainly more valuable than independence. This thesis is the result of my work whereby I have been accompanied and supported by many people. It is a pleasant aspect that I have now the opportunity to express my gratitude for all of them.

The first person I would like to thank is my supervisor Dr. M. Sudhakar, NCAOR, Goa. I have been associated with him since 2002. During these years I have known Dr. M. Sudhakar as a sympathetic, principle-centered person and was always available for me whenever I needed his advises. His overly enthusiasm and integral view on research and his mission for providing 'only high-quality work and not less', has made a deep impression on me. I owe him lots of gratitude for his help, suggestions and encouragement that helped me in research as well as writing of this thesis.

I am very obliged to the Shri Rasik Ravindra, Director, NCAOR, for his constant support and encouragement that finally resulted in the form of Ph. D thesis. Furthermore, I express deep sense of gratitude to the founder Director of NCAOR, Dr. P. C. Pandey, for his motivation, encouragement and support that led me to the completion of this thesis.

Thanks are due to Dr. S. Rajan, NCAOR, Goa, with whom I initially joined in NCAOR and carried my research activities. During his guidance I discussed various realms of Science and developed a research aptitude which finally reached in the form of a Ph. D thesis. Thanks are also due to Dr. N. Khare for his valuable discussions pertaining to my Ph. D thesis.

I am indebted to Dr. R. Ramesh, PRL, Ahmedabad, for providing the laboratory facilities. He has provided **Sta**ble **I**sotope **Laboratory** (**STAIL**) for the analysis of oxygen and carbon isotopes ratios in foraminiferal shells and the Radiocarbon laboratory for Carbon-14 dating of sediment samples. From the bottom of my heart I would like to say thanks to Dr. M. G. Yadava, PRL, Ahmedabad and Dr. Manish Tiwari, NCAOR, Goa for providing stable isotope data and Carbon-14 ages. I am also thankful to Dr. K. Pandarinath, previously Mangalore University, Mangalore and Mr. Girish Prabhu, NIO, Goa for providing help during clay mineral analysis of sediment samples. Heartfelt thanks to Mr. Gangadharan and K. K. Bhatt, GSI, Marine Wing, Mangalore for providing support and necessary guidance in doing the sedimentological analysis at GSI, Mangalore during my Ph. D tenure.

I would also like to thank Dr. Rajiv Nigam and members of Faculty Research Committee including Dr. B. Nagendernath, NIO, Goa and Dr. G. N. Nayak, Goa University, Goa, who kept an eye on the progress of my work in the form of yearly assessment, six monthly progress reports, synopsis etc and providing valuable comments for the improvement of my Ph. D thesis.

I am deeply indebted to Dr. R. Ramesh, PRL, Ahmedabad, Dr. M.V.S. Guptha and Dr. P. Divakar Naidu, NIO, Goa for providing valuable comments on the earlier versions of this thesis.

I express my sincere thanks to Dr. A. J. Luis, Dr. S. M. Singh and all the senior colleagues of NCAOR for a healthy understanding with me and providing necessary guidance and suggestions.

I record my sincere appreciation for Shri T. G. V. P. Bhaskar Rao, Dr. A. Shivaji, Shri. Shripati, Shri. Venkateshwarlu, Shri. N. S. Dalvi, Heads of the Logistics, Library, Finance, Procurement and Administration, the respective departments of NCAOR for having a smooth coordination with me throughout my tenure. I specially thank S. K. Pandey (Admn.), Sarita (Admn.), Kaushambi Prasad (Finance), Prabhu (Finance) for rendering their help throughout my tenure.

A very special thanks to Dr. Ravi Mishra, Suhas Shetye and Lalit K. Ahirwar for helping me in bringing my thesis to its final form. I am also thankful to Nilay Sharma, Amita Khanolker, Praveen Vohat, Pradeep Sharma, Nagoji Rao, Manoj Outurkar, Late Kaushik Saha, Mihir Dash, Upender Singh, K. N. Babu, Sushant Naik, Witty D'Souza, Kamna V. Sahai, Meena Pandey, Celsa Almeida, Ashlesha Saxena, Lasitha, Anayat Quarshi, Pawan Govil, Abhijeet Majumdar and all other colleagues of NCAOR who gave me the feeling of being at home. I also thank M. Rajeevan, John Kurian, Rajakumar and Shramik Patil for having shared the same room with me and being a good roommate during the tenure of my Ph. D.

The chain of my gratitude would be definitely incomplete if I would forget to thank my Late Nanaji who formed part of my vision and taught me the good things that really matter in life. The happy memory of my father still provides a persistent inspiration for my journey in this life. I am grateful for my Naniji, Mother, Uncle, Mausiji and Mamaji for rendering me the parental care that finally made me able to be part of an esteemed institute like NCAOR and to perceive for a highest degree. I am also thankful to my two brothers for giving a sense and the value of brotherhood. I am glad to be one of them.

The work has been carried out under the financial support from the Ministry of Earth Sciences, New Delhi.

In my opinion, doing a Ph. D broadens the horizon of understanding, develops the power of thinking, inculcates patience and persistence therefore I feel perceiving for this was definitely one of the best decisions of my life.

(Kamlesh Verma)

List of Tables

List of Figures

PREFACE

It has been elucidated by various palaeoclimatologists that the earth is punctuated by many episodes of climate change in the past which sometimes led to the mass extinction. Little ice age (LIA) and medieval warm period (MWP) offer examples of climate change in Holocene. A climate change has also been noticed during the Holocene to imply the migration of population, rise and fall of a civilization and appearance/ disappearance of river systems. The discovery of MWP and LIA resulted in discrediting the belief that the Holocene climate was relatively stable. Thus the palaeoclimatic research assumes importance specially to investigate the late Quaternary sedimentary records. The most important aspect of palaeoclimatic research is to understand the possible cause, mechanism and the effect of climatic change and also to decipher any linkage to the other parts of the globe. Pertaining to this, scientists observed that monsoon to be an important component of climate system in south and east Asian region wherein the land, sea and atmosphere regimes interact with each other. It is therefore considered that the present day monsoon has a fundamental relation with the climate in this region. Considering the large area of the tropics subjected to the influence of monsoonal climate with a huge amount of energy and moisture are involved; hence it is possible that the monsoons play an important role in modulating global climate. Any plausible theory of global climate shall necessarily address monsoon and its teleconnection with the other major climatic controls. Further, as the socio-economic importance of India and the other nations of Asia largely depend on the monsoonal rainfall, it is imperative to study

monsoon and its past variability to understand the climate change during the late Quaternary.

Indian summer monsoon is characterized by the seasonal reversal of winds driven by the thermal contrast between the Eurasian landmass and the surrounding Indian Ocean. During June-September, moisture laden winds blow from southwest towards the Indian subcontinent and results in heavy precipitation over land. Whereas during winter monsoon (November-February), winds blow from northeast and picks up the moisture from Bay of Bengal resulting in cyclonic storms and rainfall limited to the southeastern part of India. Of the two, the summer monsoon is important in terms of rainfall intensity. Monsoon not only causes precipitation, but also manifests physical/ chemical/ hydrographical and biological changes in the oceanic water column, which in turn is archived in the sediments. The present study is an attempt to investigate the sediments collected at three different locations from the eastern Arabian Sea to understand the past climatic changes and the influence of summer monsoon over the study area.

The present investigation involves a multiproxy approach on the slope sediments of the eastern Arabian Sea which makes it different from earlier studies where most of the work is confined to the shelf sediments. Important events are identified through the isotopic study of three different species of planktonic foraminifera, where the habitat ranges from surface to subsurface depths unlike some earlier reports where inferences were mostly drawn based on mono species. The events identified are also supported by the other proxy records such as clay minerals and organic carbon.

The study titled "**Palaeoclimatic conditions during the Late Quaternary- A multiproxy approach from the sediments of Arabian Sea**" is discussed in six different chapters.

A general introduction about the palaeoclimatic studies, its importance and its relation with the monsoon is described in Chapter 1. The socio-economic importance, the ultimate effect of monsoon on the sediments as well as on the overlying water column is outlined in the chapter. A comprehensive literature review consisting of different aspects of palaeoclimatic research particularly from the Arabian Sea is presented, and the objectives of the present study are drawn. The physiography, geology and oceanography of the study area are also discussed in this chapter.

The different methodologies adopted in order to study and understand the palaeoclimatic conditions are discussed in Chapter 2. The type of sediments chosen and sampling techniques to collect them is detailed in this chapter. The cores collected have been analyzed for basic sedimentological parameters along with the clay mineralogical analysis following standard techniques. Organic carbon and calcium carbonate concentrations were determined by the conventional methods. Stable isotopes of oxygen and carbon in foraminiferal carbonate were measured by standard methods/ techniques. The chronology of a given core is established either by conventional ^{14}C dating using bulk sediments or by oxygen isotope stratigraphy. All the above data are systematically presented in this chapter.

Chapter 3 describes the effect of sea level changes or the enhanced fluvial discharge on the sediment dispersal pattern through various processes like slumping, turbidity currents etc. An event representing reworking and resuspension during low sea level stand is deciphered from the core off the southwestern margin of India. Similarly, a mismatch between C-14 dates and oxygen isotope stratigraphy from the core off the northwestern margin of India is attributed to the mixing of older (relict) carbonates. Such processes are reported from the northwestern margin of India where these relict carbonates are transported laterally during low sea level stands as well as during the Holocene. This chapter deals with the various aspects of sediment mixing and its relation to the sea level changes and fluvial discharge in the study area.

Variation in Sedimentological parameters and clay mineralogy, and its implication on the palaeoclimatic studies are described in Chapter 4. Based on texture, clay minerals and organic carbon content in sediments, the probable link to the overhead surface productivity and/or its preservation are also discussed in this chapter. Clay minerals from the sediment of topographic high reveal that the dispersal of illite is regulated by the summer monsoon circulation. Based on these variations, it is inferred that the summer monsoon circulation was stronger during interglacial whereas it was weaker during glacials. Clay mineral record of core SK-172, suggests continental aridity during Last Glacial Maximum (LGM) and Younger Dryas whereas melt water pulse 1 a and b (MWP 1a and 1b) shows continental humidity. The interrelation between the various analyzed proxies as established from the core off the southwestern margin of India shows that the

intensity of SW monsoon increased during the Holocene. This chapter ends with a brief summary of inferences.

A general introduction to the oxygen & carbon isotopic variation ($\delta^{18}O$ and $\delta^{13}C$) in foraminiferal calcite and its relation with the sea surface hydrography and productivity during glacial-interglacial time scales is presented in Chapter 5. The present day sea surface hydrography of the eastern Arabian Sea is also described in this chapter. The analyzed $\delta^{18}O$ of surface dwelling foraminifera from the study region is shown and discussed in terms of past variations in the SW monsoonal intensity. The results from the core off the southwestern margin show an early intensification of the SW monsoon well before the onset of deglaciation. Deglaciation events in the form of MWP 1a and MWP 1b are also recorded. The effect of Younger Dryas is recognized here as a surface phenomenon. All such events are described in this chapter. The deciphered Holocene precipitation pattern from the cores of eastern Arabian Sea is compared with the upwelling records of western Arabian Sea. The comparison reveals that both the basins of Arabian Sea form a different monsoon domain.

The trend in palaeoproductivity through the glacial-interglacial transition is inferred from the foraminiferal $\delta^{13}C$ and the results are correlated with the other proxy records like organic carbon. The correlation reveals that during the Holocene, organic carbon content mirrors the overhead surface productivity.

In Chapter 6, the eastern Arabian Sea precipitation record documented in this study is found to be coupled with the record of Greenland ice core (GISP-2) suggesting a strong

teleconnection between these two isolated regimes. The overall conclusions pertaining to the palaeoclimatic conditions of the late Quaternary are drawn in this chapter. At the end of this chapter some key issues are suggested which need to be addressed in future for the better understanding of palaeomonsoon.

All the references used in the present study are cited in alphabetical order at the end of Chapter six. A copy of scientific articles published in standard referred journals is placed at the end of the thesis.

CHAPTER 1

INTRODUCTION

1.1 Palaeoclimatic study and its importance

In the past decade palaeoclimatologists have come to recognize abrupt climate change as a pervasive characteristic of Earth's climate record. Little ice age (LIA) and medieval warm period (MWP) are examples of climate change that occurred a few centuries ago and have been accompanied by the migration of populations, rise and fall of civilizations and appearance/disappearance of major rivers. However, palaeoclimatic records that extend beyond the age of human presence have documented many episodes of large climate oscillations (e.g. Dansgaard et al., 1993). The Holocene period, which has long been considered a stable climate interval, is now known to have undergone large climatic changes (e.g. Bond et al., 1997). Among the best documented examples are the Dansgaard/Oeschger events and the Heinrich Events that were first recognized in Greenland ice cores and high latitude marine sediment records from the North Atlantic region. These events have also been documented in environments throughout the northern hemisphere, attesting to the widespread influence. Owing to the fact that the Quaternary period has witnessed wide climatic variability, researchers have evolved very innovative techniques to probe into the past climate. Studies carried out hitherto have revealed that the main mechanism that trigger climatic changes are both the external and internal forcings. External forcing is essentially radiative forcing which affects the Earth's energy budget according to the astronomical theory proposed by the Milankovitch (1941). It involves the mean position of earth with respect to sun and invokes periodicities of the order of several thousands of years, e.g. eccentricity 400 kyr (and 100 kyr), obliquity 41 kyr and precession 21 kyr cycles. Internal forcing includes volcanic activity, oceanic circulation (thermohaline circulation), atmospheric trace gases etc.

Human interference with the pristine environment began in the 20thcentury largely by burning of fossil fuel which has substantially increased the concentration of carbon-dioxide (CO_2) in addition to the other green house gases such as Methane (CH_4). Coastal and marine habitats are being drastically altered. Rapid urbanization has transformed much of the land surface impacting an imbalance in biodiversity, nutrient cycling and soil structure. The impact of human activities have documented a warming of the lower atmosphere during the late 20thcentury that has heightened concerns, thus anthropogenic influences have begun to change the global climate.

With the quest of understanding different possible parameters affecting the climate, palaeoclimatic research has gained interest especially for the late Quaternary period. The most important aspect of palaeoclimatic research is to understand the nature, importance and causes of variations in climate, as well as how widespread, systematic and abrupt they were and how changes in one region influence or cause change to occur in other regions. Also necessary is the decoupling of natural variability from anthropogenic effects on climate.

It has been observed by the palaeoclimatologists that the Dansgaard/ Oeschger events and the Heinrich Events correlate well with the lower latitudes records and are characterized by significant hydrological change. Conceptual models that attempt to explain the origin of these abrupt climatic events have typically called upon ice sheet dynamics as a primary factor in the rapid onset of each event (e.g. Broecker et al., 1990; Bond et al., 2001; Alley and Mac Ayeal, 1994). But, evidences from high resolution marine and terrestrial records suggest that even in the absence of large ice sheets significant and equally rapid climate oscillations continued to occur at high

latitudes through the present interglacial (Bond et al., 1993; 1997; 2001). Thus to explain the recurring nature of large environmental changes under both glacial and interglacial boundary conditions it requires a persistent internal amplification mechanism that can translate a relatively small forcing into a large and wide spread response. A leading mechanism, which is often called upon to explain the abrupt changes in climate through the glacial and the present interglacial are switches in the modes of thermohaline circulation, driven by salinity changes in the North Atlantic (Broecker, 1997). Inspite of the evidences that deep water convection in the North Atlantic has undergone repeated variations, it is not clear whether the changes were the cause or were a consequence of the climate change. Hoerling et al. (2001) have suggested the recent salinity changes in the North Atlantic are consistent with the warming of tropical Pacific, which affects atmospheric latent heating and can produce down stream effects on the North Atlantic thermohaline circulation. Proxy data from the tropical Atlantic has documented longer-term changes in salinity (Nyberg et al., 2002) that may be indicative of persistent and recurring hydrologic variability at low latitudes that influenced salinities in the North Atlantic and thereby affected the ocean's convective capacity.

Similarly, many tropical records exhibit deglacial climate changes before those in the Northern high-latitudes and synchronous with those in Antarctic suggesting the potential for the tropics to play a large role in either driving or amplifying deglacial climate changes (Lea, 2003; Visser et al., 2003). Broecker (2003) suggested that precursor events to the D-O cycles could be useful in determining whether they are driven by thermohaline circulation reorganizations or tropical ocean-atmosphere dynamics. Recent work suggests that there were changes in the tropics immediately

before D-O events (Sachs and Lehman, 1999; Hendy and Kennett, 2003; Burns et al., 2003). All these evidences indicate that high latitude changes, even during the Holocene influenced the changes taking place at low latitudes. Cane (1998) suggested that the tropical ocean-atmosphere system has the capacity to affect the climate globally and a sustained change in the behavior of tropical Ocean/atmosphere system on longer time scales represents a likely candidate for causing the abrupt climate changes documented in the proxy records. Therefore, a comparison of high-resolution tropical climate records with the records of Northern high latitudes especially the North Atlantic deep-water circulation and Antarctica during the Holocene and Pleistocene become imperative to assess how susceptible the high latitude is to the variations at low latitudes. Climate models can also be used to explore the linkages between the tropics and extra-tropics. All such studies focus on the mechanisms by which both the tropics and extra-tropics are linked together through ocean and/or atmosphere, and how these may play a role in abrupt climatic change. Chronological relationship of the abrupt events at different locations may also shed light on the mechanisms involved in millennial and centennial climate change.

At present there are only a few, highly resolved climate records from low latitudes that can be compared to those from the high latitudes (e.g. Schulz et al., 1998). Until more complete and highly resolved palaeoclimate and palaeoceanographic records are available from the tropics it will be difficult to assess whether the low latitudes have been a primary "center of action" or whether the primary center of action does in fact laid at higher latitudes. So it is essential for the palaeoclimatologists to put more focus on tropics and to generate data base using marine or terrestrial archives.

1.2 Monsoon and Climate

Monsoon is considered as one of the most important air-sea interaction process of tropical climate system. Overall, half of the tropics (one quarter of the surface area of the entire globe) are under monsoonal climate. The monsoons play a significant role in modulating global climate through various forcing mechanisms. It has been documented by various palaeoclimatologists that during the last glacial episode, changes in the Indian and East African monsoons (Schulz et al., 1998; Altabet et al., 2002; Burns et al., 2003), East Asian monsoon (Wang et al., 2001; Dannenmann et al., 2003) appears to have occurred and varied synchronously with the North Atlantic climate in millennial-scales. Whereas during the Holocene, Indian monsoon (Sirocko et al., 1996; Gupta et al., 2003; Neff et al., 2001; Fleitmann et al., 2003) exhibited millennial and centennial-scale variability that have coincided with climate changes in the North Atlantic (Bond et al., 1997; 2001). From all these evidences it is certain that there exists a certain kind of teleconnection between monsoon (Tropics) and North Atlantic climate variability (Extra tropics). However, there remains considerable uncertainty in the relative timing and phasing of change between the tropical and extra tropical climate variability.

Based on proxy reconstruction it has been established that the monsoonal system is very sensitive to the external forcing mechanism and can affect other parts of the globe through the redistribution of latent heat and sensible heat (Hoerling et al., 2001). Small changes in the amount of solar radiation received at low latitudes in association with the Earth's precessional cycle have affected the strength of the monsoons over India and China (Prell et al., 1986; Clemens et al., 1991; Overpeck et al., 1996; Burns

et al., 2001; Wang et al., 1999). Besides, there are evidences of the variability in the strength of the monsoon systems at millennial to decadal time scales that correlate with the solar variability (Agnihotri et al., 2002; Burns et al., 2002; Wang et al., 1999). Therefore, considering the sensitivity and the capacity of the monsoon to affect global climate directly or indirectly, mechanism of monsoon has to be included in any plausible theory of global climate and their teleconnection to other meteorological phenomena. Apart from this, monsoon has socio-economical importance for the developing nations like India and other nations of Asia whose economy is mainly based on agriculture. Therefore it is imperative to study monsoon and its past variability as it has a direct impact on the life of common people as well as an indirect effect via climate change.

Monsoon is a term from early Arabs called the "Mausin," or "the season of winds." The term "monsoon" is now generally applied to the tropical and sub-tropical seasonal reversals in both the atmospheric circulation and associated precipitation. These changes arise from the seasonal shift of inter tropical convergence zone (ITCZ, as shown in Fig 1) due to the reversals in temperature gradients between continental regions and the adjacent oceans with the progression of the season. The dominant monsoon systems in the world are the Asian-Australian, African and the American monsoon. All monsoons share three basic physical mechanisms: differential heating between the land and oceans; Coriolis forces due to the rotation of the Earth; and the role of water which releases energy in the form of latent heat. The combined effect of these three mechanisms produces the monsoon's characteristic reversals of winds and precipitation.

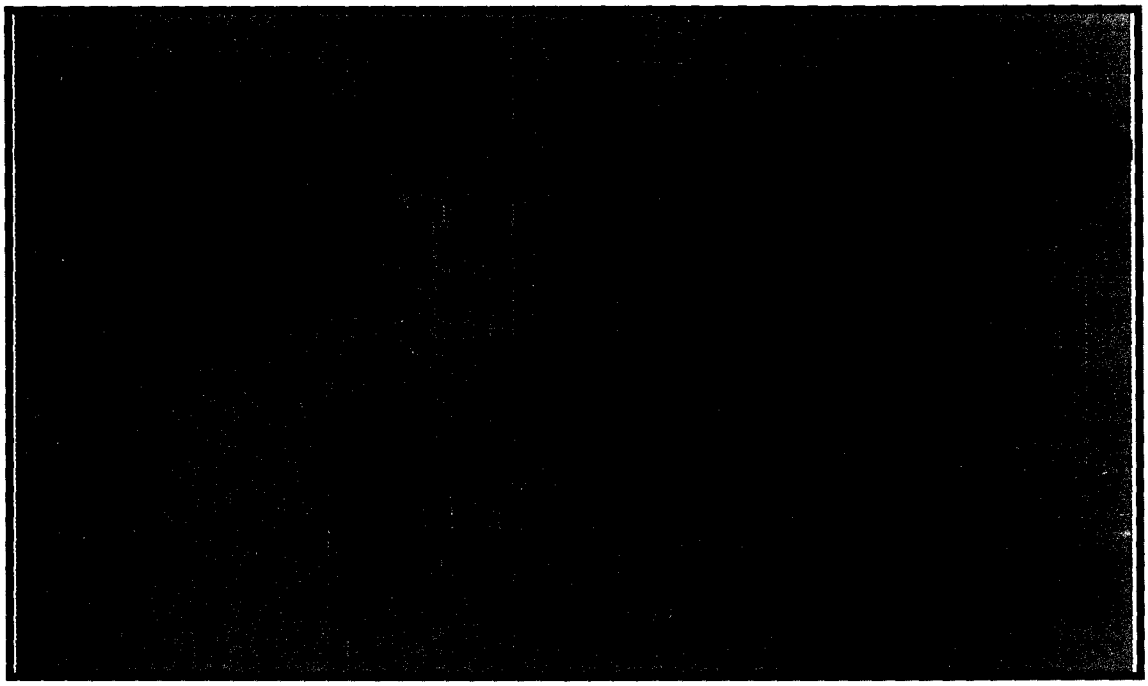

Fig 1.1. Map showing the seasonal migration of ITCZ. Solid and dashed line indicates the position of ITCZ in July and January respectively (http://www.newmediastudio.org/DataDiscovery/Hurr_ED_Center/Stages_of_Hurricane_Dev/ITCZ/ITCZ.html)

Winter monsoon (December to March): During winter ITCZ shifts to the south of equator as shown in Fig 1. And over the Tibetan plateau high pressure develops due to extensive snow cover, resulting in winter monsoon (NE monsoon) during which relatively weaker wind blows from continent to Ocean (shown in Fig 1.2). These winds are generally cold and dry, but it acquires moisture from Bay of Bengal and precipitation occurs in the southwestern part of Indian subcontinent.

Summer monsoon (June to September): During summer as the land heats faster than the ocean, a low pressure develops over the Tibetan plateau. This allows low-level moist air to blow inland from southwest hence called as SW monsoon (shown in Fig 1.2). The resulting convection and release of latent heat due to precipitation fuels the monsoon circulation. For e.g. the Asian monsoon to occur a regional meridional temperature gradient extending from the tropical Indian Ocean north to mid-latitude Asia develops prior to the monsoon through a considerable depth of the troposphere (Webster et al., 1998). To a first order, stronger meridional temperature gradient leads to the stronger monsoon. Summer monsoon typically covers large areas of Indian subcontinent and during this period it receives most of its total annual precipitation. Therefore monsoonal phenomenon (summer and winter) manifests physical/ chemical/ hydrographical and biological response in the sediments as well as in the overlying water column

1.2.1 Biogeochemical response

During the summer monsoon, longshore component of wind stress causes an upwelling in the eastern Arabian Sea particularly along the SW margin of India (Shetye

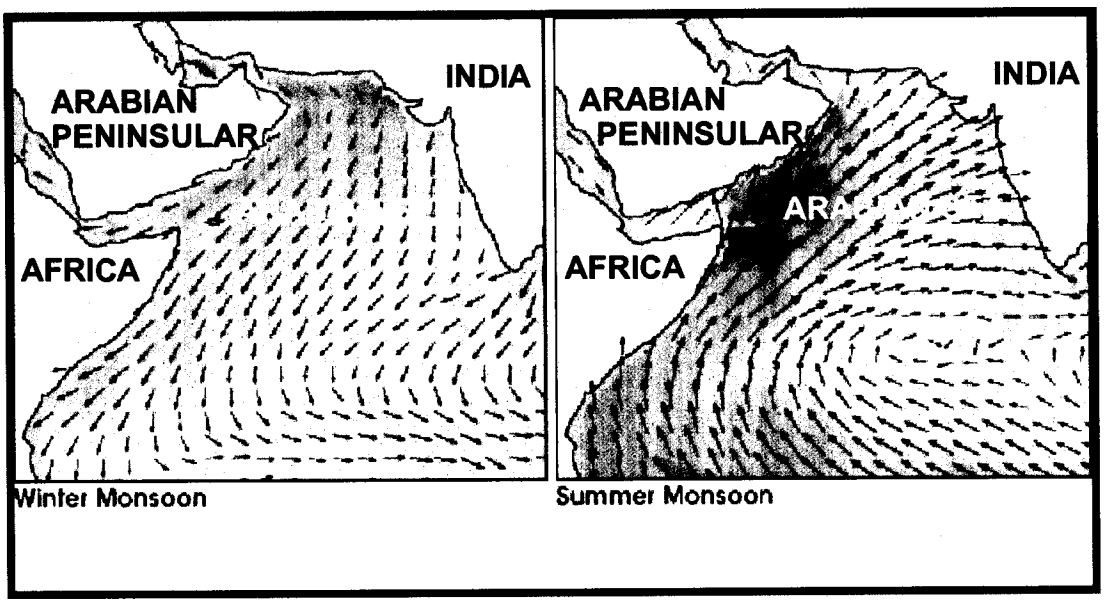

Fig 1.2. Map showing seasonal reversals of winds (arrows) during monsoon season. The length of arrow indicates wind strength.

1984 and Shetye et al., 1990), the intensity of which progressively decreases from South to North and ceases to be noticeable around north of 15^0 North (Shetye et al., 1994). The inferred spatial variability in upwelling along the western continental margin of India is found to be well correlated with the water column productivity (Bhattathiri et al., 1996). Studies of Nair et al. (1989) reported mixed layer deepening owing to enhanced southwest monsoonal wind to be the important phenomenon in increasing particle flux to the ocean bottom. Moreover it has been observed that during the winter monsoon, surface productivity increases in the northern Arabian Sea due to cold, dry northeast monsoonal winds leading to convective mixing and subsequent injection of nutrients from deeper parts into the mixed layer (Madhupratap et al., 1996). Satellite data also reveal an increase in productivity all along the eastern Arabian Sea during the summer monsoon and in the northeastern Arabian Sea during the winter monsoon (Agnihotri, 2001). Monsoon induced upwelling/ mixed layer deepening/ convective overturning brings cold, nutrient rich water to the euphotic zone, resulting in an enhanced biological productivity, the traces of which are ultimately transferred to the ocean floor in the form of organic carbon, nitrogen, calcium carbonate (foraminifers and cocolithophores), opaline silica (SiO_2) (diatoms and radiolarians). Researchers have used data on organic carbon and nitrogen (e.g. Bhushan et al., 2001; Agnihotri et al., 2003), calcium carbonate (e.g. Thamban et al., 2001; Sirocko et al., 1993), species-specific foraminiferal content (e.g. Naidu et al., 1992; Cayre and Bard, 1999) and opaline silica (e.g. Pattan et al., 2003) as proxy to reconstruct the palaeomonsoonal conditions.

The most unique feature of Arabian Sea is the depletion of dissolved oxygen in the intermediate waters column i.e. within a water depth of 150 to 1250 m in the

Arabian Sea (Wyrtki et al., 1971; Naqvi, 1987) called as oxygen minimum zone (OMZ). This is attributed to the combination of intense biological productivity in the overlying waters and a moderate ventilation of thermocline. The strength of OMZ is found to regulate the geochemical behaviour of underlying sediments by changing the oxidation state and solubility of certain redox sensitive elements like Mn, Cr and V. Mn gets enriched in the sediments in an oxic environment and in a reducing environment it changes its oxidation state and hence gets soluble in the porewater, thereby reducing its concentration in the solid phase (Yadav, 1996). In contrast to this Cr, V and U get depleted in an oxic environment, whereas it shows enrichment in a reducing environment (Dean et al., 1997). Therefore, these redox sensitive elements are used to decipher the past variability in OMZ strength and its relation to the palaeoproductivity history of eastern Arabian Sea (Schulte et al., 1999; Von Rad et al., 1999a and 1999b; Luckge et al., 2001).

Apart from the biotic component, monsoonal precipitation in the form of surface runoff through various rivers, channels and streams brings large amount of detrital materials and contribute to the sediment pool as terrigeneous component. The amount of detrital material deposited would indicate the strength of the monsoon (Agnihotri et al., 2003). Detrital materials in the form of clay mineral are widely used to study the past variability in climate. The composition of clay minerals largely depends on the climatic condition of the catchment area, geology and topography of the region (Chamely, 1989). Several studies from the Arabian Sea have suggested that the temporal variation of clay minerals can be utilized as palaeoclimatic indicators (e.g. Pandarinath et al., 1999, Thamban et al., 2002).

During monsoonal precipitation various streams, rivers, channels etc brings fine-grained silisiciclastic material mainly clay minerals into the coastal Arabian Sea. Clay minerals are mostly the weathering product of rocks and soils on land. The type of clay minerals produced mainly reflects the climatic conditions of the catchment area, geology and topography of the region. Therefore it can be used as a potential tool for palaeoclimatic reconstruction (Sirocco and Lange, 1991; Pant, 1993; Dilli and Pant, 1994; Pandarinath et al., 1999; Thamban et al., 2002), provenance (Chamely, 1989; Kessarkar et al., 2003) and palaeogeography (Doyle et al., 1968). It has been observed that the clay minerals from the eastern Arabian Sea mainly reflects the climatic condition of the hinterland (Thamban et al., 2002; Anilkumar et al., 2005) and can be used for palaeoclimatic reconstruction. Among the clay minerals assemblage, researchers are using kaolinite, gibbsite, and K/I ratio as a humidity proxy (Chamely, 1989) whereas chlorite is unstable in humid climate and hence represents arid condition. Illite along with chlorite represents the dominance of physical weathering and Himalayan source (Rao and Rao, 1995). However, it is reported that Al rich illite forms in humid conditions (Petschick et al., 1996) and easily be identified by knowing illite chemistry (Gingele, 1996). Based on these proxies and from southeastern Arabian Sea core, Thamban et al. (2002) reported decrease in the intensity of summer monsoon during late glaciation with distinct events of intensification during 28 and 22 kyr. Early strengthening of SW monsoon during 15.7 -14.8 kyr is also observed in their study along with the aridity during late Holocene. They suggested that the Holocene precipitation maxima lagged behind the precessional forcing. From the study of Kessarkar et al. (2003) it is concluded that the provenance and transport pathways for clay minerals are similar throughout the glacial interglacial transition. The clay minerals carried by NE monsoonal currents into the southeastern Arabian Sea which

was earlier thought by Chauhan and Gujar (1996) seems to be insignificant (Kessarkar et al., 2003). In this study clay minerals are also used as one of the proxy for deciphering the palaeoclimatic condition and the records are correlated with the other available proxies.

1.2.2 Hydrographic response

During summer monsoon precipitation, Indian subcontinent receives a large amount of precipitation in addition to the wind induced upwelling/ mixed layer deepening and consequent surface biological productivity. However, average annual precipitation along the western and northwestern Arabian Sea is low but the coastal regions of the eastern Arabian Sea receives heavy precipitation due to the orographic effect of the *Sahyadri* (Western Ghats). The annual precipitation over these region ranges from 1000-4000 mm yr^{-1} i.e. there exists a steep gradient of precipitation (~350mm/ degree) from regions off Saurashtra (~22^0N) to off Cochin (~10^0N) (Sarkar et al., 2000b). The heavy precipitation on the *Sahyadri* quickly drains in to the coastal Arabian Sea through various rivers, streams. This freshwater influx tends to float on the surface affecting the upwelling dynamics (Thamban et al., 2001; Agnihotri et al., 2003) and creating a low salinity plume along the coastal Arabian Sea (Tiwari et al., 2005a and the reference therein). Thus a direct relationship is expected between the surface run off and the intensity of summer monsoon rather than a wind speed or wind induced changes like upwelling.

Studies have established that the calcite shells of surface dwelling planktonic foraminifera bears the signals of monsoon/climate linked sea surface hydrography in

the form of isotopic ratio i.e. $^{18}O/^{16}O$ or $\delta^{18}O$ (e.g. Rostek et al., 1993,1997; Sarkar et al., 2000b; Naidu and Niitsuma, 2003; Tiwari et al., 2005b). In this regard different species of planktonic foraminifera i.e. *Globigerinoides ruber* (*Gs. ruber*), *Globigerinoides sacculifer* (*Gs. sacculifer*) and *Globorotalia menardii* (*Gr. menardii*) are used to measure isotopic ratios as a proxy to reconstruct the palaeosalinity/palaeomonsoonal changes in the eastern Arabian Sea (Sarkar et al., 2000b; Tiwari et al., 2005a; Chodankar et al., 2005).

1.3 Literature review

Voluminous data exists on the investigation of palaeoclimates from the Arabian Sea and in particular from the western Arabian Sea (e.g. Naidu, 2004; Naidu and Niitsuma, 2003; Sirocko et al., 2000; Gupta et al., 2003) and northwestern Arabian Sea (e.g. Reichert et al., 1997; 2002; Von Rad, 1999a, b). These studies concentrate mainly on the variability of upwelling strength and its associated biological productivity induced by summer monsoon. They utilize isotopic composition of foraminiferal calcite ($\delta^{18}O$, $\delta^{13}C$) and/ or sedimentological analysis and elemental geochemistry of sediments as proxies to understand and reconstruct the upwelling intensity in the Arabian Sea. These studies have shown that the upwelling and its associated biological productivity reflect the intensity of SW monsoon. Besides it also inferred that the productivity is greater during Holocene than the last glacial times. It is also reported that in the western Arabian Sea, the role of winter monsoon is insignificant in the productivity history. Productivity pattern from the northeastern Arabian Sea when compared with the western Arabian Sea shows opposite relationship between the summer and winter monsoon strength (Reichert et al., 2002). Studies from the western

and northwestern Arabian Sea shows organic carbon, a conventional proxy for biogenic productivity (Ganeshram et al., 1999; Rixen et al., 2000) closely mimics the surface productivity in accordance with the strength of summer monsoon unlike eastern Arabian Sea where its distribution is affected by sedimentation rate (Agnihotri et al., 2003) and bottom water anoxia (Sarkar et al., 1993).

Organic carbon data from the recent sediments of the Eastern Arabian Sea invokes an argument that the organic carbon does not mimic the surface productivity (Paropkari et al., 1987, 1992, 1993). They found that the concentration of organic carbon in sediments principally depends on the intensity of preservation due to strong oxygen minimum condition (OMZ) which impinges on the continental slope of western continental margin of India (Paropkari et al., 1987, 1992, 1993; Calvert et al., 1995). However, several other factors including sedimentation rate, texture, absorption capacity of clay minerals etc are also responsible for organic carbon preservation. In contrast to the preservation characteristics of OMZ, several authors have reported that sediments hydrogen indices (HI) value, an indicator of strength of the OMZ is similar accumulating both inside and outside OMZ (Cowis et al., 1996). They suggested that HI is not a function of bottom water oxygen concentration but rather depends on the texture of sediments. They found that coarse sediments containing organic carbon, has less HI than finer sediments (Cowis et al., 1996). Later by using coulometric technique for organic carbon determination Prakash Babu et al. (1999) found that the organic carbon distribution is very well correlated with the water column productivity (Qasim, 1977). His observation is also supported by Ba concentration, another proxy for productivity (Prakash Babu et al., 2002).

Various researches involving the utilization of C_{org} as a proxy to decipher palaeoproductivity during the late Quaternary have found that organic carbon deposition does not reflect the surface water productivity (Sarkar et al., 1993; Bhushan et al., 2001). Sarkar et al. (1993) observed an enrichment of C_{org} with concomitant increase in U concentration during LGM, which was attributed to the reduced flow of North Atlantic Deep Water (NADW) due to which anoxic conditions developed in that area leading to a better preservation of C_{org}. Later, Agnihotri et al. (2003) utilized Sr and Ba (corrected for detrital contribution i.e. Sr/Al, Ba/Al) as a proxy for surface water productivity after following Reichert et al. (1997) and Sirocko et al. (1996), respectively. Their study showed that during LGM, surface water productivity showed a decreasing trend in spite of C_{org} enrichment (also observed by Sarkar et al., 1993). They concluded that C_{org} enrichment as also observed by Sarkar et al. (1993) was due to the erosion and redeposition of shelf sediments which was exposed during LGM. Studies by Thamban et al. (2002) have reported depletion in C_{org} during early Holocene, a period of maximum summer monsoon activity in Indian subcontinent (Overpeck et al., 1996). It was attributed to the stratification of ocean surface by fresh water influx leading to the suppression of upwelling. Later Agnihotri et al. (2003) by using geochemical proxies has corroborated their observation. Yet another ambiguity could arise from C_{org} deposition in sediments is its source other than marine environment. Pattan et al. (2003) reported higher concentration of C_{org} in southeastern Arabian Sea during stadials of isotope stage 5 (5.2 and 5.4) due to the contribution from terrestrial C_{org} which is brought to the core site owing to enhanced fluvial activity. All these observations suggest that the C_{org} distribution is influenced by various complex oceanographic, geological processes rather than surface productivity alone.

Similarly, calcium carbonate ($CaCO_3$) is also being used widely as a proxy for biogenic productivity (Nair et al, 1989) and used by various researchers from the Arabian Sea (e.g. Sirocko et al., 1993; Naidu and Malmgren, 1999). In eastern Arabian Sea, a lot of literature is available on the usage of $CaCO_3$ as a productivity proxy (for e.g. Sarkar et al., 1993; Agnihotri et al., 2003; Pattan et al., 2003). They suggested that reduced productivity during glacials than interglacial period. However, Thamban et al. (2001) reported increase in productivity during deglacial period and attributed this to the convective mixing owing to the strong NE monsoonal winds. Mostly $CaCO_3$ comprises foraminifers and nanofossils (Naidu et al., 1992) therefore these can be utilized as a proxy for the strength of monsoon. Among the foraminifers, researchers are using coarse fraction (fully composed of planktic foraminifera, without dissolution and dilution) (Naidu, 1991) and specific species like *Globigerina bulloides* to decipher the past variation in the intensity of upwelling and hence productivity (Naidu et al., 1992). Sediment trap studies from the northeastern Arabian Sea have revealed strong relation between monsoon and seasonal flux of cocolithophore (Andruleit et al., 2000). Therefore cocoliths also serve as a potential proxy for palaeoproductivity. Prabhu et al. (2005) utilized a specific species of cocoliths i.e. *Florisphaera profunda* and suggested that the productivity has increased during glacials contrary to the reported decrease during glacials (Agnihotri et al., 2003; Pattan et al., 2003). In addition to the productivity driven carbonate reported from the northeastern Arabian Sea, there are documentary evidences of re-deposition from relict carbonate facies due to slope failure, slumping or turbidites particularly during low sea level stand (Setty, 1972; Hussain and Guptha, 1985; Rao et al., 1988; Rao, 1989; Rao and Wagle, 1997; Guptha et al., 2002; and Anil et al., 2005). Besides, there is a source for carbonate material from continental deposits (Merh, 1995 and Bhushan et al., 2001).

Recent advances in mass spectrometry propelled the study of palaeoclimatology/ palaeoceanography. Various researchers are utilizing this technology to determine the isotopic composition of foraminiferal calcite ($\delta^{18}O$, $\delta^{13}C$) which is governed by a complex process of temperature, salinity and pCO_2 of the ambient water in which they grow. It is very well established that the monsoon (summer or winter) mainly controls the hydrography and productivity of the Arabian Sea. Therefore, isotopic composition of planktic foraminifera provides an opportunity to monitor these variations. In the eastern Arabian Sea researchers have utilized $\delta^{18}O$ of foraminiferal calcite to record past variation in E-P budget (Cayre and Bard, 1999; Sarkar et al., 2000b; Thamban et al., 2001; Tiwari et al., 2005a, 2006a; Chodankar et al., 2005; Banakar et al., 2005) and SST variation (Rostek et al., 1993, 1997). Using $\delta^{18}O$ of surface dwelling foraminifera, Duplessy (1982) has reported that the intensity of SW monsoon was much weaker and the NE monsoon was stronger during last glacial maximum. This has resulted in the reduction in salinity gradient between the Arabian Sea and the Bay of Bengal owing to the decrease in SW monsoonal precipitation and continental runoff. Vanishing of this salinity gradient could have facilitated fresh water of Bay of Bengal origin to enter in the Arabian Sea thereby decreasing the value of $\delta^{18}O$ of surface dwelling foraminifera as observed by Duplessy (1982). Sarkar et al. (1990) corroborated this by using $\delta^{18}O$ of five different species of planktic foraminifera (surface to subsurface dwelling) in two ^{14}C dated (bulk carbonates) cores. However most recently Tiwari et al. (2005b) with better age control opined that the signal of stronger NE monsoon as seen in Sarkar et al. (1990) is actually during early deglacial period i.e. ~19-17 kyr rather than during LGM. They attributed this discrepancy to the dating technique adopted by Sarkar et al. (1990) (Tiwari et al., 2005b and references therein). Rostek et al. (1993; 1997) using alkenone and $\delta^{18}O$ estimated SST for the southeastern Arabian Sea spanning 170 kyr and

suggested that during LGM SST was minimum (25.5 ^{0}C) as compared to that of present day (28 ^{0}C) which is in contrast to the CLIMAP project members who suggested that the Holocene-LGM SST amplitude is insignificant. Early deglacial warming and early intensification of SW monsoon is also noticed in the record of eastern Arabian Sea (Thamban et al., 2001).

Sarkar et al. (2000b) reconstructed E-P budget of Holocene for the entire western margin of India by using $\delta^{18}O$ variation of *Gs. sacculifer* and *Gr. menardii*. Their study suggests that the excess of evaporation over precipitation has decreased from 10–2 kyr and attributed this to the increase in the intensity of SW monsoon. They further observed that the forcing mechanism for Indian and Chinese monsoon on millennial/ centennial scale is similar to that of high latitude forcing mechanisms. The Holocene record of Tiwari et al. (2005a) shows a direct control of the solar variability on Indian summer monsoon.

Some work has been done on $\delta^{13}C$ of the planktic foraminifera (for e.g. Kroopnick et al., 1985; Wefer and Berger, 1991; Beaufort et al., 1997) in contrast to the $\delta^{18}O$ where voluminous literature is available. Similar to $\delta^{18}O$, $\delta^{13}C$ variation in foraminifera has a global component like changes in $\delta^{13}C$ of ΣCO_2 in relation to the deep water formation, circulation and wind induced productivity. Thus, subtracting the total signal from global component a local effect can be evaluated. But unlike $\delta^{18}O$ it is strongly influenced by the vital effects (Wefer and Berger, 1991) and therefore a cautious evaluation is suggested in this regard. However, studies on the interpretation of $\delta^{13}C$ of foraminifera in terms of palaeoproductivity estimation have been done from the Arabian Sea particularly from the western and northwestern Arabian Sea (Kroon

and Ganssen, 1989; Niitsuma, 1991; Curry et al., 1992; Steens et al., 1992; Peeters, 2000). Using a core from the Oman margin Naidu and Niitsuma (2003) recorded a positive excursion in $\delta^{13}C$ of *Uvigerina excellens* (benthic species) during 9-8 kyr coinciding with the SW monsoon intensification phase. They attributed this to the outflow of Red sea intermediate water and its relation with the strength of SW monsoon. From the same core, Naidu (2004) has established $\Delta\ \delta^{13}C_{sacculifer\text{-}dutertrei}$ (the difference between $\delta^{13}C$ of *Gs. sacculifer* and *Neogloboquadrina dutertrei*) as a proxy for determining the strength of upwelling. The study compared the results with *Gs. bulloides* flux an established proxy for upwelling and found a positive correlation between them.

In the eastern Arabian Sea, data on $\delta^{13}C$ is sparse. Sarkar et al. (2000a) recorded palaeoproductivity data using $\delta^{13}C$ of five different species of foraminifera ranging from surface to sub surface depth habitat. During LGM, Sarkar et al. (2000a) observed enrichment in $\delta^{13}C$ of surface dwelling foraminifera whereas depletion during 9 ^{14}C kyr with no significant change in deeper dwelling *Pulleniatina obliquiloculata* throughout the last 25 ^{14}C kyr. They attributed this to the reduced upwelling/productivity during LGM and enhanced upwelling during 9 ^{14}C kyr.

In this study an attempt is made to decipher the past variability of productivity by utilizing $\delta^{13}C$ of foraminifera from different depth habitat. A comparison is also made between the record of $\delta^{13}C$ and C_{org} & $CaCO_3$.

1.4 Study Area

Eastern Arabian Sea receives abundant monsoonal precipitation (an important element of monsoon) in contrast to most of the earlier works that have been done in western/northern Arabian Sea that receives meager precipitation. Further, it has been seen from the literature review that most of the studies were concentrated on the eastern Arabian Sea shelf sediments whereas the present thesis involves slope sediments which makes it different from the earlier studies. Moreover slope sediments fall in the oxygen minimum zone therefore a core chosen would be minimally bioturbated and C_{org} can also be used as a proxy for palaeoproductivity. In view of the aforesaid, sediments from the eastern Arabian Sea are found to be best suited locale for monitoring past variation in the monsoon/ climate and three sediment core has been collected from the Eastern Arabian Sea as shown in Fig 1.3, based on the following reasons:-.

- The monsoon induced upwelling results in the production of organic carbon (C_{org}), opaline silica in the form of radiolarians and diatoms as well as calcareous microorganisms such as foraminifera and coccolithophores.

- The formation of oxygen minimum zone (OMZ) due to intense primary productivity.

- Monsoon fed rivers like Narmada and Tapti, flow along with the detrital input derived from continent, into the Arabian Sea. So, the variation of these inputs can serve as a monsoonal proxy.

- Clay minerals are reported to be derived from hinterland thus it can serve as a proxy for monitoring the past variation in climate.

- The core location falls in a low salinity plume developed due to surface runoff from the *Sahyadri* (Western Ghats) during summer monsoon. Therefore, from the $\delta^{18}O$ variation of surface dwelling foraminifera change in salinity and hence summer monsoonal strength can be deciphered.

1.5 Objectives of the present study

In order to understand and reconstruct the palaeoceanographic settings of the eastern Arabian Sea during the late Quaternary period, a multiproxy approach has been adopted in the present study Major objectives of the present study are:-

- To examine and document various proxies to be used as potential tools of palaeoclimate in the study area.

- To understand the processes responsible for the organic carbon enrichment.

- To obtain a high-resolution record of palaeoclimate/ palaeoceanography during the late Quaternary period.

- To correlate the palaeomonsoonal record with the records of Greenland ice core (GISP2) and to establish a teleconnection if any, between the eastern Arabian Sea and Northern high latitudes.

- To decipher the variability of the Indian monsoon strength by using different proxies.

1.6 Physiography, Geology and Oceanography of the study area

Physiography

The *Sahyadri* (Western Ghats) runs almost parallel to the western Indian coast or the eastern Arabian Sea with elevation up to ~1000 m. It is an important feature because it has a significant influence on the intensity and distribution of rainfall (mainly orographic precipitation) over the SW coast of India. The influence of *Sahyadri* is seen from the sharp north south gradient in summer monsoon rainfall along the west coast i.e. south of Goa receives 4000 mm of rain (e.g. Mangalore) whereas in north, Saurashtra and Kutch receive only 300 mm of rain (Sarkar et al., 2000b). The *Sahyadri* acts as a mountain barrier for the moist air that flow from the adjacent Arabian Sea during summer monsoon. When the moisture laden air ascends, the windward slope receives abundant rainfall. Most of the monsoon rainfall over the *Sahyadri* quickly drains into the Arabian Sea through a number of large and small rivers that originate and drain through the steep slopes of the *Sahyadri*. The rivers and streams approximately cover an area of about 54000 km^2 and annually discharge about 95.58 km^3 into the eastern Arabian Sea (Rao, 1979).

Geology

The hinterland geology of eastern Arabian Sea (see Fig 1.3) comprises predominantly of Deccan trap basalts of tertiary age in the north (north of Goa) and to the south the principal rock types are gneiss, schists and charnokites of Precambrian age (Krishnan, 1968). To the further south upto the southern tip of India Mesozoic

windows in the form of Varkala and Quilon beds appear at isolated locations. It is mainly ferrugenised sandstone with clay intercalations. At certain places the rocks along the coast are extensively lateritised and all along the coast of SW India recent alluvium occurs.

Oceanography

In response to the seasonal reversals of the annual winds, the tropical Indian Ocean undergoes large circulation transitions, seasonally reversing circulation (Shetye et al., 1990), strong annual and semi-annual variations in SST and upwelling/downwelling activities in the upper ocean.

Monsoonal current: The most peculiar feature of the equatorial and the northern Indian Ocean is the seasonally reversal of monsoon currents (shown in Fig 1.4 a and b) that flow across the breadth of the north Indian Ocean. The branches of the summer monsoon current (SMC) and winter monsoon current (WMC) that flow around the Lakshadweep high and low (LH & LL) in the south-eastern Arabian Sea (Bruce et al., 1994) link the circulations in the Arabian Sea and Bay of Bengal.

S-W monsoon: During summer monsoon Indian monsoon current (Tchernia, 1980), Somali current- its associated gyre in the western Arabian Sea (Schott et al., 1990) and the north equatorial current which brings water from south into the northern Arabian Sea. During summer monsoon, western Indian coastal current (WICC) flows equatowards. The summer monsoon current (SMC) flows eastwards from the south of Sri Lanka into the Bay of Bengal. It is fed by Somali current (SC) and its associated

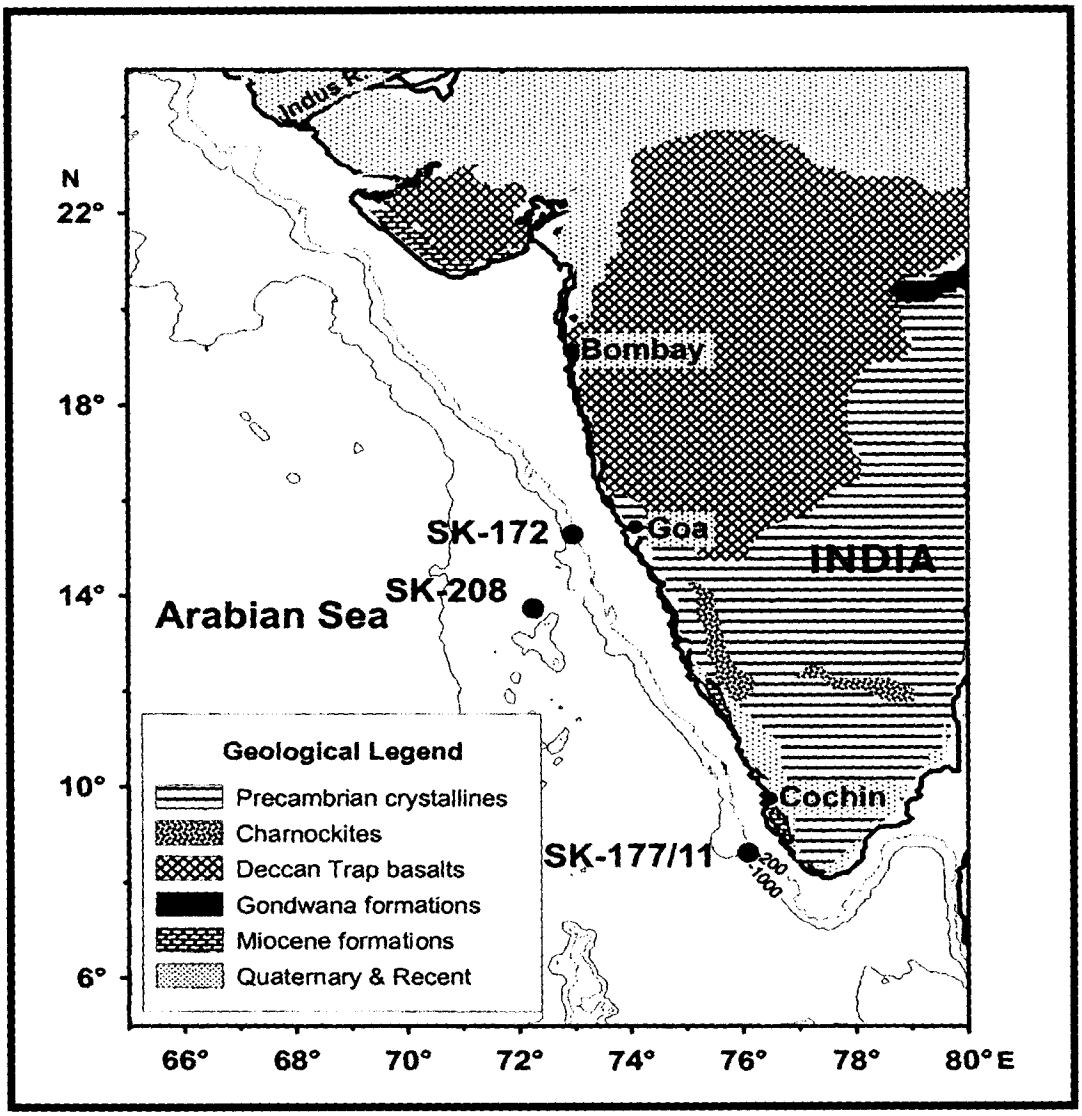

Fig 1.3. Map of India showing geology and bathymetry (modified after Thamban et al., 2002). The locations of cores used in this study are also shown.

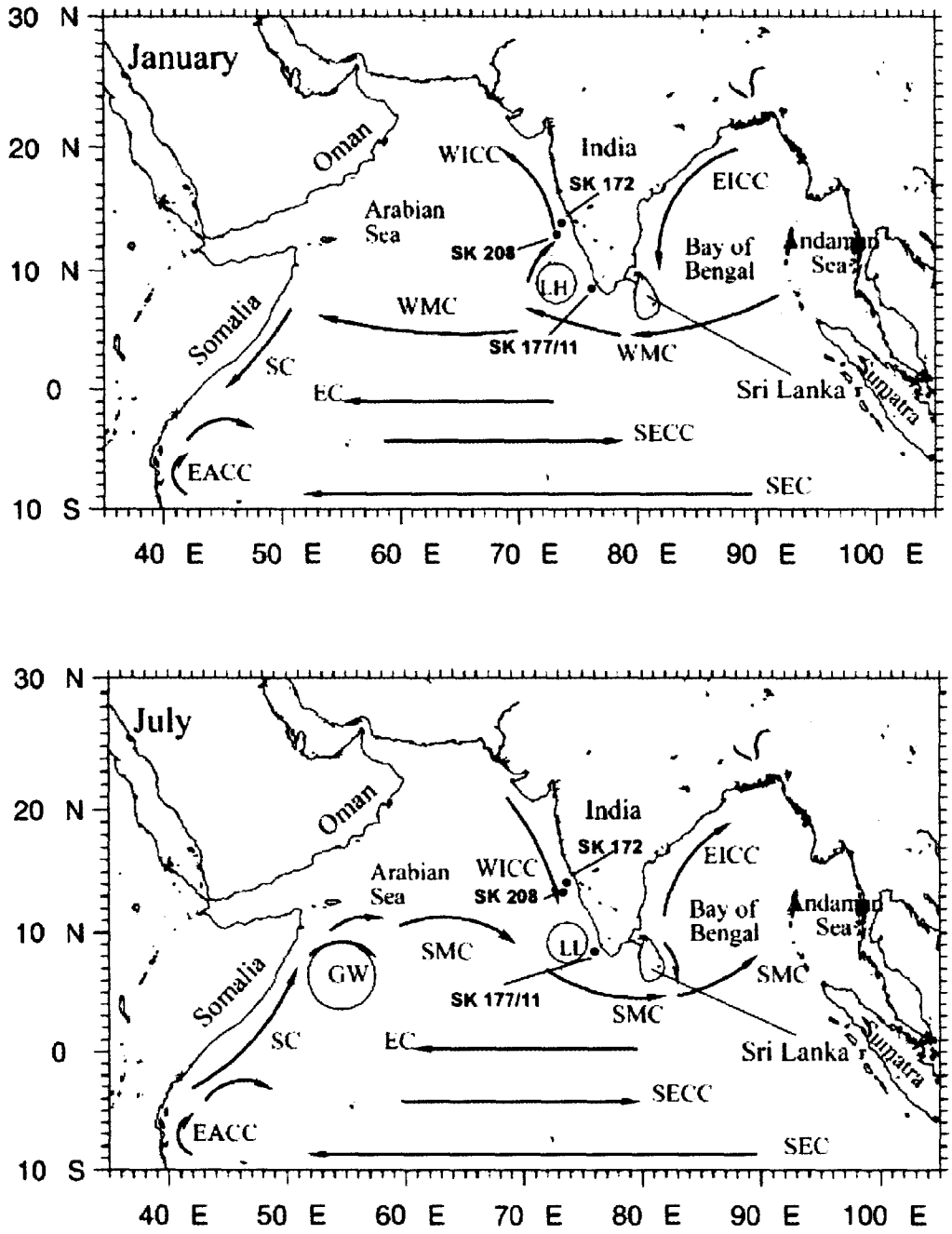

Fig 1.4. Schematic representation of the circulation, in the Indian Ocean during January (winter monsoon) and July (summer monsoon). The abbreviations are as follows: SC, Somali Current; EC, Equatorial Current; SMC, Summer Monsoon Current; WMC, Winter Monsoon Current; EICC, East India Coastal Current; WICC, West India Coastal Curent; SECC, South Equatorial Counter Current, EACC, East African Coastal Current; SEC, South Equatorial Current; LH, Lakshadweep high; LL, Lakshadweep low; and GW, Great Whirl (modified after Shankar et al., 2002).

gyre (Schott et al., 1990) at the southwest and by WICC at Lakshadweep low (Shankar et al., 2002).

N-E monsoon: During winter monsoon current (WMC), (EICC) and (WICC) reverses its circulation pattern. The East Indian coastal current (EICC) feds the westward flowing WMC at the east of Sri Lanka which in turn supplies water to the northward flowing West Indian coastal current after circulating around the Lakshadweep high (Bruce et al., 1994). Somali current receives inflow from East across the Arabian Sea in several branches and then flows southward to meet Northward flowing East African Coastal current (EACC) at 2-4^{0}S. The two flows then supply Eastward flowing South Equatorial Counter Current (SECC).

CHAPTER 2

MATERIALS AN D MATHODS

2.1 Samples and sampling technique

In order to understand the influence of summer monsoon over the study area in the past, three sediment cores collected at three different locations i.e. northern, central and southern parts of the eastern Arabian Sea wee chosen for this study. The location of three gravity cores collected on board ORV Sagar Kanya is shown in Table 2.1 and in Fig 1.2 (Chapter 1). Three gravity cores (SK172, SK-177/11 and SK-208) were collected from the continental slope off Goa, continental slope off Quilon and from the continental rise off Karwar, respectively. Except for SK-208 which lies on the edge of the oxygen minimum zone, the other two core locations fall in the present day oxygen minimum zone (Wyrtki, 1971).

These gravity cores were sub-sampled onboard at different discrete intervals using clean tools. During sampling process, litholog of each core including colour (using standard colour charts), odour was also recorded. After sub-sampling, the sediment samples were packed in a labeled polythene bag and stored in a cold, dry place. Later, in laboratory, the samples were dried in a hot air oven at ~60° C, powdered using Agate mortar and stored in clean vials for further analysis.

Northern part of eastern Arabian Sea core (SK-172): The core SK-172 was sectioned at every 2 cm interval.

Central part of eastern Arabian Sea core (SK-208): Top 100 cm of core SK 208 was sectioned at 1 cm interval and below 100 cm sampling was done at 2 cm interval.

Table 2.1 Details of core and core locations.

S. No	Cruise no.	Water Depth (m)	Total recovery (m)	Location
1	SK-172	740	5.93	LAT: $15^0$10'4" N LONG: $72^0$45'58" E
2	SK-177/11	776	3.63	LAT: $8^0$12'263" N LONG:$76^0$28'58" E
3	SK-208	383	4.84	LAT: $13^0$49.54' N LONG:$73^0$05.20' E

Southeastern Arabian Sea core (SK-177/11): Top 50 cm of core SK 208 was sectioned at 1 cm interval and between 50- 350 cm, it was sampled at 2 cm interval. Below 350 cm sampling was done at every 4 cm interval.

2.2 Sedimentological studies

Sedimentological study is important because it reflects the different sedimentary processes like transportation and depositional history of the medium, post digenetic changes etc. It is also very helpful in identifying the source rock characteristic. These sedimentological processes are in turn dependent upon the prevailing climate and hence serve as an important tool as far as palaeoclimatology is concerned. Similarly, the type of clay minerals produced indicate the rock type and climatic condition of the adjacent hinterland (Singer, 1984; Chamely, 1989). However, its dispersal is governed by a complex oceanographic process which has to be identified before drawing any conclusion. Considering the importance of such a study all the three cores were subjected to the basic sedimentological analysis including texture (with carbonate and carbonate free basis) and clay mineralogy.

2.2.1 Textural analysis

Textural analysis (Pipette Method)

In this method about 8-10 gm of dried sample was treated with 10 ml of 30% H_2O_2 in order to remove organic matter. Carbonate was removed (for carbonate free basis) from samples by adding 1 N HCl. The remaining aliquot was wet sieved by using

63 micron sieve and collected in a 1000 ml measuring cylinder. Later, the content of measuring cylinder was subjected to pipette analysis following the standard procedure (Folk, 1968).

2.2.2 Clay mineralogy

A) Sample preparation: 40-45 samples were selected from SK-172 and SK-208 for X-ray diffractometry. In this method, about 8-10 gm of sediment was wet sieved for each sample, using 63-micron sieve and collected in a 1000 ml measuring cylinder. The clay minerals (>2-μm fraction) were separated following standard technique of Folk, 1968. Following the procedures of Rao and Rao (1995), the separated clay aliquots were treated with 10 ml of H_2O_2 (30%) and 10 ml of acetic acid (10%) in order to remove organic carbon and calcium carbonate, respectively. The excess H_2O_2 and acetic acid was removed by repeated washing with distilled water. Finally the concentrated clay suspension is prepared by decanting distilled water and from this concentrated clay suspension 1 ml is uniformly pipetted on a glass slide (to avoid size sorting). The glass slide is then allowed to dry in air. X-ray diffraction studies were then carried out on these untreated slides from $3\text{-}22^0$ 2θ at a speed of 1.2^0 2θ/min on a Phillips X-ray diffractometer (1840 model) and Brukers X-ray diffractometer using nickel filtered Cu Kα radiation.

B) Glycolation: Glycolation technique is extensively used for the identification of expanding clays like smectite. The untreated slides of clay minerals were glycolated for 1 hour following Carroll (1970). These glycolated slides were then scanned from $3\text{-}22^0$ on X-Ray diffractometer with a scan speed of 0.02^0 2θ/sec. For separating Kaolinite

and Chlorite, slow scanning method was adopted (Biscaye, 1965) and the slides were scanned from 24-26^0 with the scan speed of 0.01^0 2θ/ sec.

C) Clay mineral identification and quantification: The identification of clay minerals involves the identification of peak (in X-Ray diffractogram), conversion of 2θ to d-spacing and later matching the calculated d-spacing with the standard data sets. The complete set of minerals and their corresponding d-spacing is published in the form of tables by the American Society of Testing Materials and is known as A.S.T.M powder data file. The quantification of clay minerals was done following Biscaye, (1965). Relative percentages of smectite, illite, kaolinite and chlorite were estimated by weighting the integrated peak areas of basal reflection in glycolated X-ray diffractogram. It follows the following equation.

1 Smectite (17Å) + 4 Illite (10 Å) + 2 Chlorite and Kaolinite doublet (7 Å)..... (1)

The weighted 7 Å peak common to both kaolinite and chlorite is divided in proportion to the fraction of each mineral in the total area under the 3.54/ 3.56 Å.

Normalize the clay mineral distribution by summing the weighted peak-area weights, and dividing the weighted peak-area weight of each mineral times 100 by the sum of the weighted peak-area weights. Illite crytallinity was measured by both half-height width and ratio of height to width of 10 Å illite peak and its chemistry was assessed by the ratio of 5^{0}Å/10 Å peaks (Gingele, 1996).

2.3 Geochemical Analysis

Geochemical analysis involves the quantification of organic matter and calcium carbonate in the sediment sample.

2.3.1 Estimation of Organic carbon

Determination of organic carbon (C_{org}): In order to remove salts, the samples were washed repeatedly with distilled water and dried in an oven. The dried samples were then grounded to pass 100 mesh and stored in a pre-cleaned vials. Later a few milligrams of samples were taken for titration following the method suggested by El Wakeel and Riley, 1957.

Organic carbon (mg) = 1.15 X 0.6 X Volume of Ferrous ammonium sulphate...(2)

2.3.2 Estimation of Calcium carbonate

Determination of Calcium carbonate: Calcium carbonate was determined by measuring Ca^{++} by EDTA titration method following Barnes (1959). In this method, a few milligrams of powdered sample was digested in a 2% acetic acid. The leachete was extracted (3-4 times) by using a centrifuge and collected in a beaker. This leachete was diluted to 100 ml and from this 100 ml an aliquot of 25 ml was taken for EDTA titration. Later the Ca^{++} was converted to calcium carbonate by using the following equation.

Wt of $CaCO_3$ (in gms) = 100 X M X 4..... (3)

where; M is the molarity of sample volume i.e. leachete (in litres), calculated by titrating it with standardized EDTA [prepared by titrating it with standard $CaCO_3$ (known)] and 4 is the dilution factor (i.e. because 100 ml of leachete was prepared out of which 25 ml was taken for titration).

2.3.3 Stable isotope ratios of oxygen and carbon in planktonic foraminifera

Stable isotopic analysis of oxygen ($\delta^{18}O$) and carbon ($\delta^{13}C$) were carried out on 30 clean handpicked planktic foraminiferal species i.e. *Gs. ruber* (white variety), *Gs. sacculifer* (without the sac-like final chamber), *Gr. menardii* and *N. dutertrei* with in the size range of 350-500 μm, using a Europa-PDZ Geo 20-20 mass spectrometer at Physical Research Laboratory, Ahmedabad, India. The schematic diagram of the instrument is shown in Fig 2.1 a and b. The samples (~30 clean foraminiferal species) were loaded in a vial, placed in a carousel maintained at 80^0C. For liberating CO_2 from the samples, pre-determined dose of phosphoric acid was dispensed in a vial through a valve V5. The evolved CO_2 was passed through a water trap (maintained at -100^0C) to remove moisture and frozen onto a dedicated cold finger (through valve V6, V7, V9 and V10), positioned near the mass spectrometer in-let. Throughout the CO_2 generation process the valves V4, V5, V8 and V11 were kept closed. After the completion of CO_2 generation, the whole assembly is evacuated through valve 8 in order to remove "memory effect". During evacuation valves V4, V5, V10 and V11 were kept closed. The whole assembly is called as CO_2 preparation line of 20-20 mass spectrometer and shown in Fig 2.1 a

Fig 2.1 b shows the schematic diagram of dual inlet system. The dual inlet system was devised to ensure that both sample gas and reference gas introduced into the analyzer at the same pressure and handled in the same way, ensuring that flow conditions remain the same for both sample and reference gas. This allows continuing alternating measurement of sample and reference necessary to attain precise and reproducible ratios. Sample gas from Fig 2.1 a is introduced in to the dual inlet system through valves V11, V12, V13 & V14 and from changeover valve it goes into the analyzer. During this process the valve V22 is kept closed and after completing, the whole line is evacuated by a high-speed vacuum pump through valves V14, V13 and V12. Similarly, the reference gas was introduced into the analyzer through changeover valves, V18, V17, V16 & V15 and evacuated through valves V15, V16 and V17.

Finally the two isotopic mass ratios i.e. 45/44 ratio (δ45) and 46/44 (δ46) of sample/reference gas was collected and measured in the analyzer. The final result of $\delta^{18}O$ and $\delta^{13}C$ ratios relative to the VPDB standard was obtained by applying the following corrections as suggested by Craig (1957).

$$\delta^{13}C_{VPDB} = (1.067544 \text{ X } \delta 45) - (0.03600782 \text{ X } \delta 46) \ldots\ldots\ldots (4)$$

$$\delta^{18}O_{VPDB} = (1.000966 \text{ X } \delta 46) - (0.00206322 \text{ X } \delta^{13}C_{VPDB}) \ldots\ldots (5)$$

2.4 Parametric assessment by statistical approach

Parametric assessment was carried out by doing repeat measurement of samples and standards and the estimate of precision is determined by knowing the coefficient of

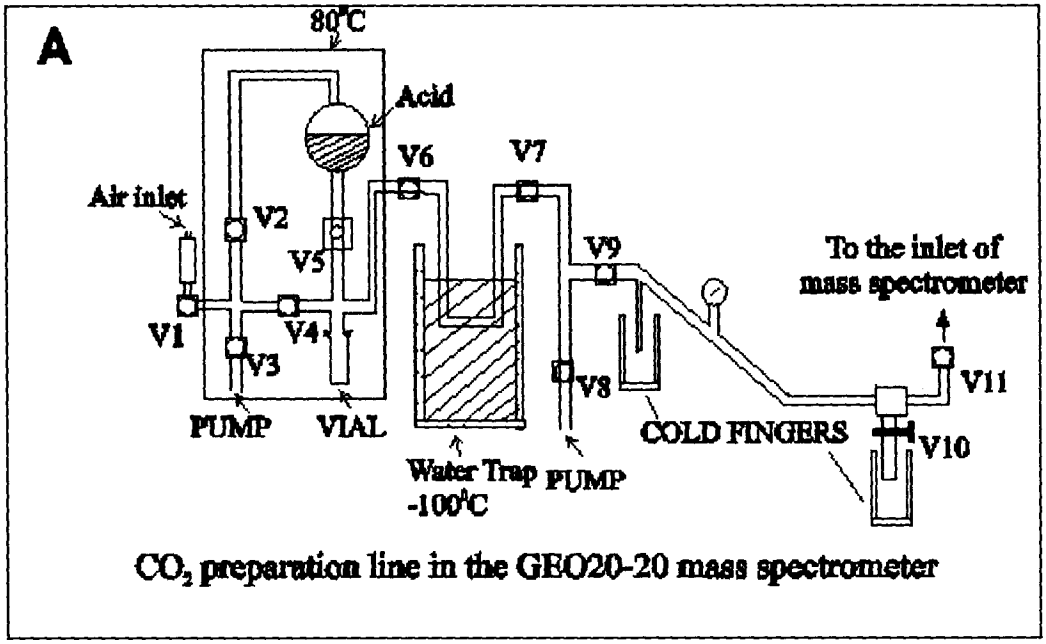

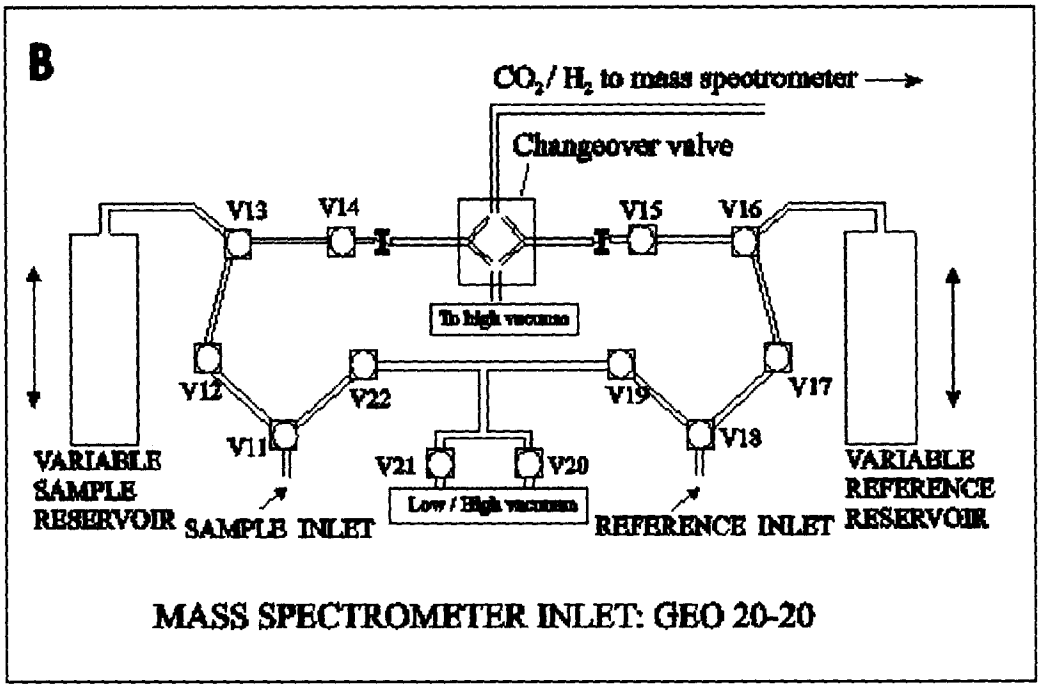

Fig 2.1 a and b. a) Shows CO_2 preparation line along with the b) mass spectrometer inlet for GEO 20-20 mass spectrometer (after Ramesh and Tiwari, 2005).

variation (C.V). The coefficient of variation is given as:

$$C.V.\% = \{1/2N\ [\Sigma\ (d_i/x_i)^2]^{1/2}\} \times 100 \ldots\ldots\ldots (6)$$

where d_i is the difference between the duplicates with mean x_i and N is the total sets of duplicates.

For geochemical parameters: The list of repeated measurement of C_{org} and $CaCO_3$ for both the sediment cores i.e. SK-172 and SK-177/11 along with the C.V. % is listed in the Table 2.2 and 2.3 respectively. The coefficient of variation (C.V) for C_{org} and $CaCO_3$ for all the eight repeat measurements is with in 5%.

For clay mineralogical analysis: The X-ray diffractometer was calibrated using internal silica standards.

For $\delta^{18}O$ and $\delta^{13}C$ measurement: $\delta^{18}O$ and $\delta^{13}C$ measurement on foraminiferal calcite were done by using a working gas (prepared in PRL, Ahmedabad). The working gas in turn is daily calibrated by using an internal calcitic standard (generally before the start of sample measurements). The external precision on $\delta^{18}O$ and $\delta^{13}C$ measurement using three daily measurements of an internal calcitic standard i.e. Z- Carrara (standard error is ± 0.02 ‰) is better than ± 0.1‰. All the $\delta^{18}O$ and $\delta^{13}C$ values are reported with respect to V-PDB.

Table 2.2 Repeat measurements of organic carbon (C_{org}) and calcium carbonate ($CaCO_3$) along with the coefficients of variation in the core SK-172.

S. No	Sample interval (cm)	C_{org} (wt%) (1)	C_{org} (wt%) (2)	C.V.% (wt%-C_{org})	Sample interval (cm)	$CaCO_3$ (wt%) (1)	$CaCO_3$ (wt%) (2)	C.V.% (wt%-$CaCO_3$)
1	4-6	3.37	3.1	5.90	4-6	57.86	57.0	1.06
2	41-43	3.41	3.25	3.39	49-51	56.36	55.9	0.58
3	83-85	2.10	2.0	3.45	71-73	53.44	52.8	0.85
4	121-123	1.69	1.69	0	89-91	49.41	48.8	0.88
5	165-167	1.45	1.4	2.48	117-119	34.83	34.0	1.70
6	243-245	2.31	2.18	4.09	203-205	46.47	45.7	1.18
7	265-267	2.07	2.0	2.43	237-239	46.2	45.2	1.55
8	289-291	1.30	1.30	0	269-271	59.54	59.0	2.04

Table 2.3 Repeat measurements of organic carbon (C_{org}) and calcium carbonate ($CaCO_3$) along with the coefficients of variation in the core SK-177/11.

S. No	Sample interval (cm)	C_{org} (wt%) (1)	C_{org} (wt%) (2)	C.V.% (C_{org})	Sample interval (cm)	$CaCO_3$ (wt%) (1)	$CaCO_3$ (wt%) (2)	C.V.% (wt%-$CaCO_3$)
1	43-44	5.5	5.7	2.53	43-44	50.3	50.6	0.42
2	56-58	6	6	0	56-58	49.2	48.5	1.01
3	80-82	5.4	5.3	1.32	74-76	47.2	45.7	2.28
4	110-112	4.3	4.5	3.21	92-94	47.2	47	0.3
5	194-196	2.8	2.8	0	170-172	53.8	52.6	1.6
6	198-200	2.7	2.8	2.57	236-240	67.2	66.7	0.53
7	288-292	3.3	3.5	4.16	288-292	65.5	65	0.54
8	348-352	3.7	3.6	1.94	348-352	64.9	64.8	0.1

2.5 Geochronology

Chronologies for the collected cores were established by ^{14}C bulk sediment dating (for core SK-172) and oxygen isotope stratigraphy/isotope derived chronology (for core SK-172 and SK-208). The details are discussed below:

2.5.1 Bulk sediment ^{14}C dating

In this method, the dried sediment was treated with ortho Phosphoric acid (H_3PO_4) to liberate CO_2. The CO_2 was purified using a chain of wet chemical reagents like $AgNO_3$, $Hg(NO_3)_2$, KI/I_2 and $K_2Cr_2O_7$ to precipitate halogens and to remove nitrogen and sulphur compounds. Silica gel and dry ice traps (-80°C) remove moisture from the gas. The purified CO_2 was then reacted with molten lithium in a stainless steel reaction vessel maintained at 800°C (furnace temperature) and placed under vacuum where it is converted to Li_2C_2.

$$\mathbf{2\ CO_2 + 10Li \Rightarrow Li_2C_2 + 4Li_2O}$$

Later, the lithium carbide (Li_2C_2) was cooled and hydrolysed to acetylene gas.

$$\mathbf{Li_2C_2 + 2H_2O \Rightarrow C_2H_2 + 2LiOH}$$

The acetylene was purified by passing through a phosphoric acid and dry ice traps to remove ammonia compounds and water vapour respectively. Finally the acetylene was trimerised to benzene using finely divided vanadium as a catalyst.

$$3C_2H_2 \Rightarrow C_6H_6$$

Benzene was then driven off the vanadium catalyst at 100°C and collected under vacuum. The benzene was then stored in a vial under refrigeration for counting. Later radiocarbon activity of benzene was detected using LKB-Quantulus ultra-low level detector at Physical research laboratory, Ahmedabad. Preparation of benzene, ^{14}C detection and other details of the method are described elsewhere by Yadava and Ramesh (1999).

Chronology of core SK-172 was established by using the abovementioned technique (^{14}C bulk sediment dating) whereas for core SK-177/11 chronology was adopted from Pandarinath et al. (2004). The chronological details are listed in Table 2.4 and 2.5 respectively.

2.5.2 Oxygen isotope stratigraphy/ isotope derived chronology

Chronology for core SK-172 is also established from the $\delta^{18}O$ variations in *Globigerinoides ruber* after identifying well known climatic events. The chronological details are tabulated in Table 2.6.

The chronology for core SK-208 is established by stacking $\delta^{18}O$ record of *Gs. sacculifer* with the standard SPECMAP curve and the different isotope stages were identified. The depth to which the tie point is identified is shown in Table 2.7 along with the corresponding age.

Based on the established chronologies, all the cores were taken for the present study. Core SK-172 shows mismatch between bulk ^{14}C carbonate dating and isotope derived chronology (discussed in chapter 3) therefore for palaeoclimatic interpretation isotope derived chronology is utilized which is discussed in chapter 4 and chapter 5.

Table 2.4 Chronological details of core SK-172 based on bulk sediment C-14 dating (using calcium carbonate of sediments).

S. No	Sample interval (cm)	Depth (cm)	^{14}C age (yr)
1	9-19	14	6920 ± 110
2	37-41	39	8780 ± 100
3	49-55	52	10110 ± 110
4	113-117	115	15000 ± 150
5	157-165	161	13740 ± 140
6	203-207	205	20970 ± 250
7	267-271	269	13600 ± 150

Table 2.5 Chronological details of core SK-177/11 based on bulk sediment C-14 dating (using organic carbon of sediments).

S. No	Sample interval (cm)	Age (kyr)	Sedimentation rate (cm/yr)
1	54-56	2.885	0.019
2	100-105	5.95	0.016
3	150-155	8.69	0.018
4	200-205	16.04	0.007
5	250-255	18.99	0.017
6	300-305	26.947*	0.006
7	360-365	33.75*	0.009

* Ages beyond 24 ka are calibrated using Bard second order Polynomial (Bard, 1998).

$$\textbf{Age (cal)} = -3.0126 \times 10^{-6} \times (\text{Age } ^{14}C)^2 + 1.2896 \times (\text{Age } ^{14}C) - 1005 \ldots\ldots\ldots (7)$$

where Age (cal) is calibrated age and (Age ^{14}C) corresponds to reservoir corrected radiocarbon dates (^{14}C dates).

Table 2.6 Chronological details of core SK-172, based on identifying climatic events on oxygen isotope variations of *Globigerinoides ruber* ($\delta^{18}O$).

S. No	Sample interval (cm)	Depth (cm)	Isotopic event	Age (kyr)
1	125-129	127	Termination of MWP1b	11
2	169-173	171	Termination of MWP1a	13.25
3	279-281	280	LGM	21

Table 2.7 Oxygen isotope stratigraphy, based on identifying tie points by comparing the $\delta^{18}O$ record of core SK-208 (*Gs. sacculifer*) with standard SPECMAP curve.

S. No	Sample interval	Depth of tie point (cm)	Age on SPECMAP curve (kyr)	Sedimentation rate (cm/kyr)
1	0-6	3	0	
2	70-71	70.5	19	3.74
3	149-150	149.5	65	1.72
4	214-216	215	80	4.4
5	280-282	281	100	3.3
6	338-340	339	110	5.8

CHAPTER 3

LATE QUATERNARY SEA LEVEL CHANGES AND RELATED EVENTS

3.1 Late Quaternary Sea Level changes

Available literature pertaining to palaeoclimatology/sea level reconstruction from various locales suggest that the late Quaternary period has witnessed various episodes of sea level changes either related to waning and waxing of continental ice volumes owing to the climate change or to the regional tectonics. Waning and waxing of continental ice volume due to climate change generally regulates the sea level and oxygen isotopic composition of seawater on a global scale (Rohling and Cooke, 2002 and the references therein). All these studies illustrates that $\delta^{18}O$ of seawater and sea level are intimately related to each other. This relation has been used by various researchers to reconstruct past sea level changes by utilizing $\delta^{18}O$ of calcareous microorganisms (e.g. Fairbanks, 1989; 1992; Bard et al., 1996b; Rohling et al., 1998; Shackleton, 2000) which grows in equilibrium with the sea water (Shackleton, 1967; Shackleton and Opdyke, 1973). Moreover, research on $\delta^{18}O$ of fossil carbonate suggests that every 0.011‰ change of $\delta^{18}O$ is equivalent to one meter of sea level variation (Shackleton, 1987; Fairbanks, 1989; 1992). This equation has led many researchers to use $\delta^{18}O$ records for past sea level reconstruction. Fairbanks (1989, 1992) has suggested that during Last Glacial Maximum (LGM), the poles were extensively covered with ice and the sea level was 120 m below than the present sea level. Using $\delta^{18}O$ records he also proposed a two step deglaciation model which indicates that the rise in sea level during deglacial period was not monotonic but was marked by two intervals of rapid sea level rise termed as melt-water pulse 1a (MWP-1a, characterized by an exceedingly rapid sea level rise of 24 m in less than 1,000 yr) and melt-water pulse 1b (MWP-1b) centered at 12,000 ^{14}C yr BP and 9,500 ^{14}C yr BP, respectively. From all these results it can be inferred that the $\delta^{18}O$ curve of all deep-sea

records contain a common ice volume component other than the local effects that can reflect sea level changes. However, on a regional scale, tectonic activity is often found to alter the relation between sea level and $\delta^{18}O$ curve (Rao et al., 2003).

The study of past sea level change is essential because it affects the sediment dispersal pattern in various ways and hence has palaeoceanographic/ palaeoclimatological implications. Records from the western continental margin of India suggests increased sedimentation rate during low sea level stand which may be due to the exposed shelf (Agnihotri et al., 2003). Additionally, the low sea level stand as well as sudden increase in sea level can trigger slumping or turbidity currents resulting in mixing of sediments from different environments (Rao et al., 1988; Rao, 1989). In order to avoid any mis-interpretation of data/results, knowledge in the past sea level variation is immensely useful for palaeoclimatologists. Considering the importance of past sea level change, several attempts have been made to reconstruct a late Quaternary sea level curve for the western continental margin of India (Hashimi et al., 1995; Rao et al., 2003). They found that the sea level shows deviation from the glacio-eustatic sea level curve indicating neo tectonic activity (Rao et al., 2003). The evidences favouring neotectonic activity are the presence of sub-marine terraces off Bombay-Saurashtra well below the glacio-eustatic sea level of that corresponding age. Furthermore, Rao et al. (2003) have also reported differential response of western continental margin of India to neo tectonic activity i.e. subsidence of 40 m in the north western margin whereas the southwestern margin gets uplifted. This is corroborated by Subramanya (1996) who reported submergence in the north and upliftment in the south due to the buckling of landmass. All these evidences suggest the lack of a reliable sea level curve for the continental margin of India.

3.2 Sea Level changes and related phenomenon like slumping, turbidity currents etc

Sediments are the natural repositories of information about the past. The sedimentary processes like slumping, turbidity currents, reworking lead to mixing of sediments from different environments which would lead to mis-interpretation of the data.

Slumping or the turbidites can disturb the stratigraphy of sediments. Slumping is a type of gravity flow where the sediment is transported downslope by the action of gravity. Whereas, turbidity currents are generated due to the density contrast between the sediment laden fluid and the ambient water due to which the sediments are carried along with the currents and gets redeposited elsewhere. Various triggering mechanism have been proposed for such kind of sediment transport for e.g. catastrophic movement like earthquake, tsunami, storm surges etc. The most vulnerable area for slumping or turbidites is the continental slope (Carpenter, 1981), particularly the upper slope. Records suggest that the northwestern continental margin of India has been subjected to extensive slumping and redeposition due to turbidity currents or slope instability during period of low sea level stand (Setty, 1972; Hussain and Guptha, 1985; Rao et al., 1988; Rao, 1989 and Guptha et al., 2002). They have reported ooids in deep sea sediments and since ooids are restricted to the shallow sea therefore its presence in the deeper part reflects turbidity currents/ slumping. Similarly, the occurrence of lime mud along the continental slope off Saurashtra-Bombay is attributed to the lateral transport from the adjacent shelf during the periods of low sea level stand (Rao and Wagle, 1997). Based on various evidences Guptha et al. (2002) and Chauhan and Almeida (1993) has

demarcated a zone of slumping/ turbidite between Saurashtra and Bombay. The presence of sharply defined portions of sea bed at the continental slope off Goa (Rao and Wagle, 1997 and the reference therein) possibly indicates the extension of slumping zone marked by Guptha et al. (2002) and Chauhan and Almeida (1993) to the region off Goa. Records suggest that apart from slumping/ turbidites, fluvial discharge due to monsoonal activity is also responsible for the sediment mixing (Bhushan et al., 2001).

As in northwestern continental margin, southwestern margin of India is also reported to have affected by slumping during the Pleistocene-Holocene transgression (Shankar and Manjunatha, 1995).

From the literature it is evident that the western continental margin of India specially the continental slope has been subjected to extensive reworking or resuspension (sediment mixing) due to slumping/ turbidity currents but none of them has suggested the convincing mechanism that could trigger sediment slumping. All these records indicate that reworking or resuspension could have occurred either due to slope instability during low sea level stand or during Pleistocene-Holocene transgression or enhanced fluvial discharge. In this chapter we are discussing this issue using a sediment core collected from two different geographic locales as shown in Fig 3.1. SK-172 and SK-177/11 are collected from the northern and southern part of Arabian Sea respectively. In the present study an attempt is also made to establish a relation between various aspects of sediment mixing with the sea level changes and/or monsoon induced fluvial discharge.

3.3 Geological setting of the sediment core site SK-172 and SK-177/11

The surficial geology of the western continental margin as shown in Fig 3.1 varies widely from north to south. It also varies with in the continental shelf. The inner continental shelf between Saurashtra and Quilon comprises terrigeneous material with sand in the near shore environment followed by a zone of silty clay. The adjacent hinterland is the main source of terrigeneous material for the inner continental shelf whereas the outer shelf represents the relict sediments (Rao et al., 2003). Between Saurashtra-Mangalore these relict sediments occur predominantly as biogenic material and between Mangalore-Quilon it consists of admixture of terrigeneous and biogenic sediments. Towards south biogenic sediments again appear on the outer continental shelf off Quilon-Cape Comorin. The relict zone is broader in the northwestern part and it narrows down towards the southwestern margin of India. The northwestern relict zone also called as carbonate platform extends up to 4°of latitude and consists of dolomite crust, *Halimeda* dominated limestone and aragonite sand. The central relict zone comprises rhodoalgal facies while the southern part is dominated by molechfer facies (Rao and Wagle, 1997).

The sediments of inner continental shelf and slope are dominated by fine siliciclastic sediments i.e. clay minerals with abundant foraminifera. Between Saurashtra and Goa, these clay minerals comprises admixture of clays that are derived from Indus and Basaltic province whereas inner shelf derives its clay minerals from the adjacent hinterland. However, the abundance of Indus borne clay minerals on the continental slope decreases from north to south indicating the decreasing influence of Southwest monsoon currents.

3.4 Geochronology of the core SK-172 and SK-177/11

3.4.1 Northern part of eastern Arabian Sea core (SK 172): The location of the core SK-172 falls in the proximity of relict carbonate deposit (see Fig 3.1), the northern extension of which is called the carbonate platform. Carbonate platform is reported to consist of carbonates of varying age i.e. from oldest dolomite crust of ~18 ^{14}C kyr to the *Halimeda* dominated limestone and aragonite sand of early Holocene age (Rao and Wagle, 1997; Rao et al., 2003). Hence reworking/ resuspension of these carbonates to the core site are expected and to understand the extent of reworking/ resuspension the collected core is subjected to multiproxy approach like sedimentology, isotope geology and geochemistry (organic carbon and calcium carbonate). Chronology as established by oxygen isotope events as well as bulk carbonate ^{14}C dating is compared and assessed along with the other records like oxygen isotope, geochemistry, coarse fraction etc. Based on this comparison, the origin of carbonates (on which the technique of bulk ^{14}C dating depends) is ascertained i.e. if chronology from both the methods matches then the carbonates can be inferred as insitu otherwise mixing of carbonates from different source can be thought as an alternate explanation and various possible mechanisms could be suggested.

Bulk carbonates ^{14}C dating: Chronology obtained by conventional bulk carbonate ^{14}C dating using liquid scintillation spectrometry (Yadava and Ramesh, 1999) is shown in Table 3.1. At 161cm and 269cm, radiocarbon ages deviate from the normal trend (i.e. showing younger age as compared to the age of overlying sediments). We have discarded these two ages and plotted an age depth model using best-fit line for the remaining five ages (see Fig 3.2). From Fig 3.2 it is evident that the Pleistocene- Holoc

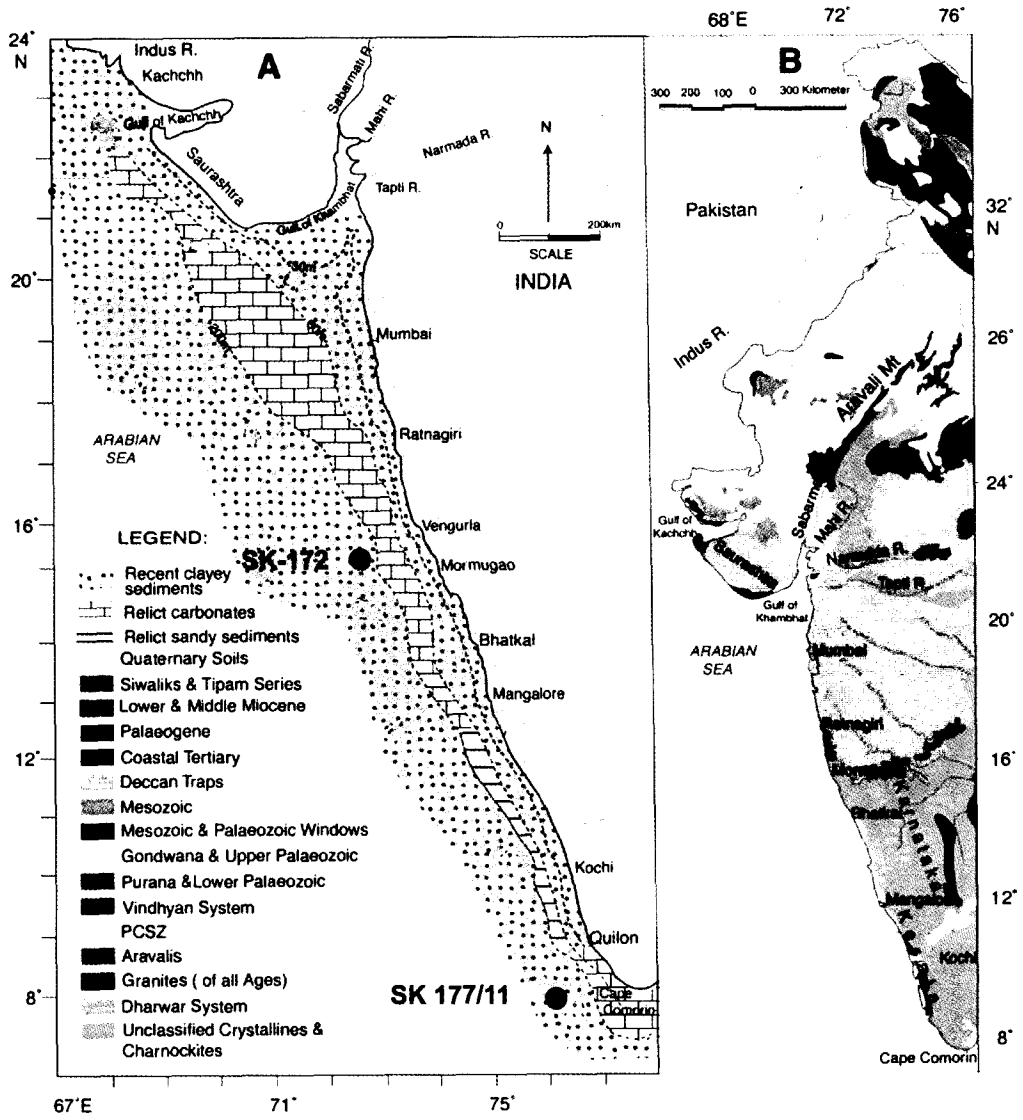

Fig 3.1 Map showing A) surficial geology of the eastern Arabian Sea and the location of core used in this study, B) hinterland geology (modified after Anonymous, 1965)

Table 3.1 Bulk sediment radiocarbon age (^{14}C yr) for core SK-172 (using calcium carbonate).

S. No	Interval (cm)	Depth (cm)	Age (^{14}Cyr)
1	9-19	14	6920±110
2	37-41	39	8780±100
3	49-55	52	10110±110
4	113-117	115	15000±150
5	157-165	161	13740±140@
6	203-207	205	20970±250
7	267-271	269	13600±150@

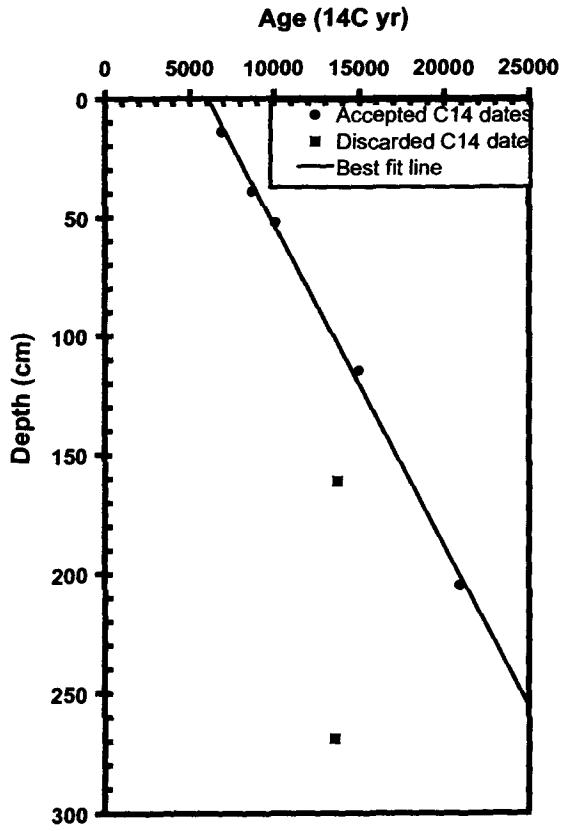

Fig 3.2 Age depth plot for core SK-172. Note: the two points are not falling in best fit line.

ene boundary arrives at 49-50 cm and upon extrapolating towards the core top it shows 6073 yr which indicates erosion of surface sediment.

Oxygen isotope ($\delta^{18}O$) derived chronology: $\delta^{18}O$ derived chronology is based on three isotopic events (as shown in Fig 3.3a) identified on surface dwelling planktonic foraminifera i.e. *Gs. ruber*. Taking these 3 events as tie points we have constructed an age depth model and shown in Fig 3.3b. The identified events are Last Glacial Maximum (LGM), culmination of melt water pulse 1 a and melt water pulse 1 b (MWP 1a and 1b). These events are global in nature and correspond to ~21 kyr (Dansgaard et al., 1993), ~13 kyr and ~11 kyr respectively (Fairbanks, 1989, 1992; Bard et al., 1996). The LGM as identified in this core is represented by the heaviest $\delta^{18}O$ value, which is in close agreement and also observed by others (e.g. Tiwari et al., 2005b; Chodankar et al., 2005; Banakar et al., 2005). On the other hand, the termination of MWP 1a and 1b are identified by a sharp negative excursion (prior to this point) in $\delta^{18}O$ value which is analogous to the eustatic sea level curve of Fairbanks (1989, 1992). All these events (summarized in the form of Table 3.2) are also identified in *Gs. sacculifer* and *Gr. menardii* along with the *Gs. ruber* (see Fig 3.4 a, b and c). From this approach the Pleistocene Holocene boundary arrives at 120 cm.

3.4.2 Southeastern Arabian Sea core (SK-177/11)

The chronology as shown in Table 3.3 is obtained from Pandarinath et al. (2004). The ages shown in Table 3.3 are calibrated using programme Calib 4.1 (INTCAL 98) (Stuiver et al., 1998). The ages beyond 24 kyr are calibrated using Bard polynomial (Bard, 1998). Based on sedimentation rate, an age depth model is obtained (Fig 3.5).

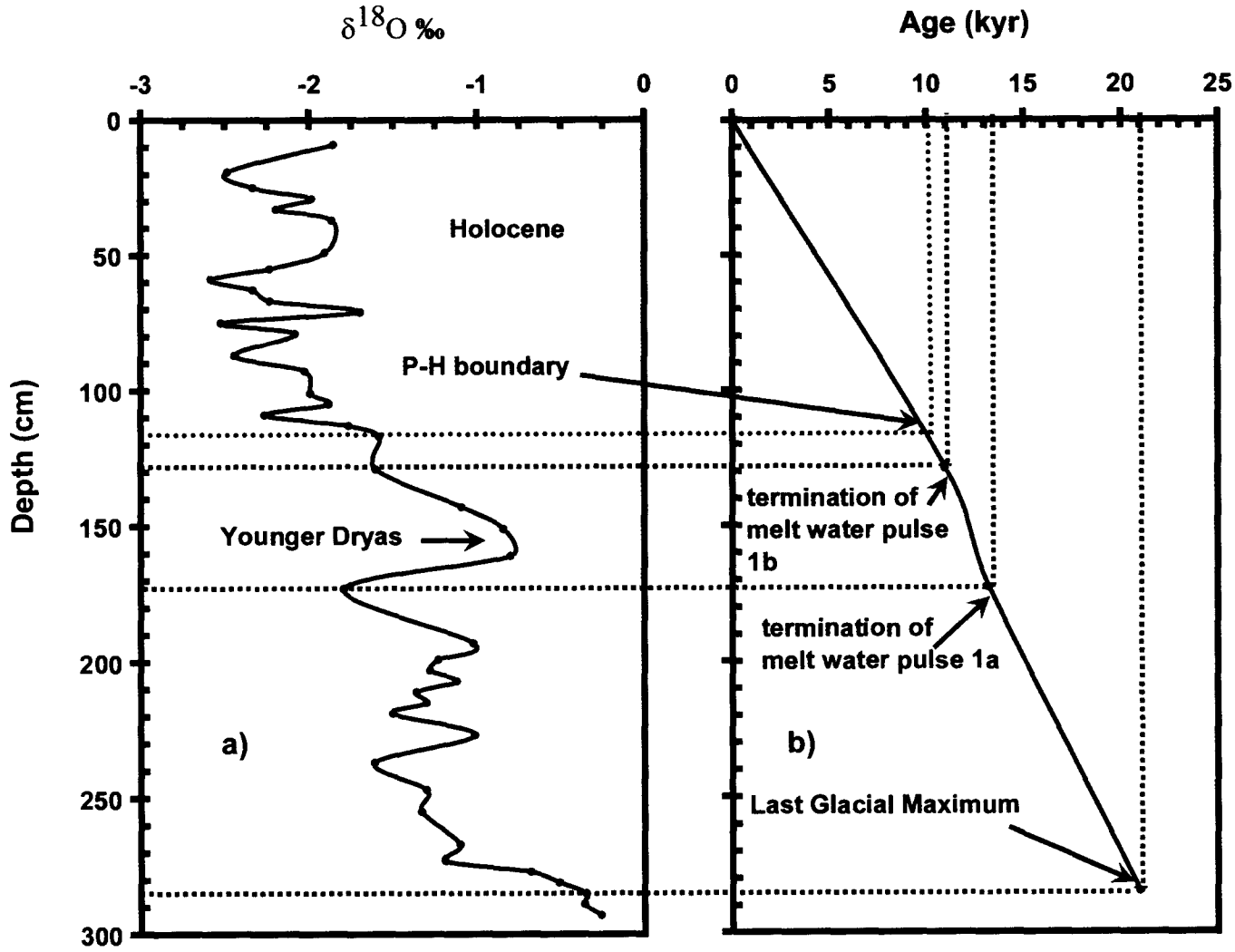

Fig 3.3. a) Downcore variation of $\delta^{18}O$ in *Gs. ruber* based on which b) age depth model for core SK-172 is constructed. Note: The arrow and the dashed lines are the climatic events based on which the chronology is established.

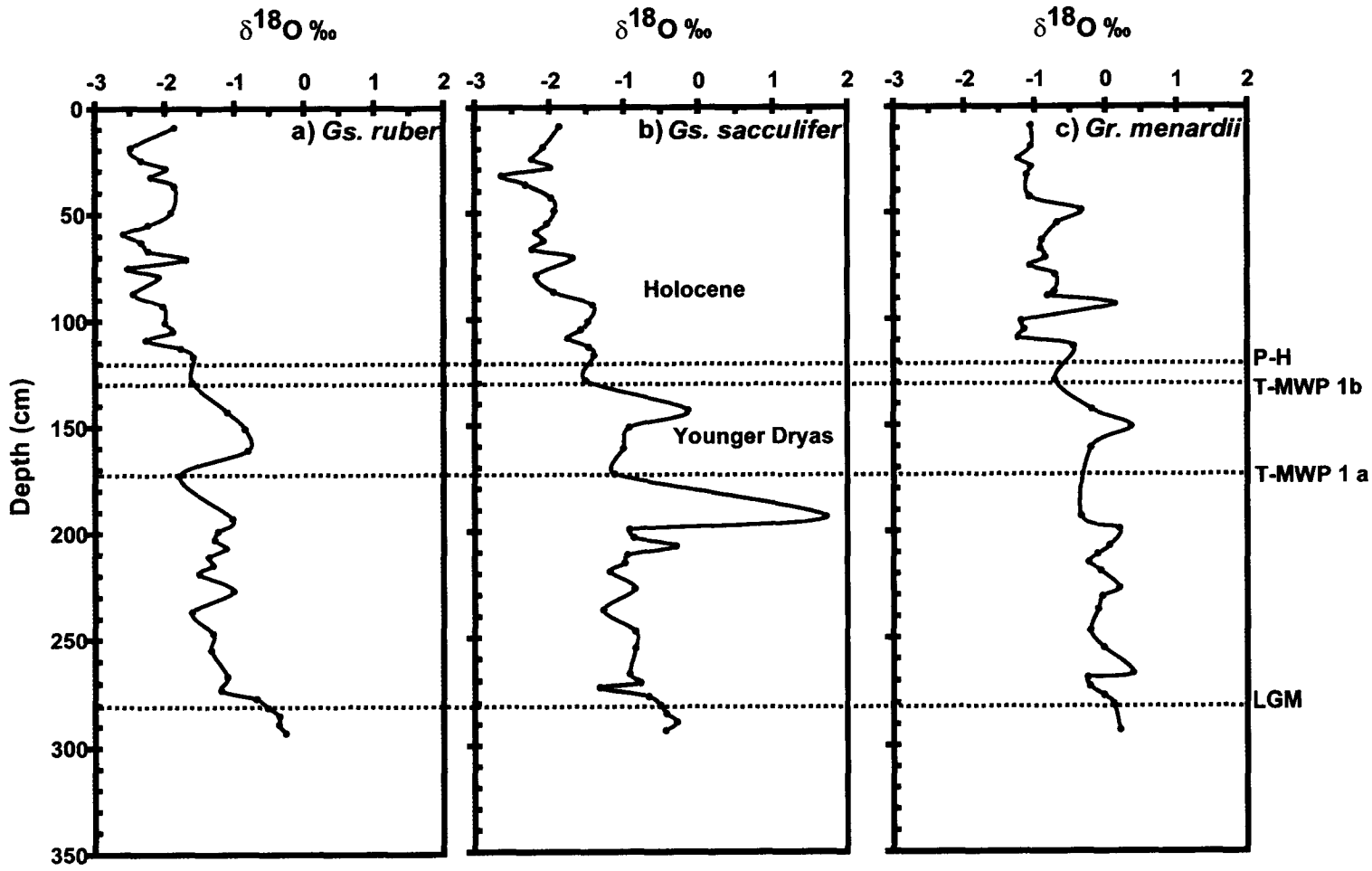

Fig 3.4. Downcore variation of $\delta^{18}O$ in a) *Gs. ruber*, b) *Gs. sacculifer* and c) *Gr. menardii* respectively in core SK-172. The dashed lines are the climatic events based on which the chronology is obtained.

Table 3.2 $\delta^{18}O$ derived chronology for core SK-172 (identified from global isotopic events).

S. No	Interval (cm)	Depth (cm)	isotope events	Age (kyr)
1	125-129	127	Termination of melt water pulse 1b (T-MWP 1b)	11
2	169-173	171	Termination of melt water pulse 1b (T-MWP 1a)	13.25
3	279-281	280	Last Glacial Maximum	21

Table 3.3 Calibrated C-14 ages (kyr) for core SK-177/11 (using organic carbon of sediments)

S. No	Sample interval (cm)	Depth (cm)	Age (calibrated) (kyr)
1	54-56	56	2.885
2	100-105	105	5.95
3	150-155	155	8.69
4	200-205	205	16.04
5	250-255	255	18.99
6	300-305*	305	26.947
7	360-365*	365	33.75

* calibrated by using Bard polynomial (Bard, 1998) rest are calibrated using Calib 4.1 (INCAL 98)

3.5 Sedimentological parameters

3.5.1 Northern part of eastern Arabian Sea core (SK-172)

Texture: Textural analyses along with different sedimentological parameters like mean, median are shown in Fig 3.6. These textural parameters were carried out on bulk sediments following the standard method of Folk (1989). The results suggest that the core is silty clay and the variation of mean and median shows progressive increase of grain size towards the core top.

Biogenic proxies

Organic carbon and calcium carbonate: The downcore variation of C_{org} is shown in Fig 3.7a. It is evident from the Fig that the C_{org} fluctuates between 1.5 and 3.5%.3.5% of C_{org} from the core top is very well corroborated by the record of Prakash Babu et al. (1999). The downcore variation of C_{org} shows enrichment from ~120 cm to the core top. $CaCO_3$ content as shown in Fig 3.7b varies between 35-60%. Similar to C_{org}, surface value of $CaCO_3$ (i.e. 60%) corroborates with Prakash babu et al. (2002). The downcore variation of $CaCO_3$ shows enrichment from ~120 cm to the core top.

Coarse fraction content: Downcore variation of coarse fraction content (>63 μm) shows variation between 1-13% (see Fig 3.7c). Below ~120 cm it remains near constant i.e. between 1-1.5% whereas it gradually increases from ~120 cm to the core top. Examination under binocular microscope shows that coarse fraction is largely comprised of planktonic foraminifera with no signs of dissolution and dilution from terrestrial material.

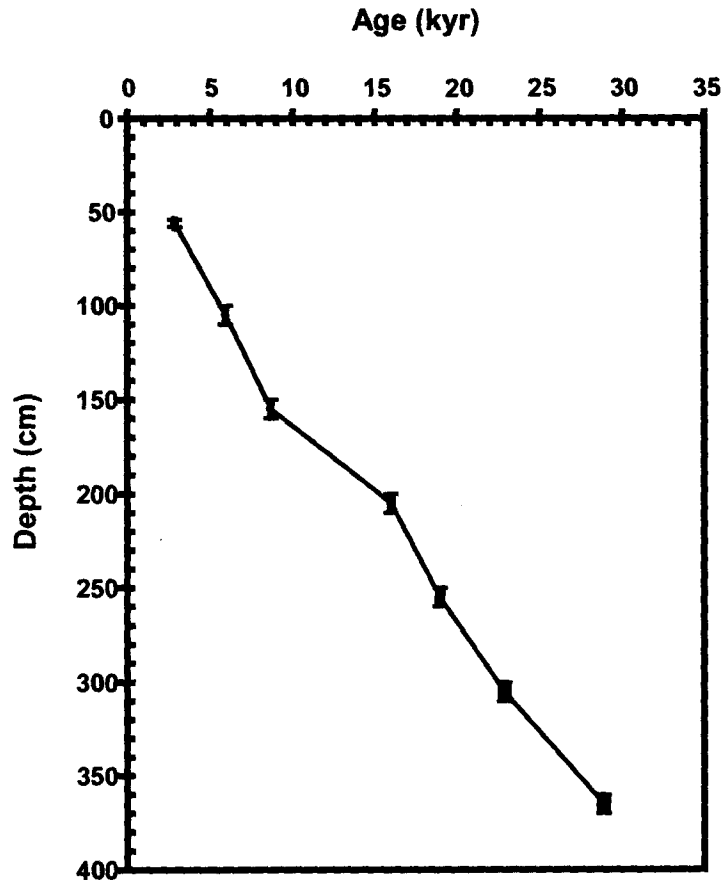

Fig 3.5 Age depth model for core SK-177/11 (after Pandarinath et al., 2004).

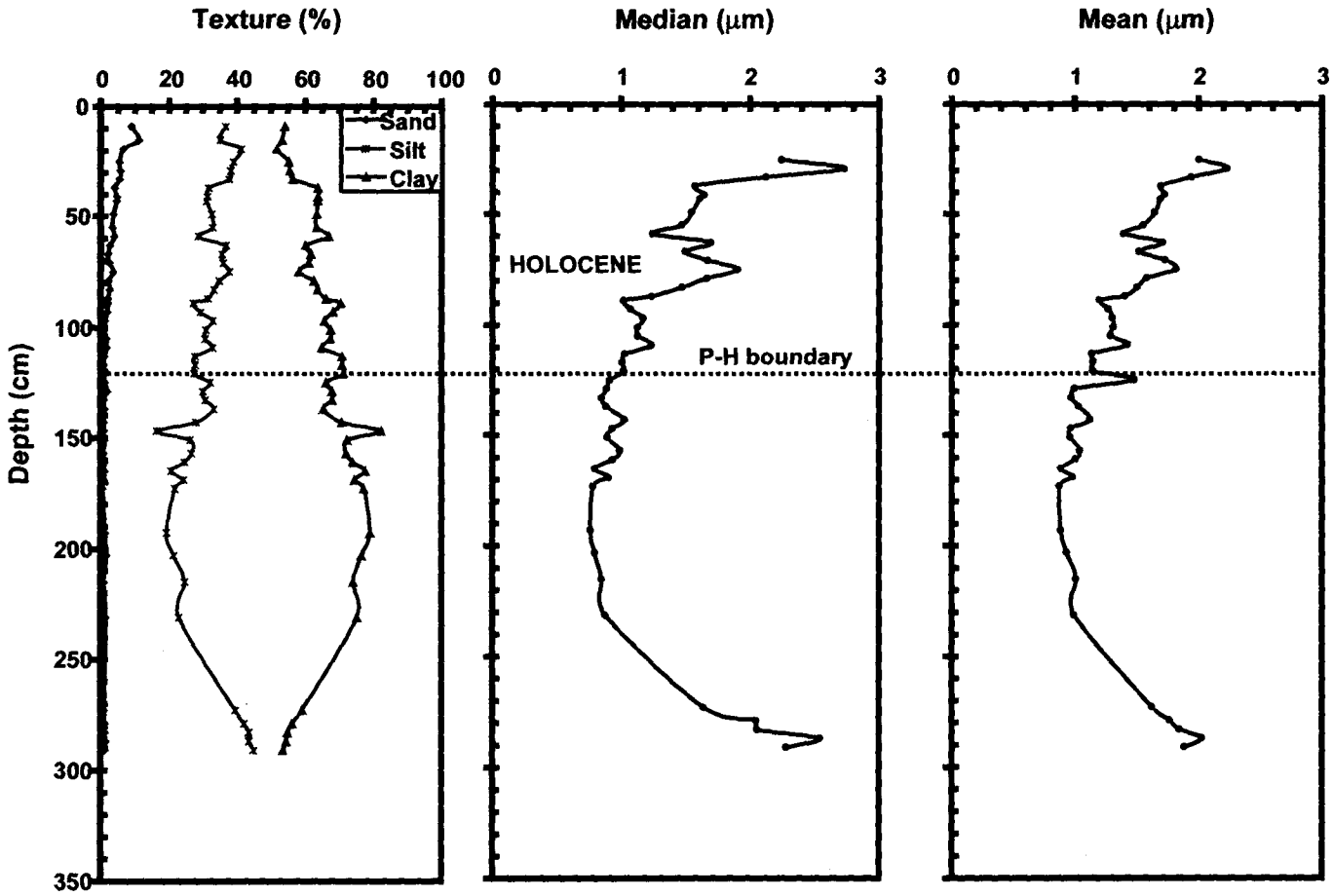

Fig 3.6 Downcore variation of textural parameters, median and mean grain size (in μm) for core SK-172. The dashed line represents the isotope derived Pleistocene-Holocene boundary.

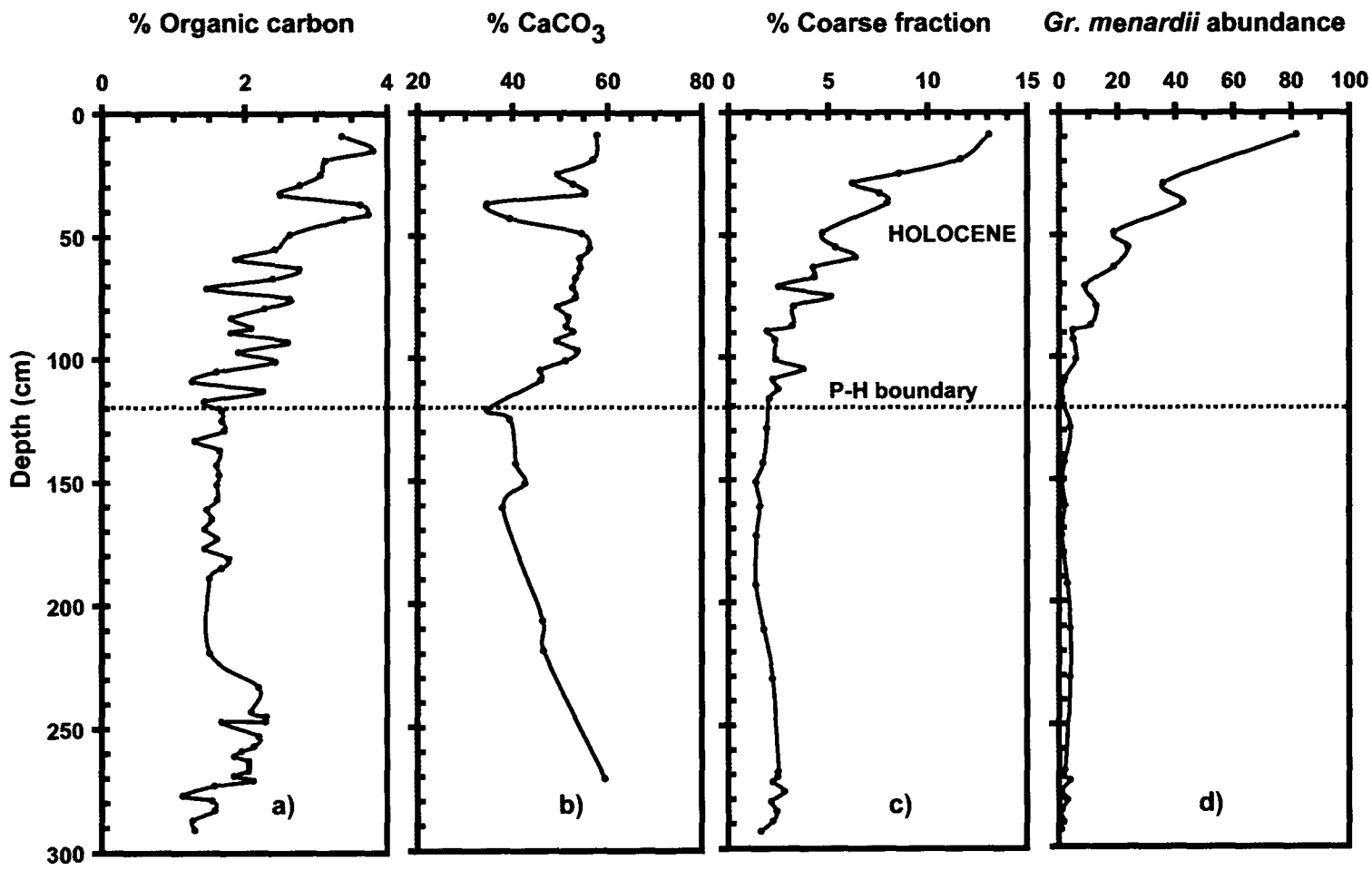

Fig 3.7 Downcore variation of a) Organic carbon, b) $CaCO_3$, c) Coarse fraction and d) *Gr. menardii* abundance in core SK-172. The dashed line represents the isotope derived Pleistocene-Holocene boundary.

Individual count of planktonic species *Gr. menardii* per gram of sample was carried out and the results are presented in Fig 3.7d. *Gr. menardii* is a tropical species which thrives at the top of thermocline (Fairbanks et al., 1982). Hence its abundance can be used as an index for the mixed layer deepening. Similar to the coarse fraction, *Gr. menardii* population shows increasing trend from ~120 cm (see Fig 3.7d).

3.5.2 Southeastern Arabian Sea core (SK 177/11)

Texture: Variation of textural parameters (carbonate free) is shown in Fig 3.8. It suggests that the core is silty clay with an average of 30% clay and 12% silt. Sand fraction (insoluble residue) being insignificant is not shown in Fig 3.8a. Temporal variation of silt and silicic fractions i.e. sum of silt and clay (see Fig 3.8a, b) shows three distinct zones i.e. MIS 1, 2 and 3. During MIS 3 and MIS 1, all the component i.e. silt, silicic fraction and clay shows enrichment whereas in MIS 2 silt and silicic fraction remained lowest at 21 kyr BP. It is interesting to note that silicic fraction is largely controlled by silt because clay remained near constant throughout the core except in Holocene where it shows a slight enrichment.

Biogenic proxies

Organic carbon and calcium carbonate: Temporal variation of C_{org} and calcium carb--onate is shown in Fig 3.8c and d, respectively. They show inverse relation with each other. During MIS 3 and 2, C_{org} decreased, whiles calcium carbonate increased and carbonate dominated the sediments between 23 and 15 kyr with an average of 67% whereas organic carbon and silicic fraction remained low. During Holocene, calcium

carbonate and organic carbon showed increasing trend which could be related to productivity.

Coarse fraction content: Coarse fraction content as shown in Fig 3.8e varies between 8 and 18%. During MIS 2 (25-15 kyr) it shows maximum enrichment of 18%. Visual examination of coarse fraction under binocular microscope reveals the presence of calcareous aggregates encrusting small foraminifera (see Fig 3.9 a, b and c). This is very common from the samples of MIS 2 (between 25-15 kyr) and possibly indicates the reworked products of relict carbonate deposits that has finally deposited at the core site during low sea level stand.

3.6 Discussion

3.6.1 A mismatch between oxygen isotopes derived chronology and bulk carbonate chronology in the northern part of eastern Arabian Sea core (SK 172)

The radiocarbon ^{14}C derived chronology (as shown in Fig 3.2 and Table 3.1) and isotope derived chronology (Fig 3.3a, b; 3.4a, b, c and Table 3.2) is compared in Fig 3.10. Both these chronologies displayed a mismatch. From Fig 3.10, it is evident that bulk carbonates ^{14}C dates are showing comparatively older ages because P-H boundary from isotope derived chronology arrives at ~120 cm whereas from ^{14}C dating it arrives at ~49-50 cm. In such discrepancy it is better to rely on oxygen isotope stratigraphy due to the following reasons:

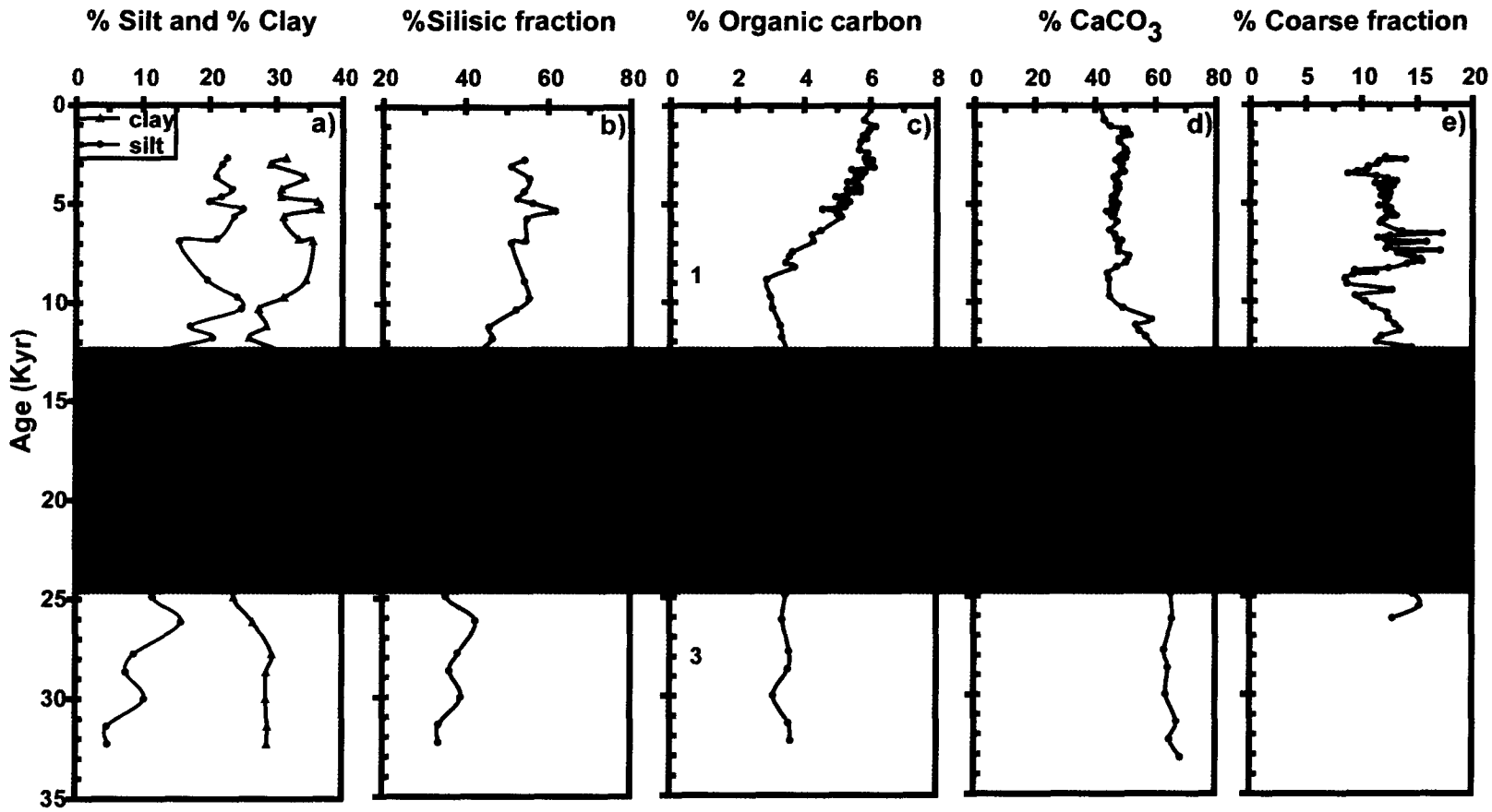

Fig 3.8. Variations in a) Silt and clay, b) Silisic fraction, c) Organic carbon, d) $CaCO_3$ and e) Coarse fraction for core SK-177/11.

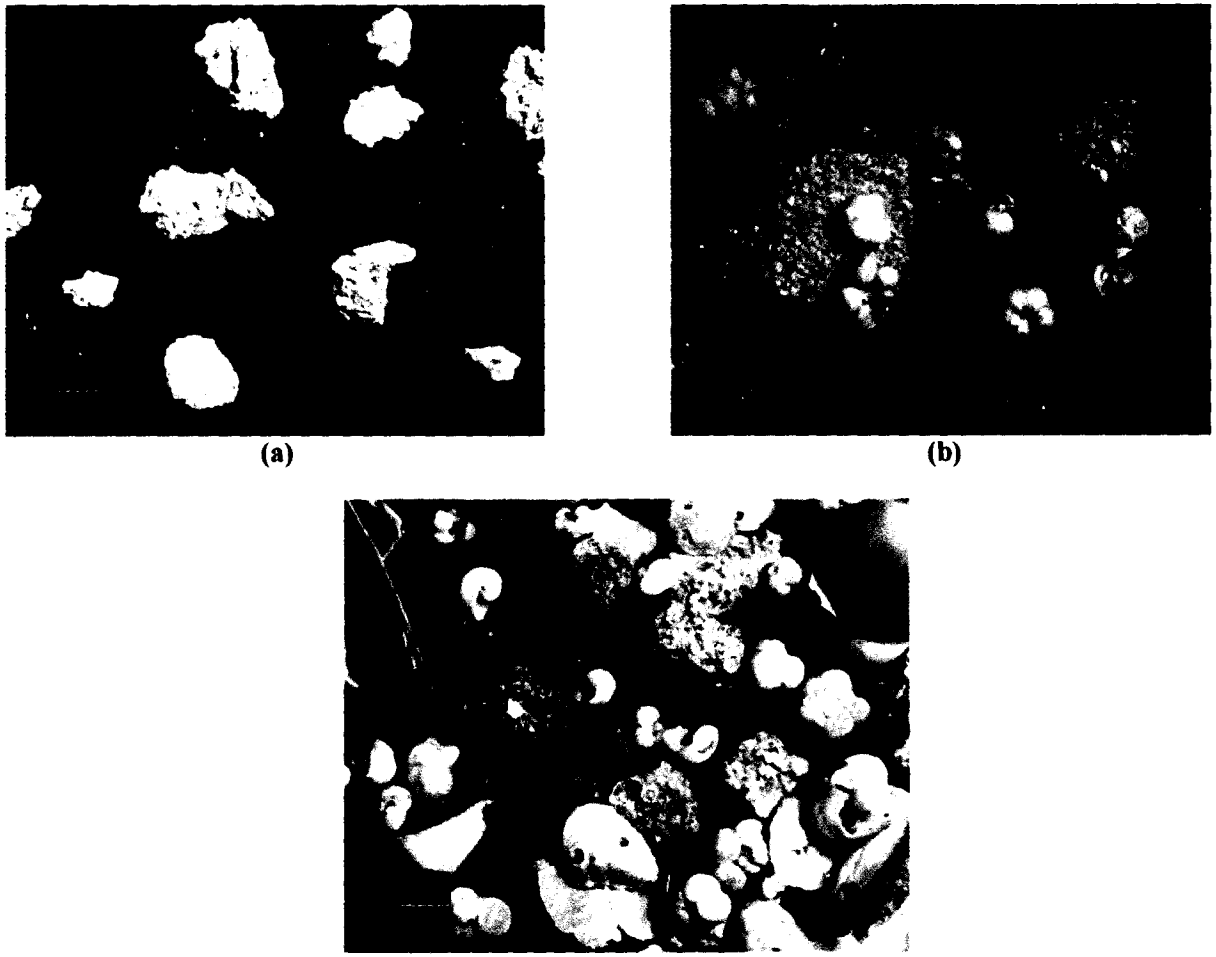

(a) (b) (c)

Fig 3.9 Photomicrographs showing calcareous aggregates as observed in core SK-177/11.

i) In the present study we have utilized clean and unstained foraminifera for the oxygen isotope analysis as suggested by Shackleton, 1972. This approach is based on the fact that clean and bright foraminiferal shells indicates freshly formed (insitu) unlike buff coloured or stained ones which indicates reworking/digenetic change.

ii) The downcore variation of organic carbon, coarse fraction- an established proxy for variation in productivity shows increased in its concentration from ~120cm to core top interval (Fig 3.7a, c). Records from the eastern Arabian Sea have reported the reestablishment of SW monsoon winds during Holocene due to which productivity has increased through wind mixing (Nair et al., 1989). Thus the recorded enrichment of productivity proxies could represent Holocene and the depth (i.e. ~120cm) from where productivity increases can be considered as Pleistocene-Holocene boundary. In addition to the productivity proxy, the abundance of *Gr. menardii*, a tropical species which thrives at the top of thermocline (Fairbanks et al., 1982) is also reported. Due to its depth habitat, the abundance of *Gr. menardii* will reflect deepening and the subsequent injection of nutrients in the mixed layer (Verma et al., 2003). Thus the section (i.e. above ~120 cm) from where *Gr. menardii* abundance increases (Fig 3.7d) represents Holocene and marking the Pleistocene-Holocene boundary at 120 cm interval. All the independent proxy records like C_{org}, coarse fraction and *Gr. menardii* abundance shows increasing trend uniformly.

Records from the eastern Arabian Sea have also suggested decrease in productivity (Agnihotri et al., 2003; Pattan et al., 2003) during glacial period. Below ~120 cm depth the proxy records like C_{org}, coarse fraction and *Gr. menardii* abundance from our study shows depletion/ less abundance. Thus the observed decrease in

concentration of C_{org}, coarse fraction and *Gr. menardii* abundance suggest a glacial period. These observations may add credence to interpretation of Pleistocene-Holocene boundary i.e. at 120 cm.

iii) The Holocene sedimentation rate of 12 cm/ kyr as deciphered from $\delta^{18}O$ technique corroborates very well with the nearby core (Paropkari et al., 1992).

The Pleistocene-Holocene boundary as concluded from the isotope derived boundary and downcore variation of organic carbon, coarse fraction, *Gr. menardii* abundance (Fig 3.3a, b and Fig 3.7 a, c and d) show close agreement with the nearby core reported by Paropkari et al. (1992). This further suggests that this approach for obtaining chronology by marking climatic events in oxygen isotope record (in this study 21kyr, 13kyr and 11kyr) seems to be correct and can be utilized for palaeoclimatic/palaeomonsoonal reconstruction. Bulk carbonate on the other hand, utilizes carbonate from two sources, the first having a marine origin (from foraminifera and coccolithophores) and second from the continents and /or other older carbonate. The later fraction (carbonate) when mixes with the sediments in the form of reworked material brought by runoff/turbidity currents/slumping from the continents/older carbonate deposits shows apparent age and the deviation from the actual age depends on the ratio of mixing of these carbonates (marine or older/dead carbonates). Therefore, the older age (compared to $\delta^{18}O$ technique) derived from bulk carbonates technique indicates the apparent age due the significant contribution from older/dead carbonate either from terrestrial or marine realm. The surface sediment showing ~6073 year is also an artifact of carbonate mixing rather than the erosion of core top. The evidences like the fluffy nature of core top (Banakar et al., 2005) and the surface value of C_{org}

content i.e. 3.5% which corroborates the surface value of Prakash Babu et al. (1999) supports the inference of intact nature of core top. Considering the core top to be intact and preserved, a corrected ^{14}C age-depth model (Fig 3.11a) has been developed. This model is made by subtracting a constant value of the surface age from the ages obtained using best-fit line. This is equivalent to shifting the best-fit line by 6073 yr towards origin of the age axis, without changing its slope (see Fig 3.11a). The corrected ^{14}C age-depth model is very close to the model obtained from the earlier approach using oxygen isotopic global events at 21kyr, 13kyr and 11kyr (see Fig 3.11b). All these observations suggest redeposition of older carbonate throughout the core depth (Holocene as well as pre Holocene) except at two intervals i.e. 157-165 and 267-271 cm. This is in contrast to the earlier records which suggests reworking during periods of low sea level stand (Rao and Wagle, 1997; Guptha et al., 2002).

Mechanism controlling the redeposition of older carbonates

To document the mechanism for the resuspension of these carbonates, we have compared bulk ^{14}C age (along with the discarded ages) with the $\delta^{18}O$ record. The comparison is shown in Fig 3.12a, b. It seems from Fig 3.12a, b that the bulk ^{14}C age at two depth horizons (157-165 and 267-271 cm) which deviates from the linear trend coincides with the Younger dryas and LGM (already discussed in section 3.4.1). Records of Sarkar et al. (2000b) and Tiwari et al. (2005a and the reference therein) suggest that the $\delta^{18}O$ of surface dwelling planktic foraminifera bears the signal of E-P budget owing to the summer monsoon precipitation and its associated surface runoff. Thus, the higher $\delta^{18}O$ value during these periods, which is also recorded by the earlier

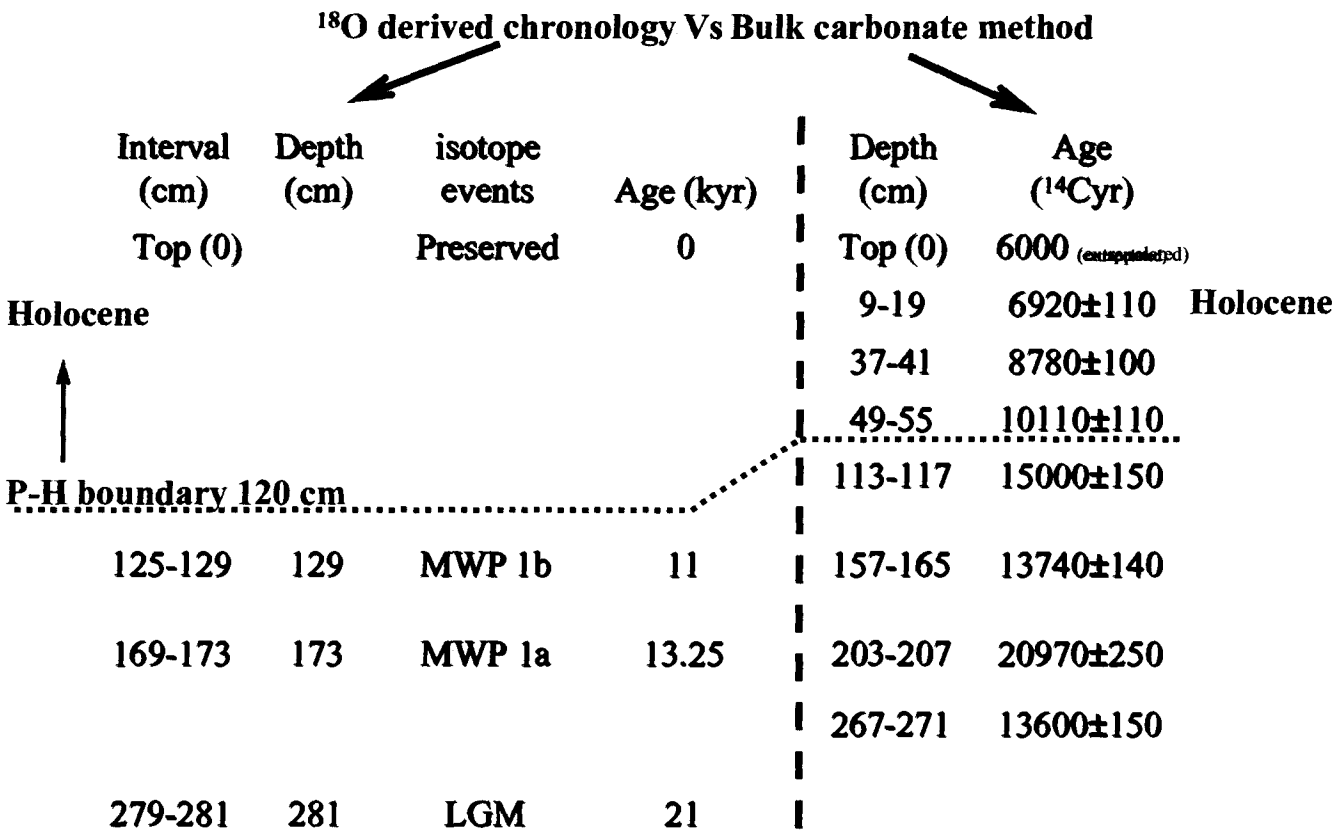

Bulk carbonate dates is showing older age compared to the isotope derived age hence inconsistency between both the technique.

Fig 3.10. A comparison between $\delta^{18}O$ derived and bulk carbonate (^{14}C) derived chronology. Note: bulk carbonates ^{14}C dates is showing comparatively older ages.

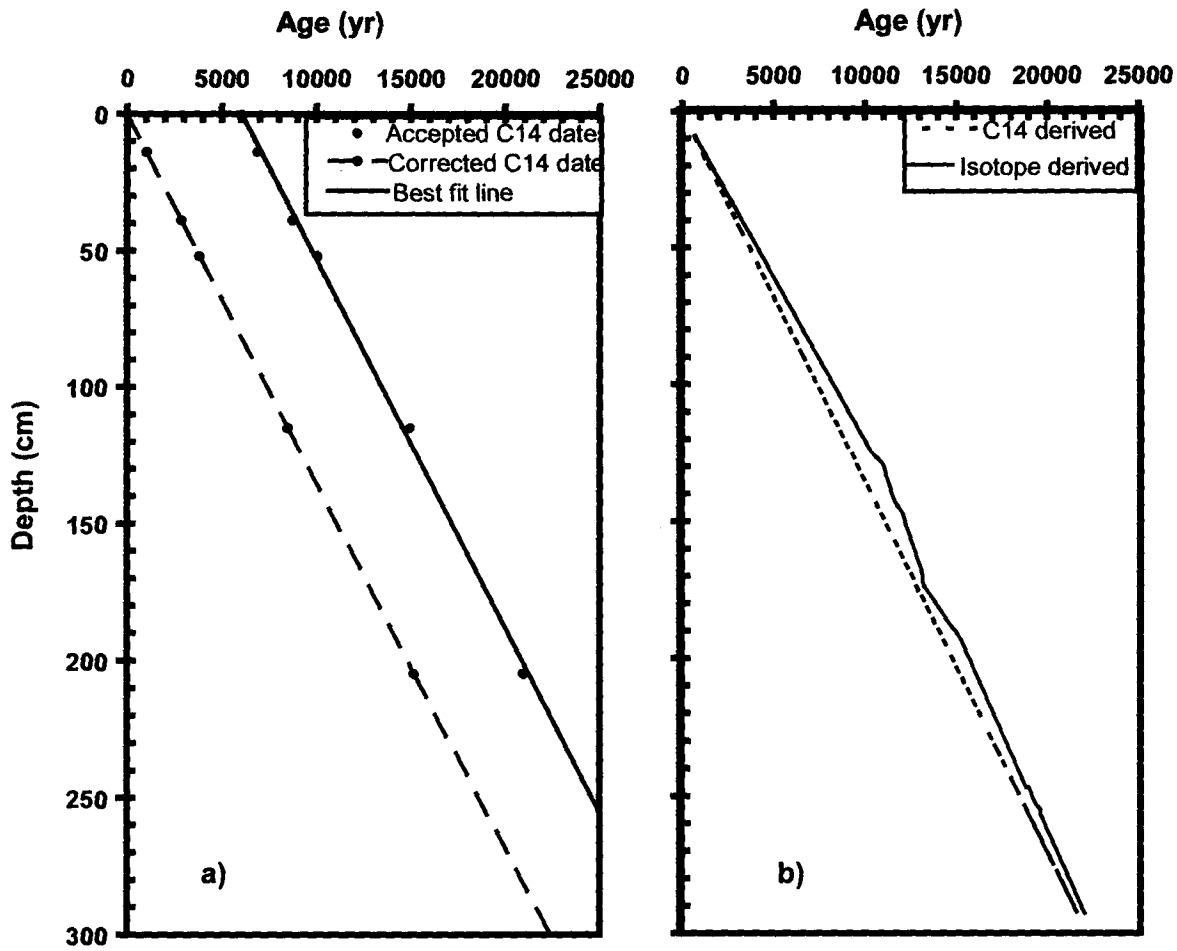

Fig 3.11 a) Age depth plot of five accepted radiocarbon dates (two were discarded and not shown in this figure) along with the corrected C-14 dates for core SK-172 b) a comparison between C-14 and isotope based chronology.

works (Duplessy, 1982; Sarkar et al., 2000a; Chodankar et al., 2005, Tiwari et al., 2005b, Tiwari et al., 2006b), reflects the reduced intensity of summer monsoon precipitation and runoff. The reduced runoff due to reduced precipitation (seen in the isotopic signature) could have decreased the runoff carrying land/marine derived older carbonates. This might have increased the relative fraction of carbonate from foraminifera containing contemporary radiocarbon, therefore, deviating towards younger ages. Or in other words, due to the reduced supply of older carbonates these sections are not showing older ages (i.e. falling away from the linear trend) as compared to the other five sections. The older ages for the other five sections (i.e. falling on the line) could be attributed to the enhanced fluvial activity owing to the strengthening of SW monsoon which in turn could have brought the run-off carrying land/marine derived older carbonates [the older carbonates is reported near the proximity of study area (Wagle et al., 1994; Merh, 1995; Vora et al., 1996; Rao et al., 2003)] to the core site directly or indirectly through monsoon currents (Shetye et al., 1994). Our results of resuspension of older/ terrestrial carbonate in the northeastern Arabian Sea is in line with the reports of Rao and Wagle (1997); Bhushan et al. (2001); Anil et al. (2005).

3.6.2 Resuspension of carbonates during LGM-early deglacial period witnessed by the Southeastern Arabian Sea core (SK 177/11)

From Fig 3.13 c, d it is evident that during 23-15 kyr silt and silicic fraction remained low with lowest value at 21 kyr which corresponds to LGM when the sea level was lower than the present sea level (Rao et al., 2003) in the Quilon-Cape Comorin region. Such discrepancy of low detrital material (except clay content) in spite

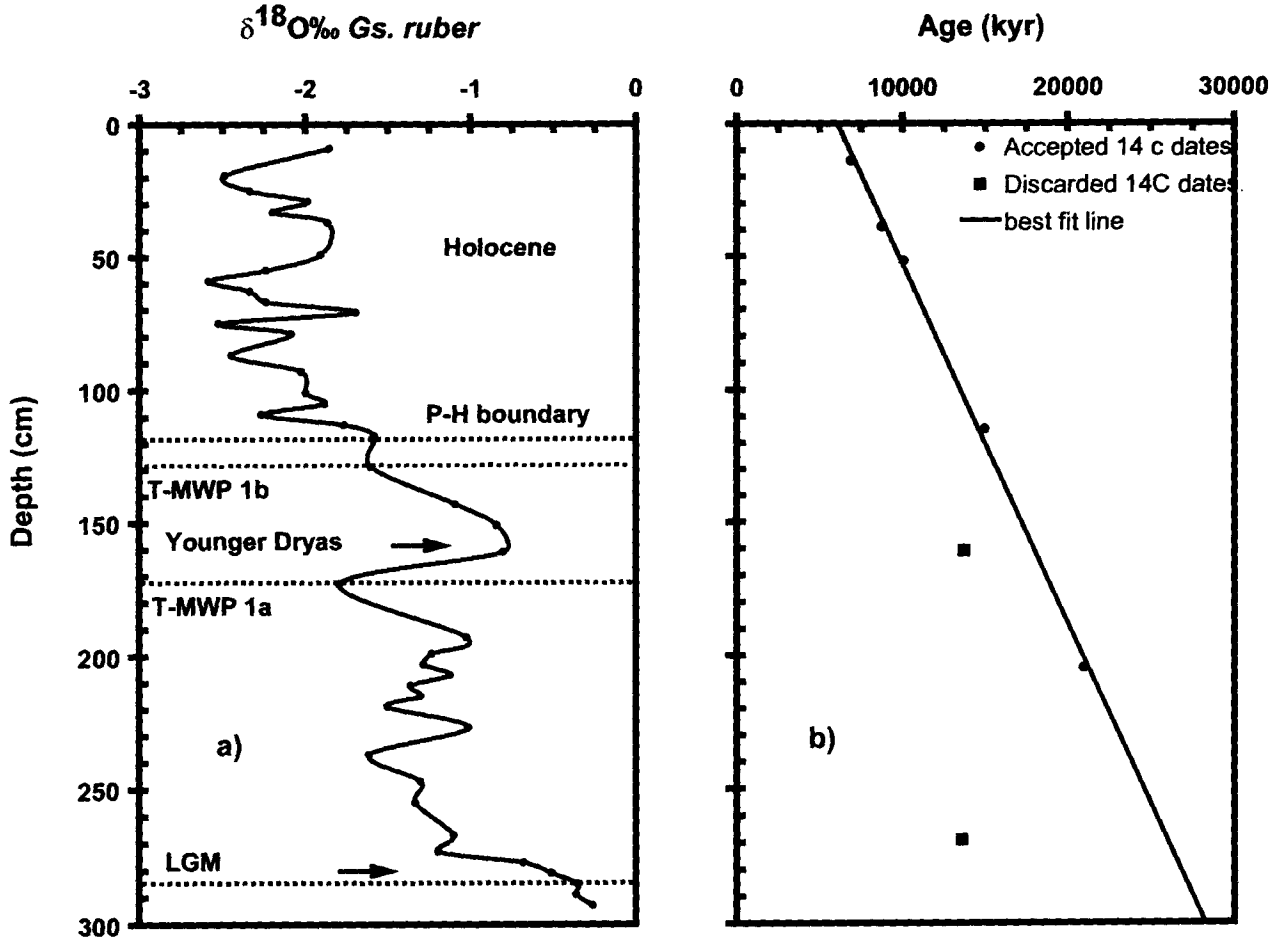

Fig 3.12. a) $\delta^{18}O$ variation of *Gs. ruber* showing dry periods marked with arrow. The dashed lines are the base for chronology. b) Age-depth model using seven radiocarbon dates on bulk sediments. Note: the discarded ages shown by filled squares coincides with the dry periods.

of exposed shelf indicates a reduced strength of erosion because of weakened SW monsoon. However, the clay content is not showing significant variation, which indicates the contribution from Warkala beds (ferruginous sandstone with clay intercalation). Clay being finer in size gets transported further offshore to the deposition site. Apart from this, one can argue that the clay minerals came from dust, as the climate was arid during this period. But this possibility can be ruled out by seeing Fig 3.13 c, d where the silicic fraction is lowest and the variation in clay content is not significant to suggest any change in provenance. This inference is also supported by the study of Kessarkar et al., 2003 that has denied any change in provenance or transport pathway through glacial interglacial time periods.

The low organic carbon during this period (see Fig 3.13a) possibly indicates towards the decreased overhead productivity due to a weaker SW monsoon (Prell et al., 1992; Sarkar et al., 2000a; Sirocko et al., 2000). On the contrary, records have also indicated increased overhead productivity during this period owing to stronger NE monsoon (Sonzogni et al., 1998; Cayre and Bard, 1999; Thamban et al., 2001). However, from this proxy alone it is not possible to ascertain whether NE monsoon was strong or weak because there could be a possibility that the overhead productivity has increased but not preserved due to low silicic fraction. But the low detrital input during this period certainly indicates weaker SW monsoon. On the other hand total carbonates and sedimentation rate (see Fig 3.13b, e) shows increasing trend which suggests the dominance of carbonate phase during this period. The dominance of carbonate phase in this time slice probably represents reworking/ resuspension from the pre-existing relict

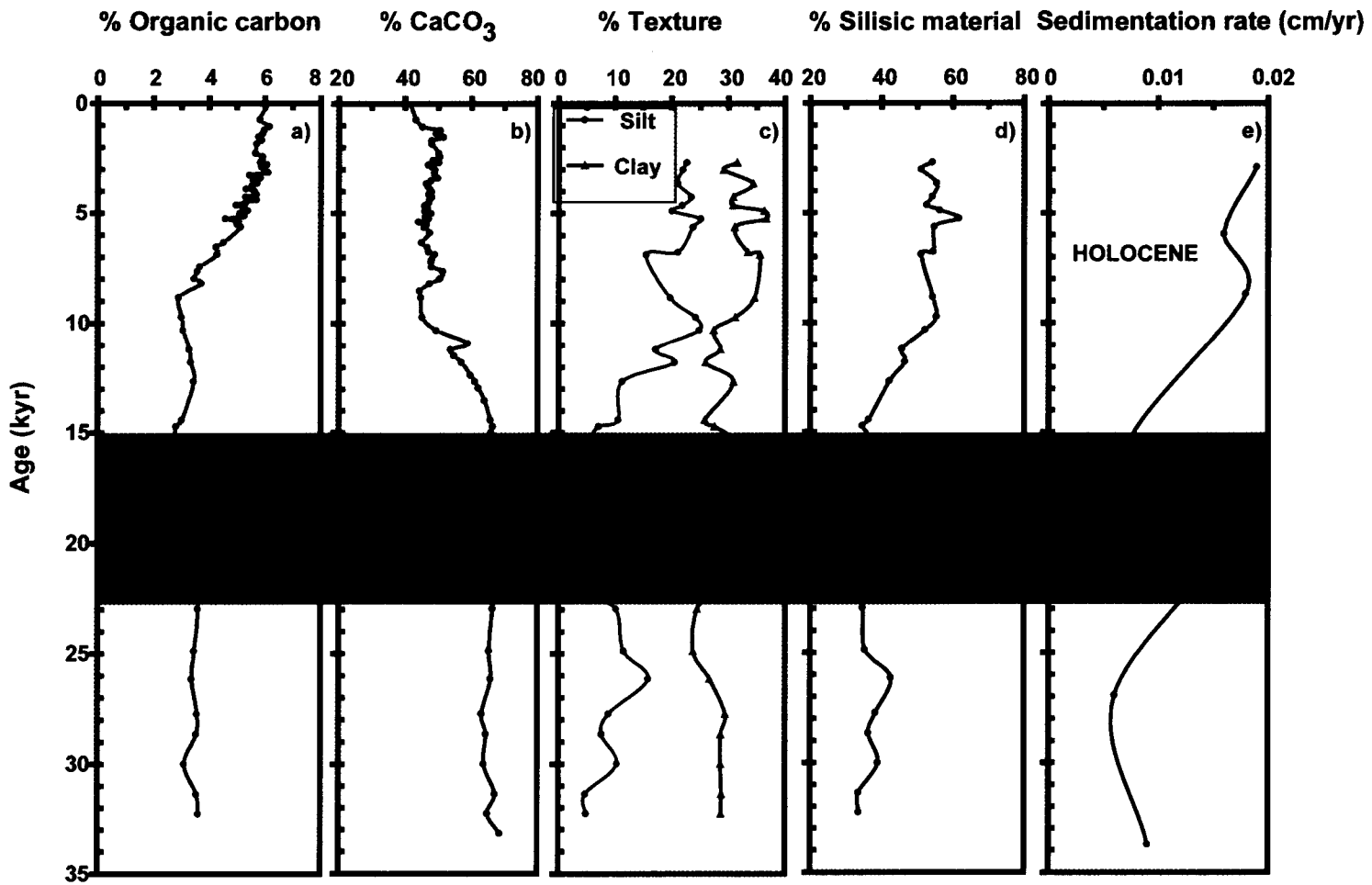

Fig 3.13 Variation in a) organic carbon, b) $CaCO_3$, c) texture, d) % silisic material and e) sedimentation rate (cm/yr) for the core SK-177/11. The dashed line represents LGM. Note: increase in sedimentation rate and the $CaCO_3$ in the shaded region.

carbonate lithofacies situated between Quilon and Cape Comorin (Rao and Wagle, 1997). This fact is supported by two reasons – firstly, the sedimentation rate which has increased abruptly is not reflected in the concentration of silicic material rather it has decreased. Secondly, the coarse fraction study shows some nodular aggregates with encrusted foraminifera and broken fragments of microfossils as shown in Fig 3.9 a, b and c.

3.7 Implication

Studies from the northeastern Arabian Sea have reported reworking/ redeposition of sediments mainly carbonates from the carbonate platform to the adjacent continental slope off Saurashtra (Rao and Wagle, 1997). They attributed low sea level stand to be the main reason for such reworking. In the present investigation using a sediment core off Goa (SK-172), we have reported reworking/ redeposition of older carbonates throughout the core (Holocene as well as pre-Holocene) due to which the ^{14}C dated section (bulk carbonate) shows an apparent age (older ages). We also report that the enhanced fluvial discharge owing to the intensity of SW monsoon could be a probable mechanism for the redeposition of older carbonate (terrestrial or relict carbonates) to the core site. Hence it is suggested from this study that the usage of bulk ^{14}C dating technique pertaining to palaeoclimatic study and carbonate content for the palaeoproductivity determination needs careful attention especially from the northeastern Arabian Sea.

Similarly, proxy records of core SK-177/11 from the continental slope off Quilon shows extensive carbonate deposition during LGM- Early deglacial period

attributed to the slumping/redeposition/resuspension from the outer shelf relict zone (discussed in section 3.6.2). However the exact mechanism for slumping could not be assessed from this study but records from the nearby region i.e. off Lakshadweep has reported slumping of sediments (Shankar and Manjunatha, 1995) for which they attributed Pleistocene-Holocene transgression (sudden sea level rise) to be the main reason.

All these observations from the northwestern as well as from the southwestern continental margin possibly show that the low sea level stand in combination with the enhanced fluvial strength could have caused the redeposition of sediments especially the carbonates. Such kind of study will help palaeoclimatologists to adopt a specific strategy while working with the samples from such zones.

CHAPTER 4

SEDIMENTOGY AND GEOCHEMISTRY OF THE LATE QUATERNARY

4.1 Introduction

Various literature pertaining to the late Quaternary climate reconstructions from the sediments of Arabian Sea, specially the western Arabian Sea focus on the summer monsoon wind strength and its associated biological productivity (Zonneveld et al., 1997; Gupta et al., 2003). These studies suggest that during the last glacial maximum (LGM) the thick ice cover over Tibetan highland has decreased the thermal gradient between land and ocean resulting in reduced summer monsoon intensity. On the other hand, during LGM the northern and northeastern Arabian Sea exhibits higher biological productivity owing to the stronger winter monsoon (Von Rad et al., 1999a & b; Schulz et al., 1998). Unlike the western Arabian Sea where the summer monsoon winds directly control upwelling, the intensity of upwelling in eastern Arabian Sea decreases from south to north (Shetye et al., 1994). During winter monsoon, convective mixing and its associated productivity occur north of 15^0N. Available records from the eastern Arabian Sea suggest that apart from the surface productivity, organic carbon content, a conventional proxy for productivity is also controlled by other factors like OMZ intensity, sedimentation rate, texture etc (e.g. Sarkar et al., 1993; Agnihotri et al., 2003; Pattan et al., 2003). Similarly, calcium carbonate (proxy for productivity) is also affected by many factors like dilution/ reworking from older carbonates (see Chapter 3) etc. Therefore, a linear model of wind strength, upwelling and productivity cannot be directly applied to this region. Records from the southeastern/ equatorial Arabian Sea however, suggest significant reduction in summer monsoon intensity and productivity during LGM (e.g. Agnihotri et al., 2003; Tiwari et al., 2006c).

In addition to the wind induced upwelling and productivity, summer monsoon results in heavy precipitation over the south Asia which brings large amount of sediments from the adjacent hinterland along with the numerous streams, channels and rivers. Thus, attempts have been made by many researchers to reconstruct palaeoclimatic conditions by using bulk sedimentary and clay mineral proxies specifically from the precipitation dominant eastern and northern Arabian Sea (e.g. von Rad et al., 1999a & b, Lückge et al., 2001; Thamban et al., 2002, Agnihotri et al., 2002, 2003). Proxies utilized include varve thickness (Agnihotri et al., 2002), abundance of specific clay minerals i.e., kaolinite (Thamban et al., 2002), bulk elemental concentration i.e., Al (Agnihotri et al., 2002, 2003) etc. These studies suggest that the varve thickness, specific clay mineral percentage, Al concentration are directly related to the monsoon induced fluvial sediment input, continental humidity and fresh water discharge, respectively. Based on these findings researchers have deciphered various wet and dry periods covering the entire late Quaternary. All these records indicate that the monsoon not only affects hydrography but also the sediment dispersal pattern through various oceanographic and geological processes. However, the data from the eastern Arabian Sea is very limited in this context as compared to the data from western and northern Arabian Sea. Therefore, the present study attempts to decipher the past variability of monsoon using the bulk properties of sediment from the eastern Arabian Sea.

4.2 Variation in organic carbon, calcium carbonate and its relation to surface productivity

The Indian monsoon is one of the most important features of tropical climate characterized by the seasonal reversal in wind pattern i.e., in summer and winter monsoon wind blows from southwest and northeast, respectively, thus also called as southwest and northeast monsoon. The seasonal reversal of winds over the Arabian Sea not only cause a change in the surface circulation and hydrography but also in the biological productivity. However, the different basins of the Arabian Sea respond differently to this changing wind pattern. During summer monsoon the wind induced surface biological productivity as well as organic carbon flux to the sea floor is reported to be the maximum in the western Arabian sea as it causes intense upwelling off Somalia and Oman (Prell et al., 1990; Clemens et al., 1991). The northern, northeastern and the region north of 15^0N of Arabian Sea shows high productivity during the winter monsoon due to the convective mixing and mixed layer deepening (Madhupratap et al., 1996; Kumar and Prasad, 1996). On the contrary, during summer monsoon eastern Arabian Sea experiences moderate upwelling (Shetye et al., 1994) and high productivity in the south (Bhattathiri et al., 1996), the intensity of which decreases from south to north. Based on these differences in upwelling dynamics, the eastern Arabian Sea can be divided into two Zones, as Zone-1 and 2 (see Fig 4.1) where present day productivity is controlled by winter and summer monsoons, respectively. At variance to this, time series sediment trap study of Haake et al. (1993) reported high interannual variation of particle fluxes during the winter monsoon suggesting its important role over eastern Arabian Sea. Thus, the Indian monsoon (summer and

winter) is critical for understanding the carbon budget of the tropics as it may directly influence the global climate through CO_2 sequestration.

In the eastern Arabian Sea, the deposition of organic carbon rich sediments is explained by two mechanisms, viz., production hypothesis (Pederson and Calvert, 1990, Prakash Babu et al., 1999) and the preservation hypothesis (Paraopkari et al., 1993). The production hypothesis suggests that organic carbon in the sediments of Arabian Sea is primarily controlled by the surface overhead productivity due to the summer/ winter monsoon induced mixed layer deepening/ convective mixing (e.g. Thamban et al., 2001; Agnihotri et al., 2003). This was also validated by sediment trap studies (Nair et al., 1989) and by surface sediment samples (Prakash Babu et al., 1999, 2002). Thus, it serves as a potential proxy to understand the palaeoproductivity variation and past variability of monsoon. However, other factors like sedimentation rate, texture, oxygen minimum zone etc play a secondary but important role (Paropkari et al., 1993; Thamban et al., 1997; Agnihotri et al., 2003). Similarly, calcium carbonate in the form of calcareous microorganisms, fluctuate during summer and winter monsoons. Microorganisms such as foraminifera and coccolithophores utilize nutrients for their growth; they produce calcitic shells as a protective covering for their soft body which ultimately reaches the sea floor after the death of microorganism. Hence, calcium carbonate also serve as an indicator for surface productivity (Tiwari et al., 2006c; Naidu and Malmgren, 1999) provided it is of marine origin and free from dissolution (i.e. the location of core should be above lysocline depth so that the dissolution will be negligible) and dilution from terrigenous inputs (Sirocko et al., 1993; Naidu et al., 1992).

In view of this, an attempt is made to understand and reconstruct the palaeoproductivity of the late Quaternary using three sediment cores, collected from different physiographic settings i.e. two from the continental slope i.e. SK-172, SK-177/11 and one from the topographic high i.e., SK-208. Moreover, the core locations also fall in different oceanographic settings of the eastern Arabian Sea (see Fig 4.1).

4.3 Sediment core from the continental slope (SK-172 and SK-177/11)

Sediment core SK-177/11 and SK-172 were collected from Zone 2 and Zone 1, respectively (see Fig 4.1). The demarcation of these zones is based on the present day response of eastern and northeastern Arabian Sea towards the winter and summer monsoon. In Zone-1 convective mixing occurs during winter monsoon (Kumar and Prasad, 1996) while in Zone-2, moderate upwelling occurs during summer monsoon, the intensity of which decreases from south to north (Shetye et al., 1994).

4.3.1 Geochronology

Core SK-177/11

The chronology of core collected from Zone-2 (see Fig 4.1) i.e., of the southeastern Arabian Sea is already discussed in Chapter 2 and 3. The age-depth model suggests that the age of this core (SK-177/11) extends up to ~35 kyr.

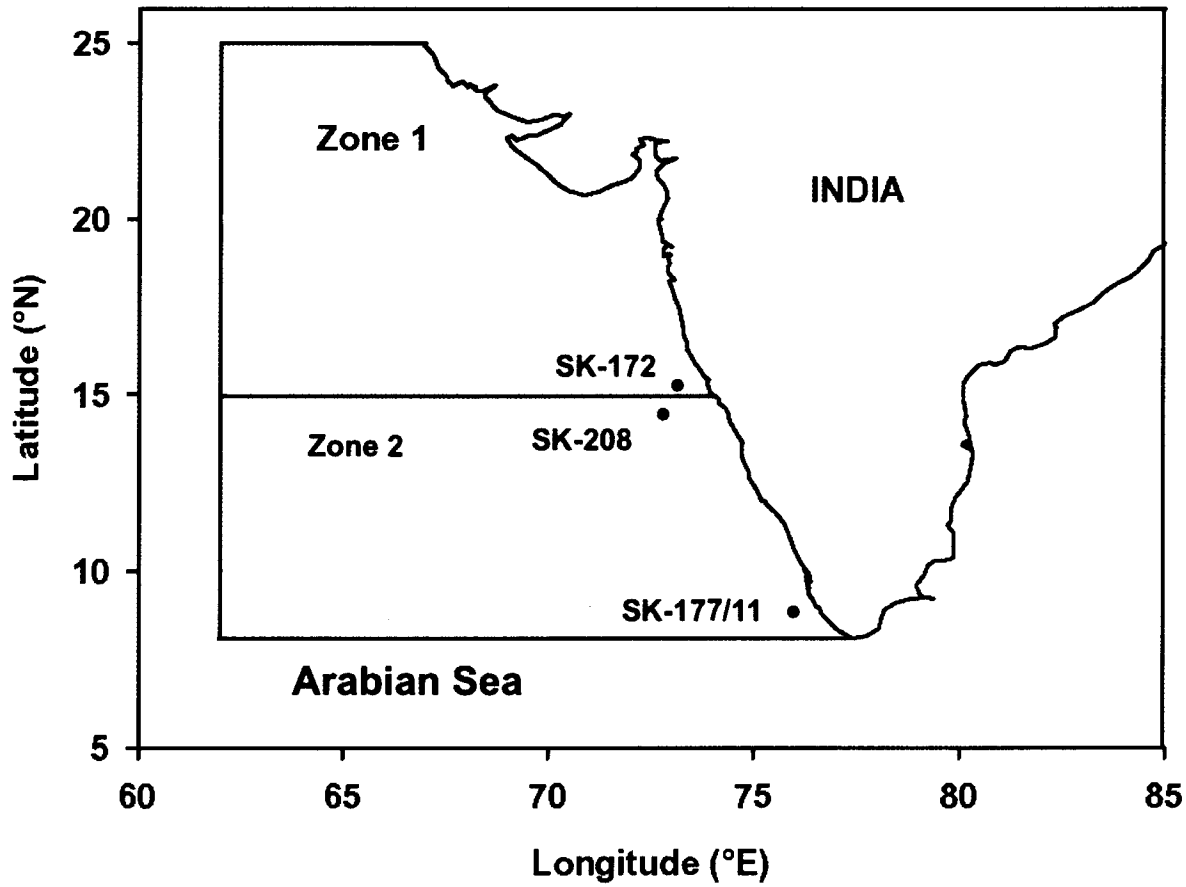

Fig 4.1 Showing locations of both the cores from eastern Arabian Sea. Based on the present day response of eastern and northeastern Arabian Sea towards the winter and summer monsoon, it is divided into 2 zones. In Zone-1 convective mixing occurs during winter monsoon (Kumar and Prasad, 1996) while in Zone-2, moderate upwelling occurs during summer monsoon, the intensity of which decreases from south to north (Shetye et al., 1994).

Core SK-172

The chronology of core collected from Zone-1 (see Fig 4.1) is based on isotope events inferred from $\delta^{18}O$ of planktonic foraminifera *Gs. ruber* and *Gs. sacculifer* (as discussed in Chapter 2 and 3) and accordingly, the age-depth model is constructed. The age-depth model suggests that the core extends up to ~22 kyr.

4.3.2 Textural, organic carbon and calcium carbonate analyses

Core SK-177/11

The sediment core spanning ~35 kyr is subjected to organic carbon and calcium carbonate analyses along with textural analysis. Results are discussed in the following sections.

Organic carbon: The variation in C_{org} content is shown in Fig 4.2 a. Organic carbon content fluctuates between a minimum of 2.5% to a maximum of 6%. During MIS 3 and MIS 2, C_{org} fluctuates between 3.5-2.7 % whereas during the Holocene it increases gradually from 3% to 6%.

Calcium carbonate: Calcium carbonate in Fig 4.2 b shows enrichment during MIS 2 and early MIS 3. From the later part of MIS 2 to early Holocene carbonate shows decreasing

trend i.e. it decreases from ~15 kyr with a value of 65% to 45% during early Holocene while in mid to late Holocene it increases gradually from 43% to 52%.

Texture: Variation of textural pattern (carbonate free) and silicic fraction shown in Fig 4.2 c, d suggest that the core is silty clay with average 30% clay and 12 % silt. Sand fraction being insignificant, is therefore neglected. Temporal variations of silt and silicic fractions show three distinct zones i.e. MIS 1 (12 kyr-present), MIS 2 (~25-12 kyr) and MIS 3 (~25-35 kyr). In MIS 1, silt and silicic fraction show an enrichment, whereas in MIS 2 there is a transition from low value to high value for both silt and silicic fraction with the lowest value at ~21 kyr (LGM). Below this section i.e. at MIS 3, silt and silicic fraction show an increasing trend peaking at 26 kyr BP. It is interesting to note that silicic fraction is largely controlled by silt because clay remained near constant throughout the age except in Holocene, where it shows a slight enrichment.

Sedimentation rate: Sedimentation rate taken from Pandarinath et al. (2004) is shown in Fig 4.2 e. It is evident from figure 4.2 e that sedimentation rate decreases during MIS 3 while it increases in MIS 2 peaking around ~19 kyr where it becomes comparable to that of the Holocene. However, a general trend of sedimentation rate shows increasing pattern during the Holocene.

Core SK-172

The sediment core spanning ~22 kyr is subjected to organic carbon, calcium carbonate and textural analyses and the results are discussed in the following sections.

Organic carbon: The downcore variations of C_{org} content is shown in Fig 4.2 f. The C_{org} content fluctuates between 1.5% to a maximum of 3.5%. The average value of C_{org} reported from the surface sediment of this region is between 2-4% (Prakash Babu et al., 1999) which is very well corroborated as the core top records 3.5% of C_{org} content. The downcore variation in C_{org} shows an increasing trend during Holocene (see Fig 4.2 f). The C_{org} content increases from 1.4% at 10 kyr to 3.3% at the core top while from 10-17 kyr it shows depletion with an average of 1.5%. Again from 17-20.5 kyr C_{org} shows slight enrichment with an average of 2%. However, the magnitude of C_{org} enrichment during this period is less than the late Holocene. During LGM the C_{org} content decreases to reach 1.3%.

Calcium carbonate: The downcore variation of $CaCO_3$ content is shown in Fig 4.2 g. The comparison between C-14 dates and isotope-derived dates suggest an uniform contribution of older/reworked $CaCO_3$ in this core (discussed in chapter 3; section 3.6.1). Even after removing the contribution of reworked $CaCO_3$ from the total $CaCO_3$, the resultant trend of insitu produced $CaCO_3$ will be similar. Thus, the total carbonate can be used as a proxy for palaeoproductivity. Following this approach, the total carbonate as shown in Fig 4.2 g is discussed in the following sections in terms of palaeoproductivity. From Fig 4.2 g, it is evident that the $CaCO_3$ varies between 15 and 30%, where it increases from 17% (at 10 kyr) to reach 30% during late Holocene. The section between 17-20.5 kyr also shows enrichment, which is almost comparable to the Holocene values. The overall trend of insitu produced $CaCO_3$ is similar to that of C_{org} content.

Texture: Textural analysis (without prior removal of carbonates) as shown in Fig 4.2 h suggests that the entire core is silty clay. During Holocene, sand and silt content show an increasing trend and clay shows a decreasing trend. Between 10 and 17 kyr clay content shows maximum and silt shows minimum value. During early deglacial period clay increases and silt decreases. In the entire core both silt and clay is inversely related to each other.

4.4 Sediment core from the topographic high (SK-208)

4.4.1 Geochronology of core SK-208

The chronology of core SK-208 is established from the oxygen isotope record ($\delta^{18}O$) of surface dwelling foraminifera i.e. *Gs. ruber* and *Gs. sacculifer*. This approach is based on the hypothesis that the carbonate shell of foraminifera precipitates in equilibrium with the surface seawater oxygen isotope composition ($\delta^{18}O$) or with a constant shift from equilibrium (Shackleton and Opdyke, 1973, Shackleton, 1974; Bouvier-Soumagnac and Duplessy, 1985). Thus, the change in surface sea water $\delta^{18}O$ composition during glacial interglacial transition is likely to be recorded in the form of foraminiferal $\delta^{18}O$. Therefore, the $\delta^{18}O$ of foraminiferal calcite can be used as a dating tool for delineating the glacial and interglacial periods, also called as "Marine Isotope Stages". In the present study, the potential of foraminiferal $\delta^{18}O$ as a dating tool is used for establishing chronology of core SK-208. The $\delta^{18}O$ record of *Gs. sacculifer*, *Gs. ruber* is correlated with the $\delta^{18}O$ record of standard SPECMAP curve (Imbrie et al., 1984) and 5 tie points were identified (Fig 4.3).

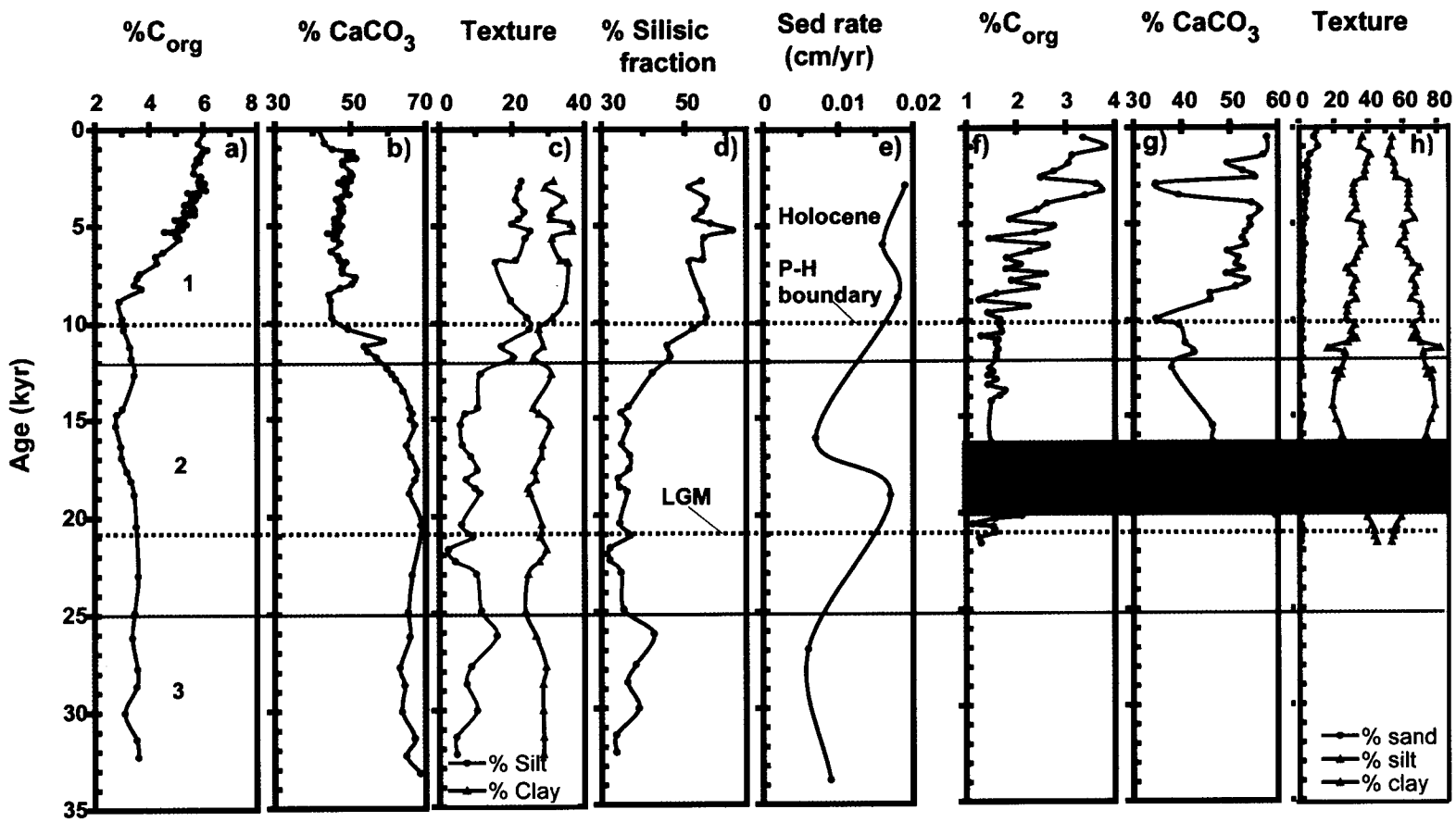

Fig 4.2 The left panel from a-e shows respective variation in organic carbon, calcium carbonate, textural analysis (carbonate free), d) % silicic fraction, e) sedimentation rate in cm/yr (adopted from Pandarinath et al., 2004) of core SK-177/11. The right panel from f-h shows respective variation in organic carbon, calcium carbonate and textural analysis of core SK-172. The cores SK-177/11 and SK-172 are collected from Zone-2 and Zone-1 respectively of the eastern Arabian Sea (for location details see Fig 4.1). Note: bold line represents the boundary between the isotope stages, the numbers indicate marine isotope stages and the shaded region in core SK-172 represents early deglacial period.

Based on these tie points, age depth model is constructed and shown in Fig 4.4. The average sedimentation rate calculated for SK-208 is 3 cm/kyr, which corroborates with the nearby core of Prabhu et al. (2004) and Paropkari et al. (1992).

The $\delta^{18}O$ record of *Gs. sacculifer*, *Gs. ruber* shows distinct fluctuations that are typical of glacial–interglacial periods and extends up to the MIS 5 (Emiliani, 1955). The $\delta^{18}O$ value varies between -2 to -0.4‰ and -1.5 to 0.7‰ for *Gs. sacculifer* and *Gs. Rubber*, respectively.

4.4.2 Texture, organic carbon and calcium carbonate variation

Variations in texture, organic carbon and calcium carbonate as shown in Fig 4.5 suggest that the sediments of SK-208 core are mostly composed of clay and $CaCO_3$ whereas C_{org}, silt fractions form a minor component. The downcore variation of silt does not show a significant variation except at MIS 2 and 100-90 kyr where it increases. The core top value of C_{org} (i.e. 2%) is found to be greater than the reported value of the surface sediments of this region i.e. <1% (Prakash Babu et al., 1999). C_{org} shows enrichment throughout the core depth except in early to mid MIS 1 where it decreases to a minimum value of 0.8%, and also shows a positive correlation with clay fraction suggesting a clay-organic interaction. On the other hand, $CaCO_3$ shows anticorrelation with organic carbon and clay fraction, which suggests a dilution from the silicic fraction (i.e. silt + clay fractions).

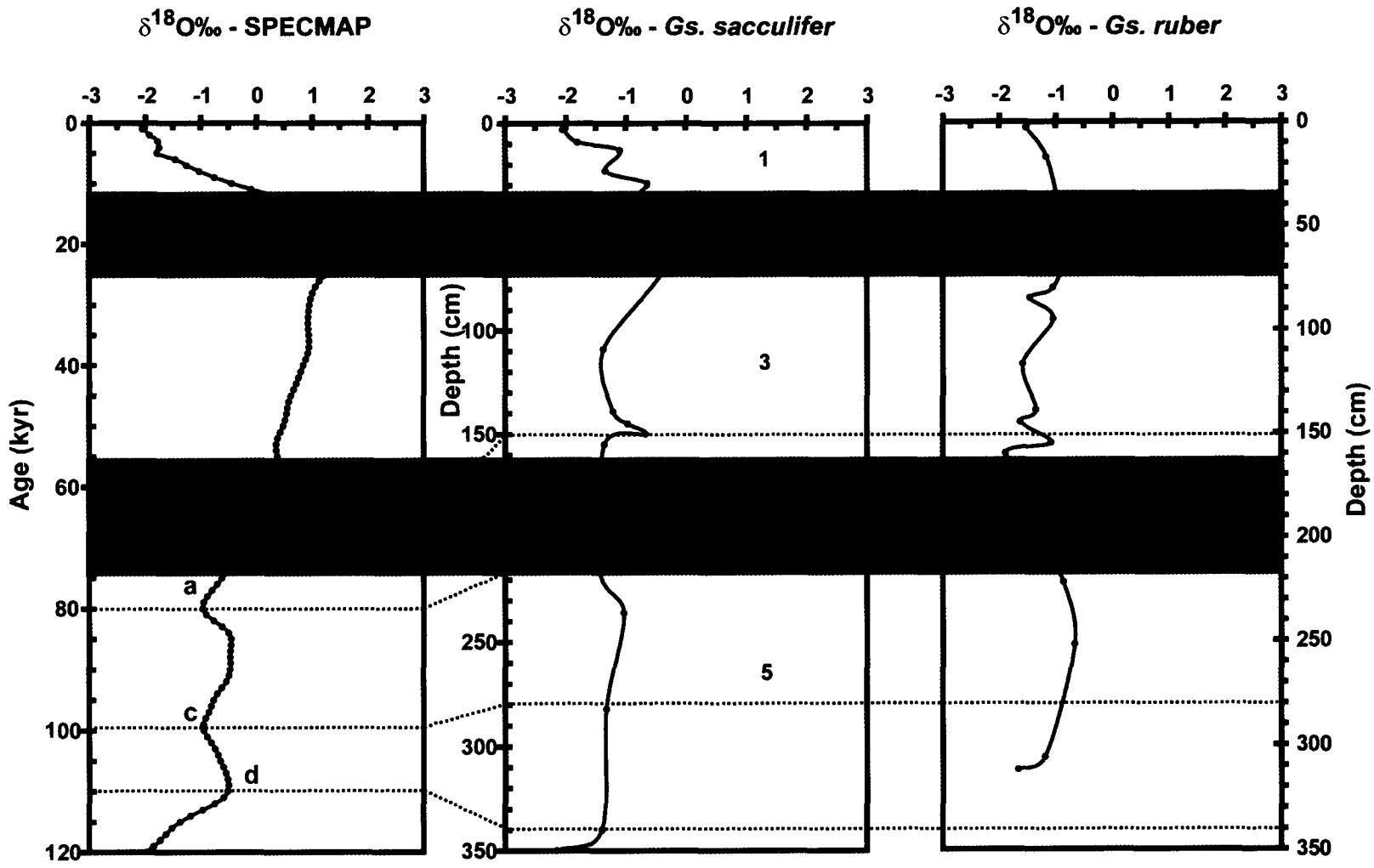

Fig 4.3. $\delta^{18}O$ stratigraphy of core SK-208 along with the SPECMAP stack. The dashed lines are the tie points based on which chronology is established. The numbers indicates marine isotope stages (MIS) and shaded areas represent glacial periods.

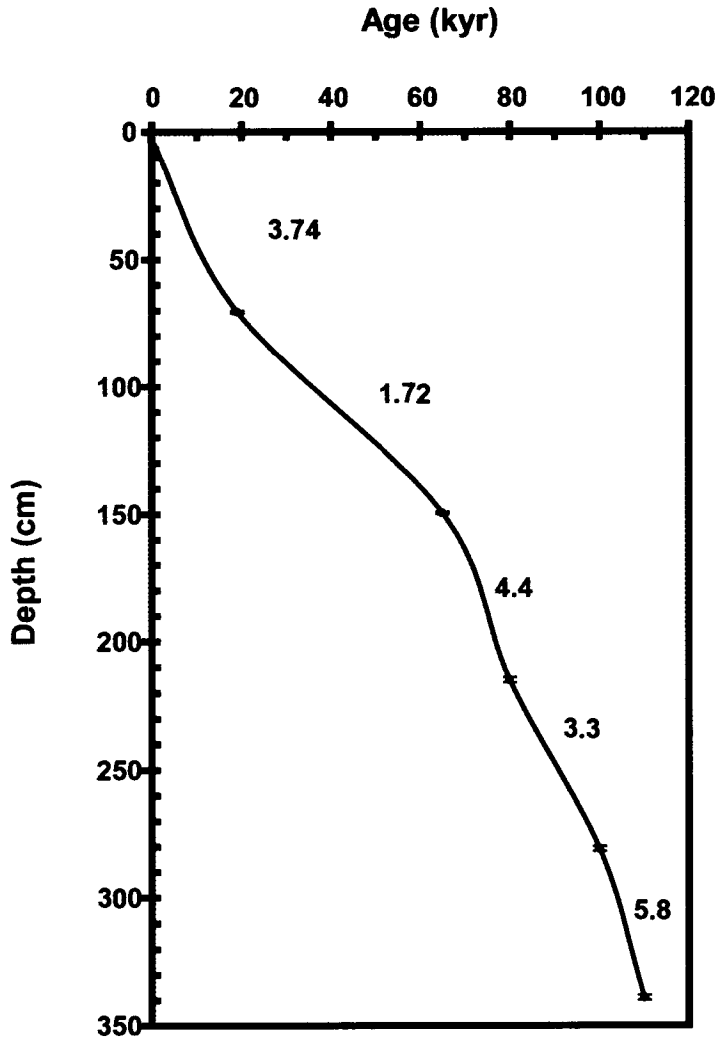

Fig 4.4 Age-depth model for core SK-208. The numbers indicates sedimentation rate in (cm/kyr).

The linear sedimentation rate (Fig 4.5) shows a maximum value of 5.8 cm/kyr during early MIS 5 (100-110 cm) whereas MIS 3 shows lowest rate of 1.72 cm/ kyr. During the mid MIS 4 (glacial period) sedimentation rate increases whereas it decreases in mid MIS 2. From the late glacial to present interglacial period (late MIS 2- MIS 1) the sedimentation increases to 3.7 cm/kyr.

4.5 Organic carbon, calcium carbonate deposition and its palaeoproductivity implications

4.5.1 Sediment cores from the continental slope

The sediment cores SK-177/11 and SK-172 were collected from the same physiographic settings (i.e. continental slope), however fall in different Zones (see Fig 4.1 and section 4.3). SK-177/11 in southeastern Arabian Sea was collected from Zone-2 where water column productivity, summer monsoon upwelling and the organic carbon in surface sediments were very well correlated (Prakash Babu et al., 2002 and the reference therein). These records suggest that the organic carbon in the southeastern Arabian Sea is primarily controlled by summer monsoon induced surface water productivity.

On the other hand, the core SK-172 was collected from Zone-1, where the present day convective mixing and its associated productivity were reported during winter monsoon (Kumar and Prasad, 1996, Madhupratap et al., 1996). Apart from this, the surface

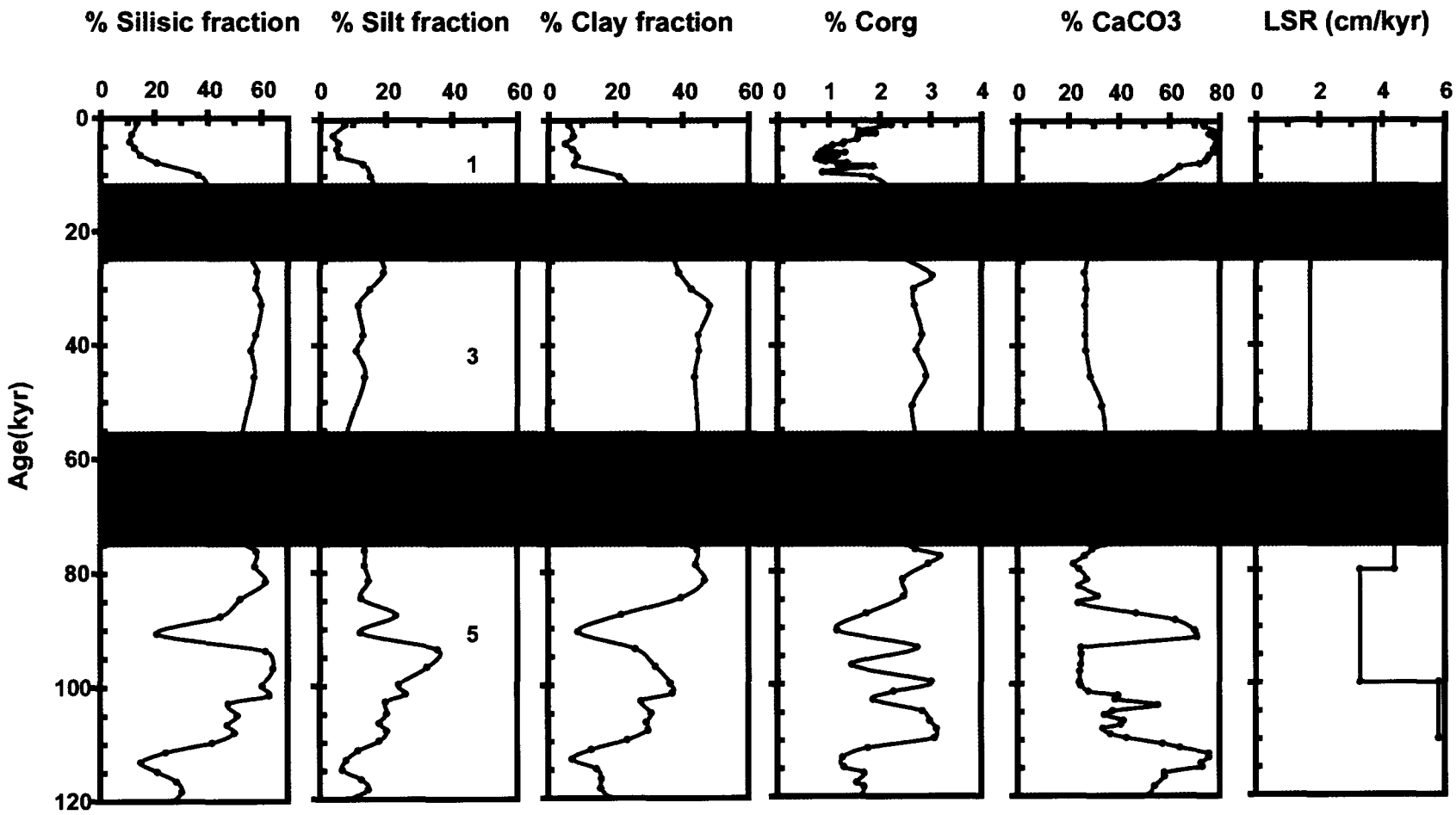

Fig 4.5. Variation in silicic fraction, silt, clay fraction, organic carbon and calcium carbonate content of core SK-208. The numbers indicate Marine isotope stages (Imbrie et al, 1984) and the shaded region represents glacial periods.

productivity in the Arabian Sea is also controlled by the mixed layer deepening owing to strong SW monsoonal winds (Nair et al., 1989).

All these records suggest that in the eastern Arabian Sea organic carbon is primarily related to the summer or winter monsoon productivity. Therefore, to reconstruct palaeoproductivity trend, the downcore variations of organic carbon and calcium carbonate are studied and discussed below.

A} MIS 3 (~35-25 kyr)

During MIS 3 (~35-25 kyr) the content of silt and silicic fraction of core SK-177/11 (see Fig 4.2 c and d) increases along with the calcium carbonate whereas organic carbon remained low through out the MIS 3 (see Fig 4.2 a and b). The enrichment in silt and silicic fraction suggests enhancement in SW monsoon, which may be due to intense strength of erosion caused by the increased surface runoff. The enhanced SW monsoon and its associated productivity during this period are corroborated by the oxygen and carbon isotope records of this core (as discussed in chapter 5, section 5.3.3 and 5.7.2). However, the low organic carbon despite increase in calcium carbonate indicates towards the poor preservation of organic carbon.

B} MIS 2

Last glacial maximum

During LGM, when the sea level was lower than the present (Fairbanks 1989, 1992), silt and silicic fraction of the core SK-177/11 (southeastern Arabian Sea; Zone-2) decreases to minimum (see Fig 4.2 c and d). Such discrepancy of low detrital material in spite of exposed shelf indicates towards the reduced strength of erosion as a result of weakened SW monsoon. Among the productivity proxies, organic carbon remained low during this period, whereas calcium carbonate shows reworking (more details are presented in Chapter 3; Section 3.6.2); hence not used for palaeoproductivity determination. This suggests decrease in the intensity of summer monsoon resulting in reduced productivity (Prell et al., 1992; Sarkar et al., 2000a; Sirocko et al., 2000). During LGM, the thick ice cover over the Tibetan plateau may have reduced the necessary thermal gradient between land and ocean resulting in a weaker summer monsoon.

The core SK-172 was collected from Zone-1, north of 15^0N where the present day convective mixing occurs due to strong NE monsoonal winds (Kumar and Prasad, 1996). On evaluating the present day response of Zone-1 (also the core site), the sea surface productivity is expected to enhance during LGM when high pressure is reported over Tibetan plateau favorable for the NE monsoon winds. Inspite of this, organic carbon (as shown in Fig 4.2 f) shows a minimum value suggesting a weaker NE monsoon. Our results of weakened NE monsoon is in agreement with the records of Tiwari et al. (2005b). Their

studies revised Sarkar et al., (1990) and suggested that despite the favorable high pressure over Tibetan plateau, the NE monsoon has not gained strength due to the lowered SST in the surrounding ocean (Rostek et al., 1993), thereby reducing the necessary pressure contrast. Thus the low organic carbon during LGM (21 kyr) could be attributed to the reduced productivity owing to the reduced intensity of NE monsoon.

Deglacial period

Due to the reworking and resuspension of carbonates from LGM-early deglacial periods in the core site SK-177/11, it cannot be used as a proxy for productivity (Verma and Sudhakar, 2006).Whereas, the low organic carbon that suggests low productivity is in agreement with the estimated foraminiferal $\delta^{13}C$ of the same core (discussed in Chapter 5; Section 5.7.2). However, the core SK-172 shows enrichment in organic carbon along with the calcium carbonate (see Fig 4.2 f, g). During this period the intensity of SW monsoon was weak due to the significant ice cover over the Tibetan plateau which has disappeared only after termination 1 a (16-18 kyr) (Tiwari et al., 2005b and the reference therein; Singh et al, 2006). The presence of considerable ice cover coupled with the early deglacial warming of the northern Indian Ocean (Rostek et al., 1993) could have established the necessary pressure gradient for NE monsoon. Thus the enrichment of organic carbon and calcium carbonate during this period could be attributed to the convective mixing caused by the intensification of NE monsoon. The results of increasing strength of NE monsoon during early deglacial period are in line with the reports of Tiwari et al. (2005b).

Unlike the core SK-172, the intensification of NE monsoon and its associated productivity is not seen in the southeastern Arabian Sea core SK-177/11. This suggests that similar to the present day, the NE monsoon and its associated productivity during deglacial period was limited to the northern part of eastern Arabian Sea because of the favorable SST and SSS conditions.

C} MIS 1

Holocene

With the completion of deglacial phase the thermal gradient between land and ocean has began to establish resulting in an enhanced SW monsoonal winds. This could have injected nutrients into the euphotic zone through wind mixing (Nair et al., 1989, Ramaswamy and Nair, 1994) or upwelling which is prominent in southeastern Arabian Sea (Shetye et al., 1994). Phytoplankton, microorganisms that utilize these nutrients for their growth, finally contribute to the pool of sedimentary organic carbon and calcium carbonate. This phenomena of ocean-wind interaction is very well reflected in the present study where the organic carbon content of both the cores, i.e., SK-177/11 and SK-172 reflect increase from 3 to 6% and 1.5 to 3.8%, respectively (Fig 4.2 a, f). A comparative enrichment of organic carbon in southeastern Arabian Sea core collected from Zone-2 (SK-177/11) is in agreement suggesting water column productivity is comparatively high in this region (Qasim, 1982; Bhattathiri et al., 1996).

During this period calcium carbonate of core SK-177/11 shows absence of reworking (as inferred from the absence of calcareous aggregates from the coarse fraction which was common in the sections of LGM-early deglacial period, discussed in Chapter 3; Section 3.6.2). Similarly, carbonates of SK-172 core site can also be considered for palaeoproductivity determination as the concentration of reworked carbonate is constant throughout the core depth (discussed in Chapter 3; Section 3.6.1). Evidently, during Holocene, the enrichment of these carbonates in core SK-177/11 and SK-172 as seen from Fig 4.2 b and g, respectively show an enhancement in productivity as a result of SW monsoon.

The enhancement in the intensity of SW monsoon during Holocene is also corroborated by the detrital input of core SK-177/11 (Fig 4.2 c, d) that could have brought down to the core site by numerous monsoon fed rivers, streams and channels prevailed in the region.

The observations from both these cores suggest that during the Holocene increased concentration of organic carbon, calcium carbonate along with the silicic fraction and sedimentation rate (see Fig 4.2) is an artifact of southwest monsoonal intensity leading to nutrient injection into the sea surface through wind mixing processes and erosion, its subsequent deposition by fluvial processes. These results of strengthening of south west monsoon during Holocene are consistent with the earlier reports (Van Campo et al., 1982; Van Campo, 1986; Naidu, 1998; Sarkar et al., 2000a; Thamban et al., 2001; Agnihotri et al., 2003; Singh et al., 2006).

4.5.2 Sediment core from the topographic high

Unlike the other two cores (SK-177/11 and SK-172), core SK-208 was collected from a different physiographic setting i.e., from the topographic high of central Arabian Sea. The core has been analyzed for organic carbon, calcium carbonate and textural analyses and the results are discussed hereafter.

A} The glacial periods MIS 2 and 4

The organic carbon shows enrichment in glacial sections and throughout the core depth it is positively correlated with the clay fraction (see Fig 4.5). Proxy records of Thamban et al. (1997 and the references therein) suggested that on the topographic high, texture (fine grained sediments) along with productivity plays an important role in organic carbon enrichment. The independent estimation of $\delta^{13}C$ of foraminiferal calcite from this core (discussed in Chapter 5; Section 5.7.1) suggests increase in productivity during glacial period. Hence, in the present study the organic carbon enrichment is controlled both by productivity and texture through the adsorption onto the clay particles. The increase in productivity during glacial period is also correlated with the results of a nearby core studied by Prabhu et al (2004) and (2005). Moreover, carbonate is not used in this study for palaeoproductivity determination because of the negative correlation between carbonate and siliciclastic fraction which suggests dilution.

B} The interglacial periods MIS 5, 3 and 1

During interglacial periods MIS 5 and 3, organic carbon and siliciclastic sediments specially the clay fractions show enrichment, whereas in MIS 1 they decrease to minimum. The $\delta^{13}C$ record from the same core (discussed in Chapter 5; Section 5.7.1) suggests decrease in productivity during interglacial periods. Thus the enrichment of organic carbon during MIS 5 and 3 and depletion during MIS 1 can be explained by the preservation alone.

4.6 Clay mineralogy of core SK-172 and SK-208

Clay minerals are the weathered products of soil and rocks, the composition of which depends on climate, geology and topography of the catchment area, therefore can be used as a potential tool for provenance, palaeogeography and palaeoclimatic reconstruction (Sirocco and Lange, 1991; Pant, 1993; Dilli and Pant, 1994). Following this, researchers have established and validated kaolinite and K/I ratio as a proxy for continental humidity (Chamely, 1989) whereas illite along with chlorite represents physical weathering process (Rao and Rao, 1995), hence reflect the continental aridity. Based on this, various records suggest that the clay mineral assemblage of the western continental shelf of India mainly reflects the palaeoclimatic conditions (Thamban et al., 2002; Kessarkar et al., 2003; Anil kumar et al., 2005). Clay mineral distribution of continental shelf shows three distinct sources, i.e., the Indus province, Deccan trap province and Gneissic province in the northern, central and southern part of the adjacent hinterland, respectively (Rao and Wagle,

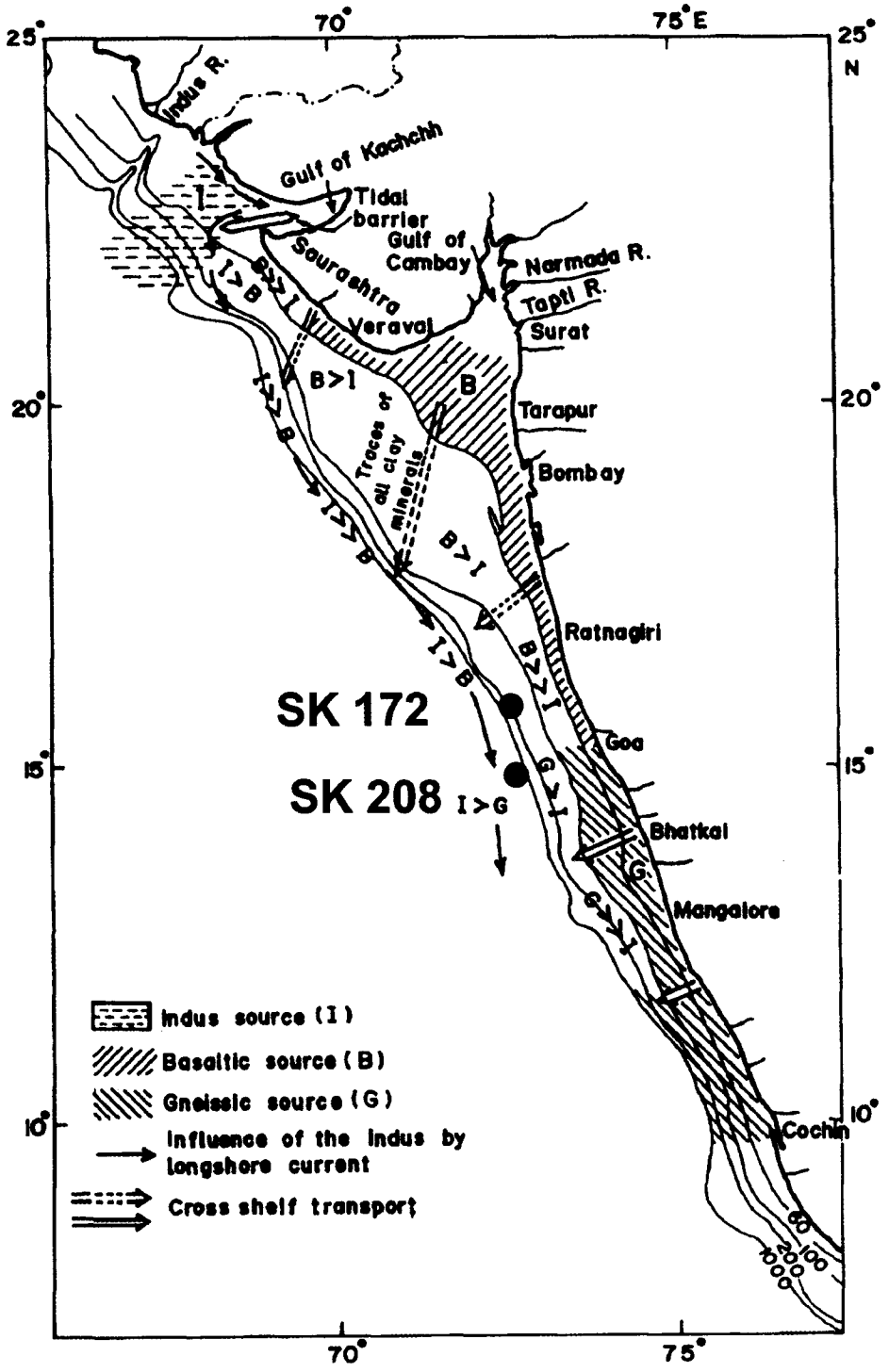

Fig 4.6. General distribution of sediments and surface currents in the study region along with the location of core (modified after Rao and Rao, 1995).

1997 and the reference therein). The continental slope between Saurashtra and Goa contains admixtures of clay derived from the Indus and Deccan trap provinces (Thamban et al., 2002 and the reference therein) and to the further south influence of Indus borne clay decreases which suggests decreasing influence of SW monsoonal currents (Rao and Wagle, 1997 and the reference therein). However, further offshore it dominates in the clay sediments (Rao and Rao, 1995). Therefore to understand the clay dispersal pattern two cores SK-172 and SK-208 as shown in Fig 4.6 were studied and discussed in terms of palaeomonsoonal/palaeoclimatic variability.

4.6.1 Clay mineral assemblage and its palaeoclimatic implications

Sediment core from the slope (SK-172)

Core SK-172 was collected from continental slope off Goa (see Fig 4.6) that represents the admixture of Indus borne and Deccan derived clay minerals. Clay mineral assemblage as shown in Fig 4.7 suggests an overall dominance of smectite and illite with and average of 35% along with the considerable amount of kaolinite (~25%). Chlorite occurs in insignificant amount. Smectite content along with the smectite to illite (S/I) ratio shows a minimum during the LGM whereas it increases around 3 to 4 kyr. Kaolinite and kaolinite to illite (K/I) ratio show a similar trends to that of smectite and S/I ratio during the LGM. Illite on the other hand shows enrichment during the LGM. Thamban et al. (2002) suggested that besides Himalayan source, illite also shows hinterland characteristics especially in the sediments off Goa. Illite chemistry and crystallinity, which is used for

ascertaining provenance is not assessed in this core. Therefore variation of kaolinite is used to decipher the intensity of continental humidity and aridity, based on which the palaeomonsoonal history is deciphered and shown in Figure 4.7 (as bold and dashed arrows).

Last Glacial Maximum

It is evident from Fig 4.7 that among the clay mineral assemblage, the LGM section is marked by the enrichment in illite and depletion in smectite, kaolinite and chlorite. The reduced supply of smectite; along with the decrease in humidity proxies like kaolinite, K/I ratio, suggests the prevalence of aridity in the catchment area. The clay mineral record suggests continental aridity during LGM which is attributed to the weakening of the SW monsoon. The inference of reduced strength of SW monsoon corroborates with the results of Chodankar et al. (2005) and Tiwari et al. (2006 b).

Deglacial period

The period between 14.8-~14 kyr is marked by the increase in humidity proxies like kaolinite content and K/I ratio along with the decrease in aridity proxy like smectite and S/I ratio (see Fig 4.7). This suggests a commencement of humid interval leading to the intense chemical weathering on land and hence enhances the formation of kaolinite. However illite does not show much variation during this period. The results of an early

intensification of the SW monsoon is in agreement with the earlier reports of Sirocko et al. (1993), Thamban et al. (2001, 2002) and Tiwari et al. (2006).

Younger Dryas chronozone

From Fig 4.7 it is evident that during Younger Dryas, clay minerals record suggests continental aridity as it shows decrease in the kaolinite and K/I ratio with an increase in illite, smectite and chlorite contents. Thus it is likely from these records that the intensity of SW monsoon was greatly reduced during this period probably due to the rebuilding of ice sheet over the Himalayan region thereby affecting the thermal gradient and hence the SW monsoon intensity.

Melt water pulse 1b

After a brief, arid interval, the clay minerals between 11.7-11 kyr show an increase in the concentration of the kaolinite and K/I ratio with decrease in smectite content (see Fig 4.7). This suggests the commencement of humid interval which is globally recognized as a melt water pulse 1b. Melt water pulse 1 b is characterized by the rapid melting of ice sheets (Fairbanks 1989,1992), which could have possibly reduced the high pressure on northern highlands (Tibetan plateau) leading to the re-establishment of necessary thermal gradient for SW monsoon. The humid interval during this period was also reported from the northeastern and equatorial Arabian Sea by von Rad et al.,(1999a & b) and Tiwari et al., (2006b), respectively.

The Holocene

The clay mineral assemblage during the Holocene suggests that this period was also marked by a fluctuation in palaeoclimatic/palaeomonsoonal conditions, and hereafter discussed as a wet and dry periods.

A} Wet period

At 8.7, 4.9, 2.7 and ~2 kyr the wet episode owing to the enhancement of the SW monsoon is marked by the increase in continental humidity in form of kaolinite enrichment along with the decrease in chlorite and smectite contents. This suggests an intense hydrolysis of trap basalts owing to the stronger SW monsoon that ultimately resulted in the formation of kaolinite.

B} Dry period

At 9.7, 5.9 and 4-3 kyr clay mineral assemblages shows enrichment in aridity proxy i.e. increase in smectite and chlorite content whereas the humidity proxy like kaolinite, K/I ratio shows decrease in concentration. This indicates that during these periods the intensity of SW monsoon was weaker.

Sediment core from the topographic high (SK-208)

In order to get a longer record of clay minerals, a core SK-208 (Fig 4.6) was collected from the topographic high off Karwar. Since the core location is far from the adjacent hinterland, the sediments comprise of an admixture of clays derived from the Indus source through summer monsoon current and basaltic/gneissic source from the adjacent hinterland through cross shelf transport (Rao and Rao, 1995). The clay mineral assemblage (Fig 4.8) shows the overall dominance of smectite and illite with an average of 40%, whereas chlorite and kaolinite are present in lesser amounts with an average of 15%. Clay distribution pattern of this core suggests that it may contain dispersed clay minerals due to the relative intensity of summer monsoon circulation and cross shelf transport. Considering this aspect, illite, a well crystalline and Fe-Mg rich (Thamban et al., 2002 and the reference therein) Indus borne clay mineral (Rao and Rao, 1995) is used as a proxy to understand the intensity of summer monsoon circulation. On the other hand smectite, a basaltic derived clay mineral which form in semi-arid condition is used as an indicator for cross shelf transport.

In the core SK 208, crystallinity of illite was measured as height width (HHW) of the 10 Å illite peak and the chemistry was assessed using the ratio of intensity of 5 and 10Å peak areas of illite (see Fig 4.8). An illite 5Å /10Å ratio below 0.5 represents Fe, Mg-rich illite and above 0.5 indicates Al-rich illites (Gingele, 1996). Based on the variations of illite, smectite or smectite-illite ratio the relative intensity of summer monsoon circulation or the cross shelf transport has been deciphered and discussed.

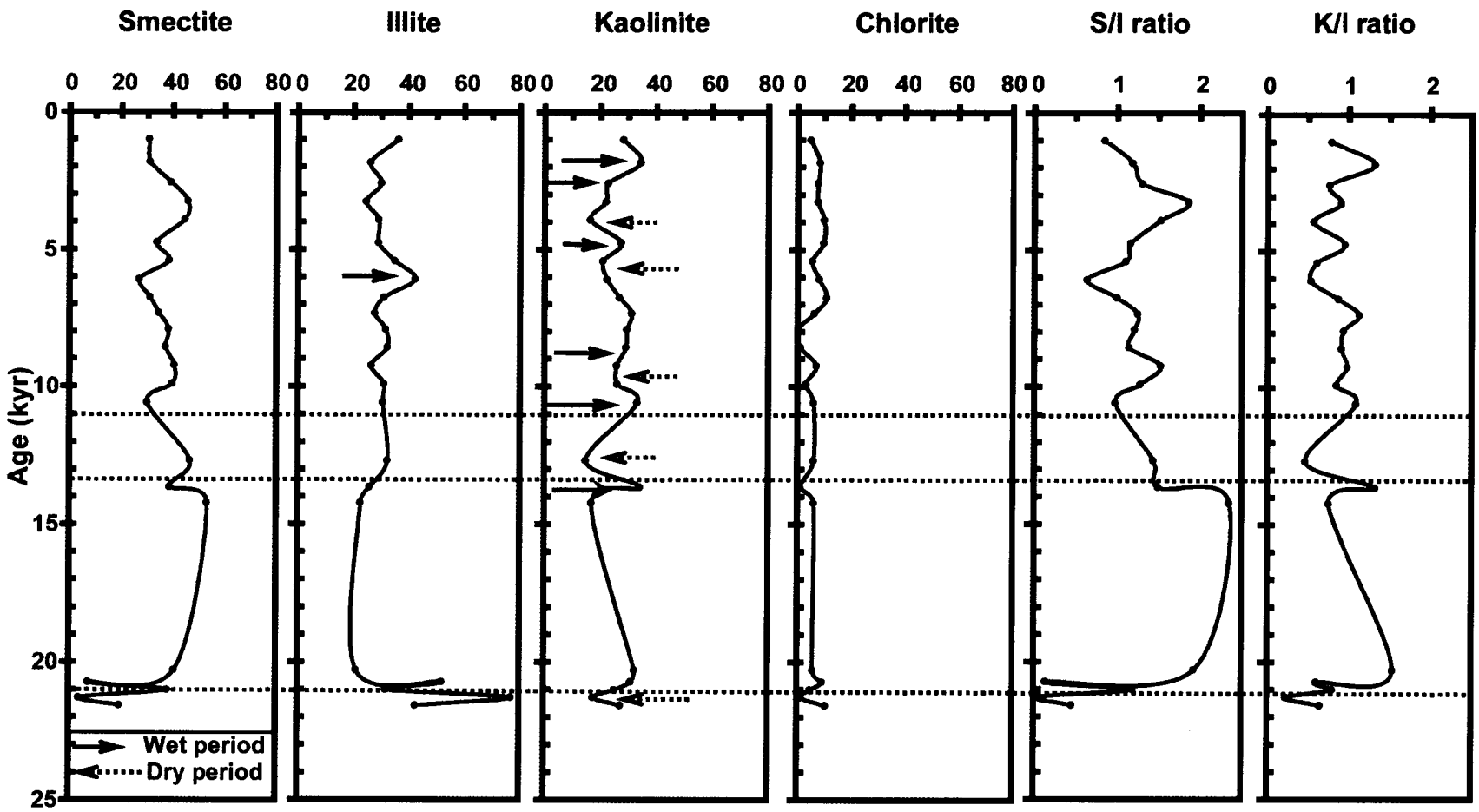

Fig 4.7. Variation in smectite, illite, kaolinite, chlorite, S/I ratio and K/I ratio for core SK-172. Dotted lines are the base for chronology. Bold and dashed arrows indicate wet and dry periods respectively.

A} Interglacial period (MIS 5, 3 and 1)

Temporal variation of clay minerals as seen from Fig 4.8 suggests that as compared to the glacial periods, the interglacial periods show increasing concentration of illite and decreasing concentration of smectite and S/I ratio. Independent estimation of illite crystallinity and chemistry shows illite to be well crystalline and Fe-Mg rich suggesting an Indus source. The increase in Indus borne illite is attributed to the increasing strength of summer monsoon circulation, which could have brought illite and deposited at the core site. The increasing influence of summer monsoon current may also have restricted cross shelf transport resulting in decrease in smectite content and S/I ratio. The changes in smectite content and S/I ratio at this core location reveals that during interglacials, the intensity of summer monsoon wind was perhaps stronger than during glacial periods which is also corroborated by the upwelling records of western Arabian Sea (Anderson and Prell, 1993; Emeis et al., 1995).

During ~110-105 kyr illite increases from 44% to 58% and smectite and S/I ratio decreases to minimum of 21% and 0.4, respectively (Fig 4.8). Similarly, during mid-late Holocene (6 kyr to present), illite increases from 26% to 42% and remains enriched throughout this period with an average of 40%. Illite crystallinity and chemistry during the above mentioned periods suggests the dominance of Indus source. All these observations suggest about the strengthening of summer monsoon circulation (as shown by bold arrow in Fig 4.8). During ~110-105 kyr, the maximum content of illite and the minimum content of smectite and S/I ratio indicates that the summer monsoon circulation/ summer monsoon

winds was stronger during MIS 5 than the present times. On the other hand, during early-mid Holocene i.e., 10-6 kyr smectite as well as S/I ratio increases from 31-44% and 1-1.6 (S/I), respectively; whereas illite decreases as compared to the mid-late Holocene time (as shown by dashed arrow in Fig 4.8). The increase in smectite and S/I ratio along with the decrease in illite is attributed to the weaker summer monsoon circulation/summer monsoon winds which could have facilitated the cross shelf transport, hence the enrichment in smectite content. The result of weaker summer monsoon during early Holocene is in contrast to the earlier reports from the western Arabian Sea (Fleitmann et al., 2003; Gupta et al., 2003). The contrasting trend of summer monsoon between the western and eastern Arabian Sea is due to the fact that they are a part of different monsoon domains as suggested by Staubwasser (2006). Information derived by the clay mineral content on the variability of SW monsoon is very well correlated with the $\delta^{18}O$ record (as discussed in Chapter 5 section 5.4) and is in agreement with the earlier reports (Prabhu et al. 2004; Chodankar et al. 2005).

B} Glacial period (MIS 4 and 2)

As compared to interglacial periods, illite of Indus origin (as seen from crystallinity and chemistry of illite) shows a decrease and smectite along with the S/I ratio shows an increase during glacial period (see Fig 4.8). The decreasing content of illite suggests weakening of summer monsoon circulation/wind, hence the arid period. The aridity during this period is also reflected by the increasing trend of smectite and S/I ratio. Various records suggest that during arid periods, the extreme rainfall events get enhanced resulting

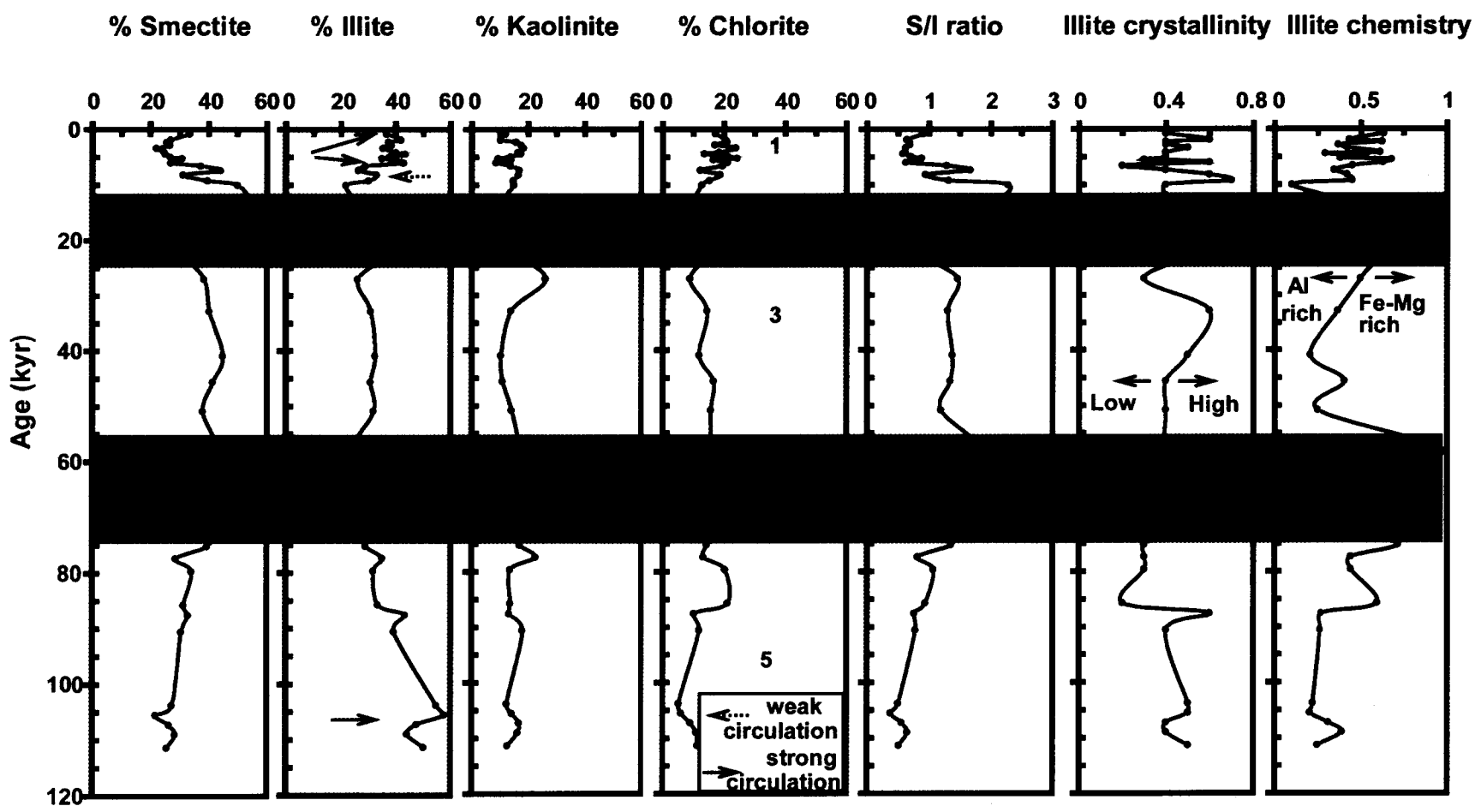

Fig 4.8. Variation in clay minerals from the core SK-208. The numbers indicates isotopes stages and the shaded region represents glacial stage. Bold and dashed arrows indicate strong and weak circulation respectively.

in a higher fluvial sediment load (Staubwasser, 2006). Therefore, considering the same analogy, the enhanced deposition of smectite at the core site (see Fig 4.8) could be attributed to the enhanced cross shelf transport due to an extreme rainfall events that known to occur during arid period. As compared to MIS 4, the enhanced concentration of smectite during MIS 2 could be attributed to the combined effect of aridity and lowered sea level [lowest recorded for the last 100 kyr (Chodankar et al., 2005 and the reference therein)] which could have favoured in the deposition of clay minerals specially smectite to the core site, as also the distance from the adjacent hinterland has reduced considerably. The clay mineral record suggests aridity during glacial period is also reflected in the precipitation records ($\delta^{18}O$ record) as discussed in Chapter 5 section 5.4. These results are comparable to that of Pattan et al. (2003); Prabhu et al. (2004, 2005); Chodankar et al. (2005).

4.7 Summary

The sedimentological, geochemical and clay mineralogical results of the two cores (SK-172 and SK-177/11) collected from the eastern Arabian Sea are summarized below:

- The variations in organic carbon from the studied cores suggest that organic carbon enrichment is controlled by overhead productivity, however texture also plays an important role.

- From the results of southeastern Arabian Sea core (SK-177/11), the depletion in organic carbon inspite of the increase in silt, silicic fraction and carbonate content during MIS 3 suggests poor preservation of organic carbon.

- During glacial periods, the intensity of NE monsoon and its associated productivity (as deciphered from organic carbon content) shows a marked increase in the sediment core site SK-208.

- Palaeoproductivity as estimated from all the cores suggests that similar to the present day, the NE monsoon and its associated productivity during late Quaternary was limited to the northern part of eastern Arabian Sea due to favorable SST and SSS conditions that prevailed.

- In the cores SK172 and SK-177/11, organic carbon and calcium carbonate shows enrichment during the Holocene which suggests increase in surface productivity owing to the enhancement of SW monsoon.

- The increase in concentration of kaolinite during 14.8-14 kyr and MWP 1b suggests intensified chemical weathering on adjacent hinterland due to the strong intensity of SW monsoon. On the other hand, the decrease in kaolinite content during LGM and Younger Dyras suggests aridity (decrease in SW monsoon intensity).

- The present study using core SK 208 also demonstrates that clay minerals can be used as an index of summer monsoon circulation along the eastern Arabian Sea rather than upwelling indices.

- The summer monsoon circulation during interglacials was stronger than glacials and during ~110 kyr the summer monsoon circulation was stronger than the present time.

- The distribution of illite in SK-208 suggests that during early Holocene the strength of summer monsoon circulation was weaker whereas it became stronger in mid-late Holocene.

CHAPTER 5

PAST VARIABILITY OF SURFACE HYDROGRAPHY AND PRODUCTIVITY

5.1 Introduction

The pioneering effort of Emiliani (1955) who deciphered the isotopic record from the deep-sea core in terms of a series of Pleistocene climate/ temperature cycle, analysis of stable oxygen and carbon isotopes from foraminiferal shells played a pivotal role in palaeoceanography. It utilizes the fact that foraminiferal tests calcify in equilibrium with the isotopic composition ($\delta^{18}O$) and temperature of the ambient seawater (Shackleton, 1974). Hence, it is likely that the $\delta^{18}O$ of foraminiferal test reflect the variations in continental ice volume locked on poles during glacial-interglacial time scale (because ice gets enriched in ^{16}O leaving the sea water enriched in ^{18}O) and the change in the sea surface temperature. However, it also records variation in sea surface temperature (SST) and sea surface salinity (SSS) caused by local phenomenon like upwelling, mixing of water masses and the fresh water influx etc. Therefore, the measured $\delta^{18}O$ of foraminiferal calcite is the sum total of all the effects operating together. Similar to $\delta^{18}O$, $\delta^{13}C$ of foraminiferal calcite has global and regional effects. Global effects includes εCO_2 induced by circulation, global productivity owing to change in wind strength and the regional component like upwelling can produce a significant effect on the $\delta^{13}C$ of foraminiferal calcite. Therefore, a careful investigation and prior knowledge of global and regional signal is needed to evaluate the effect caused by the regional phenomenon.

Researchers have utilized the potential of foraminiferal $\delta^{18}O$ to decipher the past variation in the hydrography of Arabian Sea. It is suggested that the hydrography of Arabian Sea has fluctuated in the past on a glacial interglacial time scale (e.g. Chodankar et al., 2005; Tiwari et al., 2005a & b; Thamban et al., 2001; Sarkar et al.,

2000b; Beufort et al., 1997; Rostek et al., 1997; Sarkar and Bhattacharya, 1992; Duplesy, 1982). These records suggest that during LGM the intensity of summer monsoon was effectively reduced (Chodankar et al., 2005). Sarkar et al. (2000a) reported that during LGM, Arabian Sea was saltier by 1-2‰ than the present, whereas the equatorial and northern Arabian Sea witnessed increased precipitation and evaporation, respectively. On the other hand, records from eastern Arabian Sea suggests stronger winter monsoon during this period resulting in the intrusion of low salinity waters of Bay of Bengal through winter monsoon currents (Sarkar et al., 1990). Recently, Tiwari et al. (2005b) suggested a revision indicating an early deglacial strengthening of northeast monsoon and its associated oceanic currents rather than during LGM. During late deglacial period i.e., at ~15 kyr summer monsoon and its associated precipitation is reported to have regained the strength (Thamban et al., 2001). Apart from monsoonal changes, Arabian Sea shows the evidence of classical two step deglacial melting of ice sheets termed as Melt water pulse 1a and 1b i.e., MWP 1a and 1b (Thamban et al., 2001).

In order to understand the palaeoclimatic/palaeomonsoonal conditions and its possible linkage with the forcing mechanism, various studies have been undertaken in the eastern Arabian Sea covering the Holocene (Tiwari et al., 2005a; Thamban et al., 2001; Sarkar et al., 2000b). Of these records, some suggested a direct relation with the summer insolation maxima and the early-mid Holocene precipitation maxima (Van campo, 1986; Sirocko et al., 1993), whereas Thamban et al. (2001) observed a time lag of ~3 kyr reporting a nonlinear response of monsoon towards summer insolation. Tiwari et al. (2005a) suggested solar cycle to be the most dominating factor controlling the intensity of southwest monsoon especially after 8 kyr because during this time

thermohaline circulation had stabilized and thereby monsoon circulation responded directly to solar forcing (Fleitmann et al., 2003). Similarly, Sarkar et al. (2000b) studied E-P budget (excess evaporation over precipitation) of this region, a sensitive climate indicator, and observed a decreasing trend from ~10 kyr to ~ 2 kyr due to the increase in summer monsoon rainfall. They have also reported teleconnection of Indian monsoon with the high latitudes.

Like sea surface hydrography, sea surface productivity of the eastern Arabian Sea is also driven by the intensity of monsoons either through upwelling or wind induced mixing/ convective overturning (Nair et al., 1989; Madhupratap et al., 1996). Studies by Sarkar et al. (2000a) have shown that the $\delta^{13}C$ variation of foraminiferal calcite indicates palaeoproductivity fluctuation either due to the change in the concentration of CO_2 or to the upwelling process (Naidu and Niitsuma, 2003). Palaeoproductivity records based on $\delta^{13}C$ has indicated that during LGM strength of upwelling has reduced whereas it became vigorous in early Holocene i.e. ~ 9 kyrs (Sarkar et al., 2000a). The decrease in upwelling and the associated productivity during LGM is also corroborated by the other proxy records of the eastern Arabian Sea (Thamban et al., 2001, Agnihotri et al., 2003; Pattan et al., 2003).

All these records suggest that the $\delta^{18}O$ and $\delta^{13}C$ of foraminiferal calcite can potentially be used as a proxy to reconstruct the palaeoclimatic condition through deciphering the sea surface hydrography and palaeoproductivity. Most of the above mentioned studies are based on the records of a sediment core that have been archived from the shelf region of eastern Arabian Sea, whereas the present investigation involves slope/ deeper sediments. Also the climatic events as identified through the isotopic

study ($\delta^{18}O$ and $\delta^{13}C$) of foraminiferal calcite are based on three different species of planktonic foraminifera, where the habitat ranges from surface to subsurface depths unlike the earlier reports where inferences were mostly drawn on mono specific species.

5.2 Present day sea surface hydrography and productivity

Present day sea surface hydrography of eastern Arabian Sea is modulated by complex monsoon system (Wyrtki, 1973) characterized by upwelling and associated productivity during summer monsoon. The spatial variability of summer monsoon upwelling along the eastern Arabian sea is continuous up to 15^0 N and ceases around 20^0 N (Shetye et al., 1994). Such variability is very well reflected in water column productivity (Bhattathiri et al., 1996). However productivity increases during winter monsoon due to convective mixing which is reflected north of 15^0N latitude (Madhupratap et al., 1996). The sea surface temperature (SST) shows seasonal variation of ~3^0C with the lower value recorded during monsoon period (minimum during August) which reaches to high value during intermonsoon period (maximum during May).

Variation in sea surface salinity (SSS) along the south eastern Arabian Sea is influenced by both summer monsoon precipitation and the transport of low salinity water from Bay of Bengal during winter monsoon (Wyrtki, 1971; Duplessy, 1982). The northward flowing poleward coastal current (PCC) (Shetye et al., 1991), which is a part of winter monsoon current (WMC), seems to advect the low salinity water from Bay of Bengal to the eastern Arabian Sea (Shankar et al., 2002). During the period of summer

monsoon, the abundant precipitation over Western Ghats i.e. between 20^0N - ~ 10^0N quickly drains in to the coastal Arabian Sea through various streams, channels and rivers that resul in the decrease of sea surface salinity as shown in Fig 5.1. The reduction in salinity is evident from the north-south trending salinity contours with values ranging from 34 psu to 36 psu away from the coast (Tiwari et al., 2005a and the reference therein).

All these studies suggest that the sea surface hydrography and productivity of the eastern Arabian Sea is regulated by a complex monsoon system. This provides an opportunity to reconstruct and understand the past variability of monsoon using oxygen and carbon isotope of foraminiferal calcite of sections of a sediment core.

5.3 Late Quaternary sea surface hydrography and monsoon variability

Records from the Arabian Sea pertaining to late Quaternary palaeomonsoonal reconstruction using marine sediments mostly relied on the connection between summer monsoon wind and upwelling (e.g. Overpeck et al., 1996; Anderson et al., 2002; Wang et al., 2005). They have utilized various monsoon (wind/upwelling) proxies such as pollen, foraminifera, stable isotopes (δ^{18}O, δ^{13}C), eolian dust etc and found a good correlation between wind/upwelling strength and summer monsoon. As the eastern Arabian Sea does not show such a strong connection between upwelling and monsoonal strength (e.g., Thamban et al., 2001 and Agnihotri et al., 2003), implying that the summer monsoon can be viewed in terms of precipitation (Sarkar et al., 2000b; Thamban et al., 2001; Tiwari et al., 2005a) rather than wind proxies. Sediment trap data from the Arabian Sea (Open Ocean) shows a strong peak of planktonic foraminifera

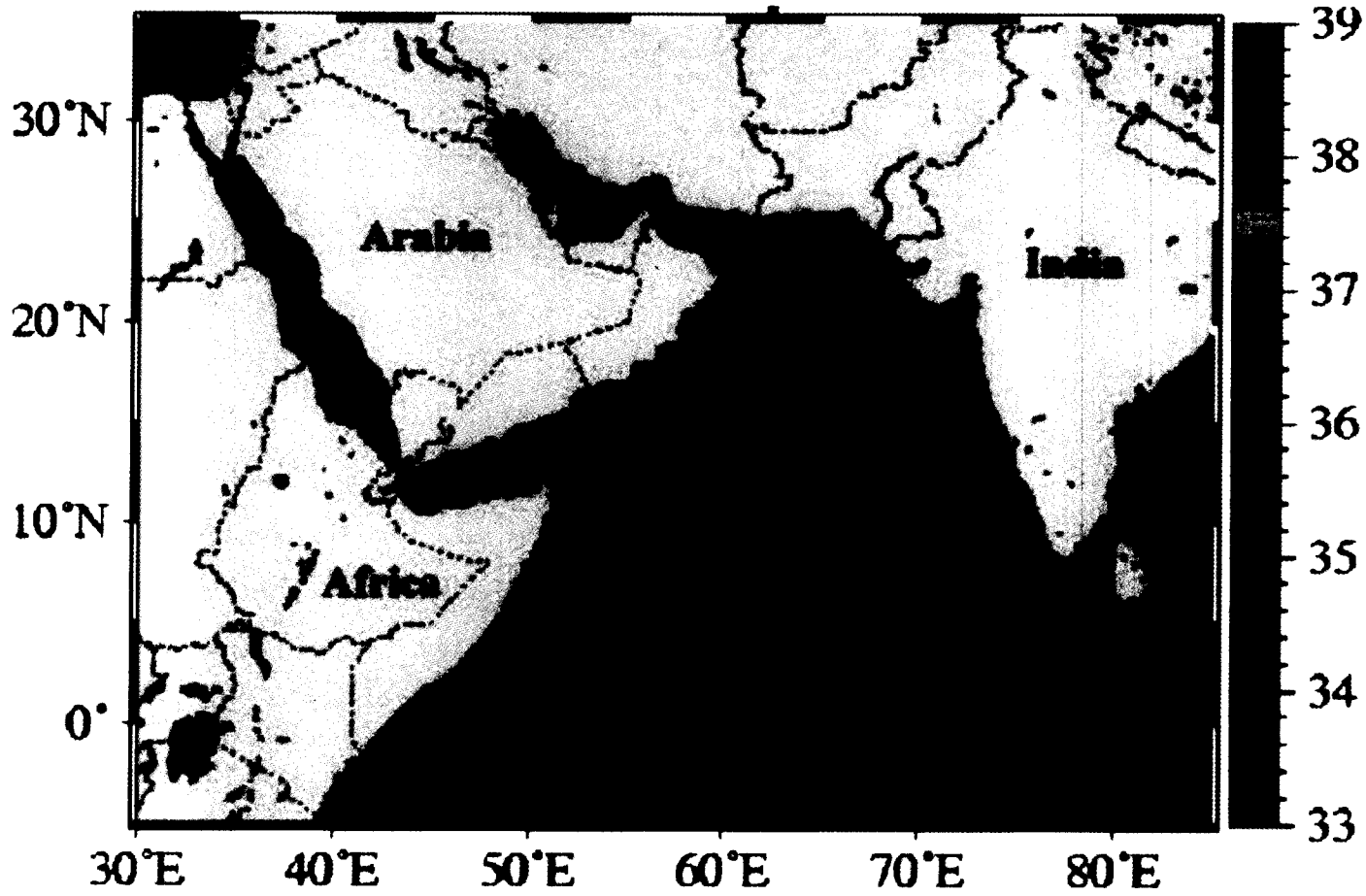

Fig 5.1. Map showing sea surface salinity (in PSU) during summer monsoon (modified after Tiwari et al., 2005a). Note: The locations of core falls in the low salinity region.

during summer monsoon (Curry et al., 1992). Therefore, the $\delta^{18}O$ variation of planktonic foraminifera is likely to reflect the variation in summer monsoon. The present study attempts to reconstruct the Holocene and pre-Holocene (late Quaternary) palaeomonsoonal conditions from the $\delta^{18}O$ record of surface dwelling foraminifera in sediment cores collected from three different locales. Two cores SK-172 and SK-208 are form the northern and one core SK-177/11 is from the southern part of eastern Arabian Sea (see Fig 5.1).

5.3.1 Northern part of eastern Arabian Sea core SK-172

The location of core SK-172 falls with in the low salinity plume generated by monsoonal runoff (see Fig 5.1). Therefore to reconstruct the intensity and variability of low salinity plume-an index of summer monsoon, the $\delta^{18}O$ record is obtained from three different species of planktonic foraminifera viz *Gs. ruber*, *Gs. sacculifer* and *Gr. menardii*. The habitat of these species ranges from surface to subsurface depth. *Gs. ruber* is subtropical warm water species with preference for warm, stratified water (Ganssen and Sarnthein, 1983) and inhibits at top 25 m. *Gs. sacculifer* dwells at 50m depth, a tropical water species has preference for water masses with low seasonality in SST and vertical temperature gradient (Tiwari et al., 2005a and the reference therein; Fairbanks et al., 1980, 1982) whereas *Gr. menardii* dwells at the top of thermocline i.e. ~100m (Fairbanks et al., 1982). The recorded variation in $\delta^{18}O$ of each species is reported with respect to VPDB and shown in Fig 5.2.

The $\delta^{18}O$ record of these species i.e. *Gs. ruber, Gs. sacculifer* and *Gr. menardii* (as shown in Fig 5.2) shows fluctuation between -2.5‰ to -0.2‰, -2.6‰ to 1.72‰ and –1.2‰ to 0.3‰ respectively.

5.3.2 Southeastern Arabian Sea core SK-177/11

The southeastern Arabian Sea core, like the other cores falls in the low salinity plume generated by the monsoonal runoff. It is also characterized by weak upwelling system which starts before the onset of monsoon (Shetye, 1984) and gets enhanced with the onset of SW monsoonal winds (Levitus and Boyer, 1994; Levitus et al., 1994). During the winter monsoon transport of low salinity water from the Bay of Bengal into the eastern Arabian Sea (core site) is also reported (Shankar et al, 2005, Shenoi et al, 2005). Hence, to trace the variability of monsoon during late Quaternary, a similar approach of oxygen isotope ($\delta^{18}O$) is adopted. Pertaining to this, $\delta^{18}O$ record of planktic foraminifera viz *Gs. ruber*, *Gs. sacculifer* and *N. dutertrei* is documented in Fig 5.3. The depth habitat of *Gs. ruber*, *Gs. sacculifer* is discussed in the previous section while *N. dutertrei* is deeper, thermocline dweller ~150-200 m depth (Fairbanks et al., 1982). The $\delta^{18}O$ value of all the species as shown in Fig 5.3 is reported in ‰ with respect to V-PDB.

The $\delta^{18}O$ value of *Gs. ruber* fluctuated between 1.14‰ to -3.16‰ whereas *Gs. sacculifer* fluctuated between -0.03‰ to -2.5‰. The deeper dwelling *N. dutertrei* fluctuated between 0.6‰ to -1.8‰. During early deglacial period heaviest value is recorded for all the three species while during Holocene lightest value is recorded. The average $\delta^{18}O$ value for the Holocene period [taken as a point with maximum occurrence of same or near same values (except events)] is -2.4‰ for *Gs. ruber*, 2.1‰ for *Gs. sacculifer* and 1.3‰ for *N. dutertrei*.

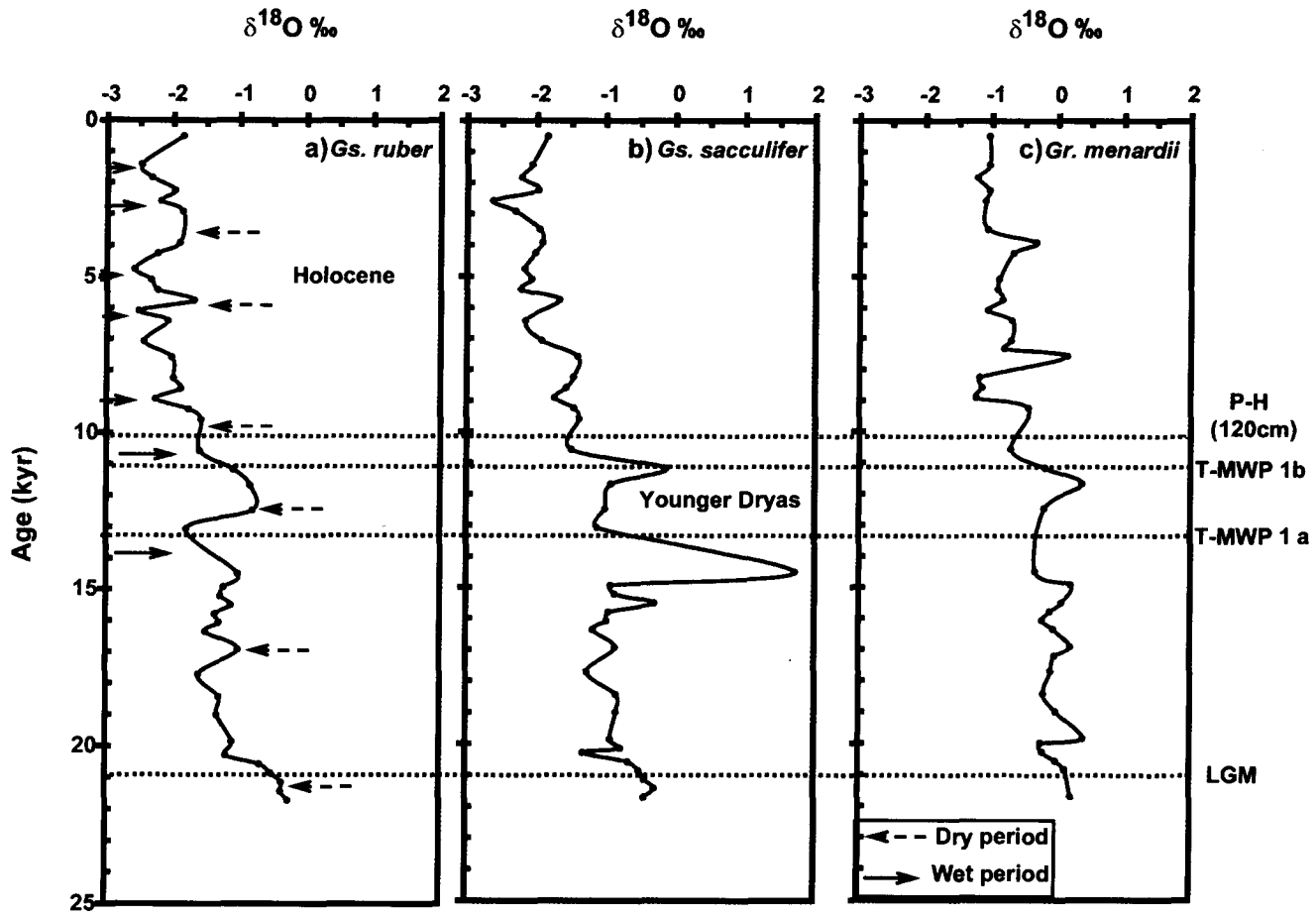

Fig 5.2. Variations in $\delta^{18}O$ of *Gs. ruber, Gs. sacculifer* and *Gr. menardii* respectively for core SK-172. The dashed lines are the base for obtaining chronology.

In addition, the upper ocean stability structure as determined from the $\delta^{18}O$ gradient is also used to reconstruct the palaeomonsoonal condition. The $\delta^{18}O$ gradient ($\Delta\delta^{18}O_{gradient}$) is obtained by subtracting the $\delta^{18}O$ value of surface dwelling *Gs. ruber* and *Gs. sacculifer* with the deeper dwelling *N. dutertrei* (see Fig 5.3). The gradient is called negative when the surface dwellers (*Gs. ruber* and/or *Gs. sacculifer*) show lighter value as compared to deeper dweller (*N. dutertrei*) whereas it is called positive when surface dwellers shows heavier value as compared to deep dwellers.

5.3.3 $\delta^{18}O$ variability and its palaeomonsoonal implications during pre Holocene

The $\delta^{18}O$ variation of core collected from different end of eastern Arabian Sea (i.e. SK-172 and SK-177/11) is compared and discussed in terms of monsoonal variation during pre-Holocene period.

A} MIS 3

At ~26 kyr, the $\Delta\delta^{18}O_{gradient}$ of core SK-177/11 shows the lightest value for the surface dwelling *Gs. ruber* suggesting the enhanced summer monsoon precipitation making the surface water lighter. These results of increasing intensity of summer monsoon are very well correlated with the records of Chodankar et al. (2005).

B} MIS 2

Last Glacial Maximum

In core SK-172, the LGM-Holocene shift in $\delta^{18}O$ value ($\Delta\delta^{18}O$) is calculated

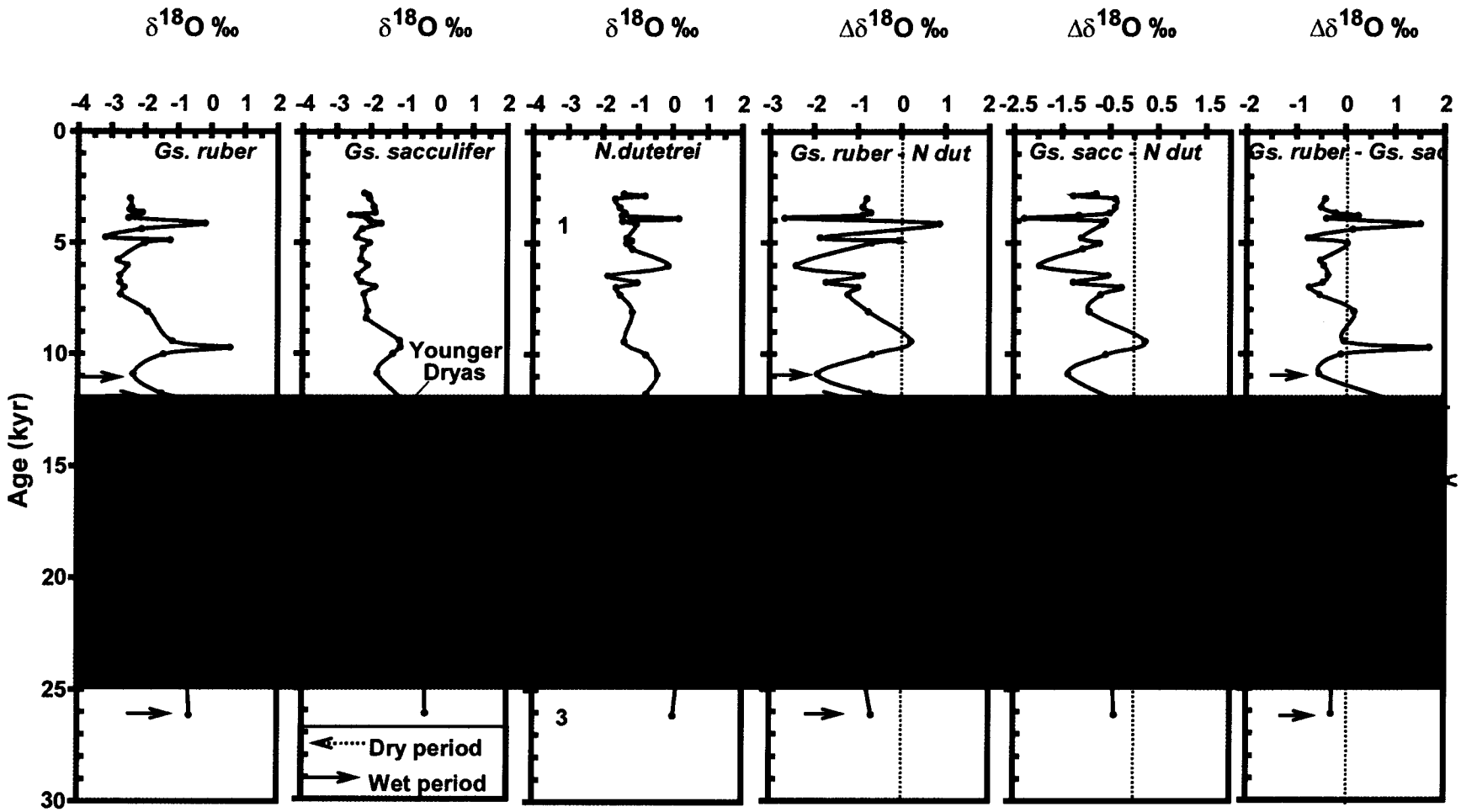

Fig 5.3. Variations in the $\delta^{18}O$ of *Gs. ruber, Gs. sacculifer* and *N. dutertrei* along with the isotopic gradient ($\Delta\delta^{18}O_{gradient}$). The numbers indicates isotopes stages, shaded region represents glacial period. Bold and dashed arrows represent wet and dry periods respectively.

from the difference of average value from the LGM section and the average value from the Holocene section (excluding the extreme events). The recorded LGM-Holocene shift ($\Delta\delta^{18}O$) for *Gs. ruber, Gs. sacculifer* and *Gr. menardii,* are ~2‰, ~1.5‰ and ~1.2‰, respectively. The $\Delta\delta^{18}O$ could be attributed to the combination of ice-volume effect i.e.1.2‰ (Fairbanks, 1989, 1992), SST (Rosenthal et al., 2003) and SSS effect (Banakar et al., 2005). The recorded $\Delta\delta^{18}O$ suggests increase in E-P budget due to the reduced summer monsoon precipitation. The inference of reduced strength of SW monsoon corroborates with the results of Chodankar et al. (2005) and Tiwari et al. (2006b). However, the different magnitude $\Delta\delta^{18}O$ in these species could be due to the depth habitat (Fairbanks et al., 1982) and/or species specific e.g. *Gs. ruber* is surface dweller and more temperature sensitive compared to the *Gs. sacculifer* (Mulitza et al., 1998) therefore it is likely to have recorded the maximum LGM-Holocene $\delta^{18}O$ shift ($\Delta\delta^{18}O$).

Deglacial period

During early deglacial period various records suggest that the sea surface hydrography of eastern and equatorial Arabian Sea has witnessed a fluctuation in the intensity of summer monsoon precipitation (Thamban et al., 2001) and/or winter monsoon circulation (Tiwari et al., 2005b). In the present study, both the cores (i.e. from northern and southern part of eastern Arabian Sea SK-172 and SK-177/11) shows positive excursion in $\delta^{18}O$ value during early deglacial period. This is contrary to the earlier reports of equatorial Indian Ocean showing depletion in $\delta^{18}O$ value owing to the enhancement of NE monsoon (Tiwari et al., 2005b). The magnitude of $\delta^{18}O$ variation for core SK-172 (northern part) is 0.6‰, 0.4‰ & 0.3‰ for *Gs. ruber, Gs. sacculifer*

and *Gr. Menardii*, respectively; whereas the magnitude is slightly higher in core SK-177/11 i.e., 0.7‰ & 0.5‰ for *Gs. ruber* and *Gs. Sacculifer*, respectively. However, the thermocline dwelling *N. dutertrei* does not show any significant variation (see Fig 5.3). During LGM-early deglacial period the ice melting episodes were less (Fairbanks, 1989) hence its contribution to the $\delta^{18}O$ record is insignificant (as seen from the $\delta^{18}O$ variation of *N. dutertrei*). Further, any SST increase during this period would have reduced the $\delta^{18}O$, however, is not reflected in the present study. Thus the positive excursion in $\delta^{18}O$ (in both the cores) during this period is attributed to the enhanced evaporation. Evaporation being a surface phenomenon is strongly reflected in *Gs. ruber* as compared to deeper dwelling *Gs. sacculifer* and *Gr. menardii.*

During ~16.2-15.6 kyr, core SK-177/11 (southern part) shows positive excursion in $\delta^{18}O$ value of *Gs. ruber* whereas the deeper dwelling *N. dutertrei* does not show any variation. The stratification structure of the upper column of sea surface ($\Delta\delta^{18}O_{gradient}$) shows positive gradient i.e. higher value for *Gs. ruber* than *Gs. sacculifer.* All these observations suggest a reduced precipitation/ enhanced evaporation due to the weakening of summer monsoon. The enhanced evaporation could have stratified the surface ocean resulting in the enhancement of $\delta^{18}O$ value of sea surface, which is reflected in the $\delta^{18}O$ of surface dwelling *Gs. ruber.* On the other hand, core SK-172 (northern part) does not show any significant variation in $\delta^{18}O$ of *Gs. Rubber* when compared to SK-177/11 (southern part). This could be due to the fact that the hydrography of southern part of eastern Arabian Sea is more sensitive to the precipitation changes because it receives more rain in summer monsoon than the northern part (Sarkar et al., 2000b and the reference therein). These results suggest

reduced precipitation during this period which is also reported from the equatorial Arabian Sea (Tiwari et al., 2006b).

During ~15.6 – 14.4 kyr

From 15.6-15.3 kyr, Fig 5.3 (core SK-177/11) shows negative excursion of 0.8‰ in the $\delta^{18}O$ value of *Gs. ruber*. The negative excursion suggests an early intensification of summer monsoon that is in agreement with the earlier records of Sirocko et al. (1993), Thamban et al. (2001) and Thamban et al. (2002). After the early intensification of summer monsoon, a period between ~15.3 – 14.4 kyr also shows a negative excursion of 1.1‰. Although this period coincides with the Termination 1 a (Fairbanks, 1989, 1992) but due to low melting rates of ice cover (Fairbanks, 1989, 1992) the contribution from change in $\delta^{18}O$ of sea water is insignificant. Therefore the negative excursion of 1.1‰ can be explained entirely due to the combined effect of summer monsoon precipitation and SST that rose to ~2^0 C in the southeastern Arabian Sea (Sonzogni et al., 1998; Cayre and Bard, 1999). The 2^0 C rise in SST will account for a reduction in the $\delta^{18}O$ value by ~0.5‰. Hence the remaining 0.6‰ could be ascribed to the enhanced summer monsoon precipitation. The $\Delta\delta^{18}O_{gradient}$ showing (see Fig 5.3) a sharp negative gradient (lighter values for *Gs. ruber*) corroborates the inference of enhanced summer monsoon precipitation. The wet period as recorded by core SK-177/11 during the entire period of 15.6-14.4 kyr is not reflected in the records of SK-172 (see Fig 5.2). This dissimilarity in the hydrographic response of southern and northern end of eastern Arabian Sea could be attributed to the sensitivity of southeastern Arabian Sea towards the precipitation changes [as the southern part of eastern Arabian Sea receives more rainfall than northern part (Sarkar et al, 2000b)].

Melt water pulse 1a

It is evident from Fig 5.2 that during 14.5-13 kyr, core SK-172 shows negative excursion of 0.8‰ in the $\delta^{18}O$ of *Gs. ruber*. Similarly, the negative excursion of ~0.5-0.6‰ is also recorded from the core SK-177/11 (see Fig 5.3). The recorded event coincides with the global melt water pulse 1a (Fairbanks, 1989, 1992; Bard et al, 1996) which has decreased the $\delta^{18}O$ of global sea water by nearly ~0.2-0.3‰ (Fairbanks, 1992). Therefore for core SK-172 and SK-177/11, the remaining 0.5‰ and 0.3‰, respectively can be ascribed to the enhancement of summer monsoon precipitation. The decrease in salinity is very well reflected in $\Delta\delta^{18}O_{gradient}$ of core SK-177/11 which shows lighter values for surface dwelling *Gs. ruber*. However, in the later part of MWP 1 a (13.2 kyr) *Gs. ruber* shows heavier value compared to the *Gs. sacculifer* which suggests a dry phase and may be attributed to the reduced strength of summer monsoon.

Younger Dryas chronozone

During Younger Dryas, the $\delta^{18}O$ record of core SK-172 (shown in Fig 5.2) shows positive excursion in all the three species i.e. *Gs. ruber*, *Gs. sacculifer* and *Gr. menardii* (more pronounced in *Gs. ruber*). Similarly, the southeastern Arabian Sea core (SK-177/11) shows a positive excursion of 1.4‰ and 0.7‰ for *Gs. ruber* and *Gs. sacculifer* respectively whereas deeper dwelling *N. dutertrei* does not show any significant variation (see Fig 5.3). The $\Delta\delta^{18}O_{gradient}$ shows positive gradient (heavier value for *Gs. ruber* as compared to the *Gs. sacculifer* and *N. dutertrei*). All these records suggest an increase in E-P budget i.e., reduced runoff/ precipitation or enhanced evaporation

owing to the reduced intensity of summer monsoon precipitation. The rebuilding of ice sheet over the Himalayan region could have reduced the necessary thermal gradient for SW monsoon which ultimately might have resulted in the weaker summer monsoon.

Melt water pulse 1b

It is evident from Fig 5.2 and Fig 5.3 that during later part of Younger Dryas, the $\delta^{18}O$ value of *Gs. ruber* for core SK-172 and SK-177/11 shows negative excursion of 0.6‰ and 0.9‰ respectively. Contrary to this, *N. dutertrei* of core SK-17/11 shows a positive excursion of 0.3‰. The recorded positive excursion is discussed separately in section 5.5. The negative excursion of 0.6‰ and 0.9‰ as recorded in both the cores coincides with the second melt water pulse (MWP 1b) which suggests a depletion of ~0.35‰ in $\delta^{18}O$ of global sea water (Fairbanks 1989, 1992). On compensating for the global sea water change, the $\delta^{18}O$ value shows a remainder of 0.25‰ and ~0.5‰ for the core SK-172 and SK-177/11 respectively. This remainder can be ascribed to the decrease in E-P budget due to summer monsoon precipitation. Moreover $\Delta\delta^{18}O_{gradient}$ of core SK-177/11 shows negative gradient i.e. lighter value for *Gs. ruber* (see Fig 5.3) which suggests presence of lighter water at the sea surface. All these observations suggest enhancement in summer monsoon precipitation and are very well corroborated with the records of equatorial Arabian Sea (Tiwari et al., 2006b), northeastern Arabian Sea (Von Rad et al., 1999a).

5.3.4 Sediment core from the topographic high (SK-208)

Like other sediment cores, SK-208 is also collected from the low salinity plume

induced by summer monsoon precipitation and its associated surface runoff (see Fig 5.1). The core is analyzed for $\delta^{18}O$ variation of surface dwelling foraminifera *Gs. ruber*, *Gs. sacculifer* and deeper dwelling *Gr. menardii*. But due to low sedimentation rate, it provides a longer record (~120 kyr) than the other two cores. The $\delta^{18}O$ record as shown in Fig 5.4 shows fluctuation between -1.8 to -0.6‰, -2.1 to -0.4‰ and -1.3 to 0.5‰ for *Gs. ruber*, *Gs. sacculifer* and *Gr. menardii*, respectively. The dry and wet periods as deciphered from these variations are discussed hereafter.

A} Glacial period (MIS 2 and 4)

Figure 5.4 suggests that the glacial period is characterized by heavier value of $\delta^{18}O$. The $\Delta\delta^{18}O$ amplitude (the difference between the glacial and present interglacial $\delta^{18}O$ value) for MIS 2 and MIS 4 shows a value of 1.7 and 1.4‰ respectively. The recorded amplitude ($\Delta\delta^{18}O$) is typical of glacial-interglacial period and is in agreement with the earlier records of eastern Arabian Sea (Rostek et al., 1993). The respective ice-volume effect reported for MIS 2 and MIS 4 are 1.2‰ (Fairbanks, 1989, 1992) and 0.7‰ (Shackleton, 2000). Therefore the remaining 0.5‰ and 0.7‰ could be ascribed to the combined effect of decrease in sea surface temperature and increase in sea surface salinity. The increase in sea surface salinity suggests a stronger convective mixing owing to the stronger winter monsoon. This interpretation is also supported by the record of organic carbon content (discussed in Section 5.7.1 and also in Chapter 4; Section 4.5.2). These results of intense convective mixing during glacial period corroborates with the records of Thamban et al., (2001) and Prabhu et al., (2004, 2005).

B} Interglacial period (MIS 1, 3 and 5)

Palaeoprecipitation record of core SK-208 (as obtained form the $\delta^{18}O$ of *Gs. sacculifer*) shows 3 distinct periods of precipitation changes apart from the changes that have occurred during glacial-interglacial periods. The lightest $\delta^{18}O$ value of -2.1‰ (*Gs. Sacculifer*) is recorded during 110-105 kyr (shown by bold arrow in Fig 5.4) suggesting an intensification of summer monsoon precipitation. Apart from this the $\delta^{18}O$ fluctuations of stage 5 correlates with the sub stages of SPECMAP stack showing low value during warmer intervals (5a and 5c, i.e. at ~80 and 100 kyr respectively) and high value during colder intervals (5b, i.e. at ~86 kyr). This can be explained by the enhanced/reduced summer monsoon precipitation during the periods of warmer/colder interval. However due to deeper depth habitat such fluctuations are not recorded by *Gr. menardii* except at the sub stage 5c indicating summer monsoon precipitation to be stronger than the sub stage 5a. The records of Prabhu et al. (2004) corroborate well with the present results of enhanced/reduced summer monsoon precipitation during the periods of warmer/colder interval.

During Holocene the general trend of $\delta^{18}O$ as recorded by *Gs. sacculifer* shows two distinct intervals, i.e., the early Holocene showing positive excursion in $\delta^{18}O$ value and the late Holocene showing negative excursion in $\delta^{18}O$ value (see Fig 5.4; bold and dashed arrows). The positive excursion/negative excursion suggests decreasing/increasing intensity of summer monsoon precipitation.

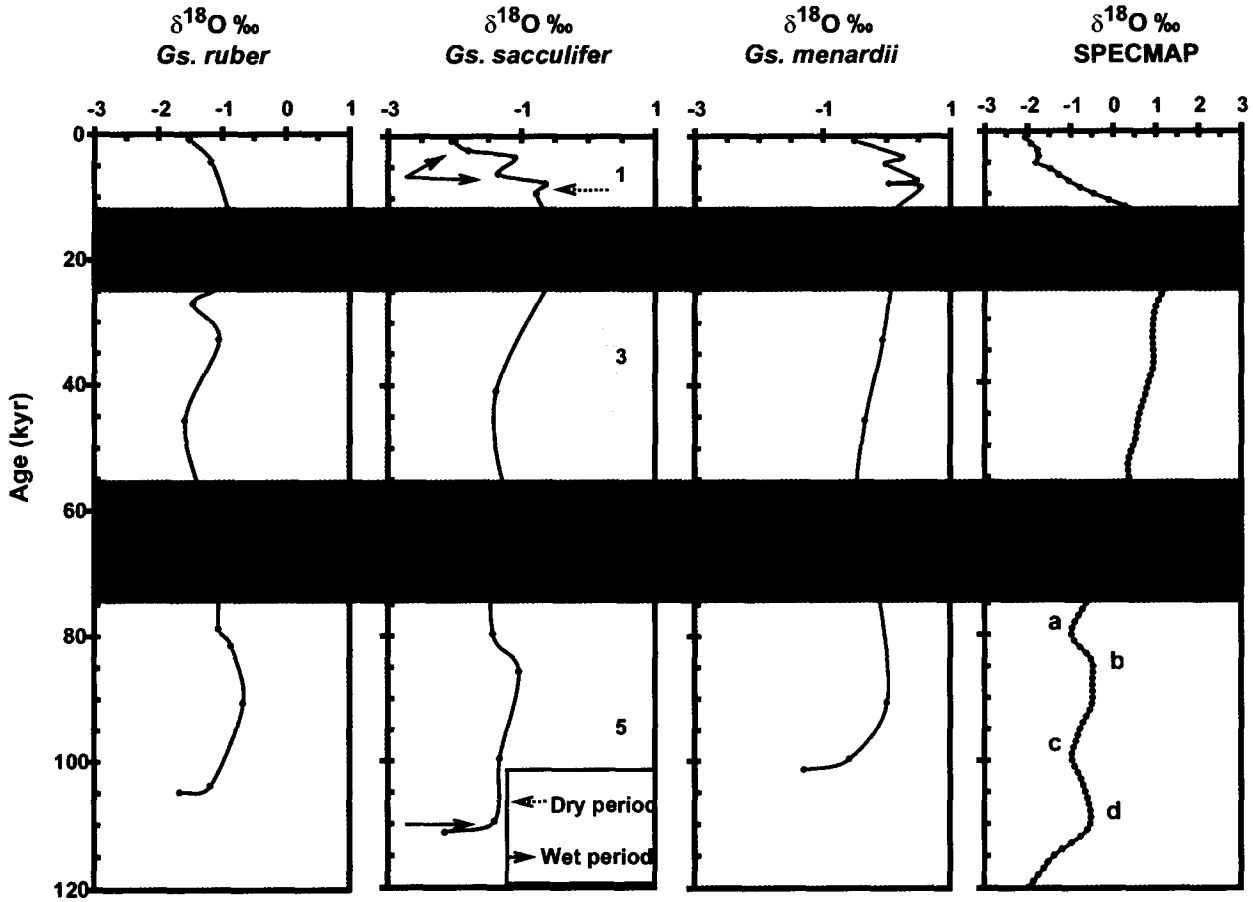

Fig 5.4. Variations in $\delta^{18}O$ of *Gs. ruber, Gs. sacculifer* and *Gr. menardii* respectively for core SK-208. Numbers indicate different isotope stages (Imbrie et al., 1984) and the shaded region indicates glacial periods. The inferred wet and dry periods are indicated by bold and dashed arrows respectively.

5.4. Pre Holocene surface hydrography and monsoon variability along the eastern Arabian Sea

To understand the palaeomonsoonal variability along the entire eastern Arabian Sea, records from both the cores SK-172 and SK-177/11 along with the other tropical/equatorial records are compared. The precipitation records from the studied core and the equatorial records of Tiwari et al. (2006b) show similar fluctuations in summer monsoon intensity during the late Quaternary (except Holocene). Northern Arabian Sea on the other hand, shows an increase in concentration of fluvial derived sediments (Von Rad et al., 1999a) when enhanced summer monsoon is reported on the Indian peninsular region. All these observations point that during the late Quaternary eastern, northern and the equatorial Arabian Seas were a part of a common monsoonal domain.

5.5 Monsoon controlled sub-surface hydrography of the southeastern Arabian Sea

In the southeastern Arabian Sea core, the recorded variation in $\delta^{18}O$ and $\delta^{13}C$ of *N. dutertrei* (thermocline dwelling) is shown separately in Fig 5.5. The variations in $\delta^{18}O$ as well as $\delta^{13}C$ show unusual positive excursions at certain intervals (see Fig 5.5; marked by bold arrows). At ~11 kyr, when the period is characterized by the reduction of 0.35‰ in the $\delta^{18}O$ of global sea water, *N. dutertrei* shows positive excursion of 0.3‰. Thus the net $\delta^{18}O$ change will be the sum of these two (i.e. ~0.7‰). Similarly, the positive excursion of 1.7‰, 1.6‰ and 0.8‰ is also recorded at 6, 3.89 and 2.88 kyr, respectively, thus provides a strong evidence for the recorded signal to be true rather than an error (manual or instrumental). The period showing enrichment in $\delta^{18}O$ coincides with the periods showing positive excursion in $\delta^{13}C$.

The heavier value of $\delta^{18}O$ and $\delta^{13}C$ recorded by deeper dwelling *N. dutertrei* possibly indicates the presence of high salinity water mass of probably Red Sea (RSW) and/or Persian Gulf (PGW) origin. In the present day their presence up to 12.5^0 N is noted at the Indian continental slope (Shankar et al., 2005) and even farther south (Shenoi et al., 2005). These two high salinity water masses occur below 200 m depth and sometimes appears as a single, mixed water mass (ASW). They have observed coastward (on the slope) and poleward increase in the concentration of RSW along the entire Indian west coast. Based on these observations, they have suggested two possible routes for the advection of this high salinity water mass. First one is the coastal route, starting from the Gulf of Aden to the continental slope of Oman, Pakistan and finally to the Indian coast. The other route is via deep monsoon currents flowing across the basin to reach the northern end of Indian west coast. Various studies suggest an eastward spreading of RSW into the Arabian Sea during summer monsoon (Gamsakhurdiya et al., 1991; Beal et al., 2003), but none of these are conclusive (Shankar et al., 2005). Upon considering these facts it is likely that the core site (SK-177/11) is bathed by these high salinity water masses at subsurface depth. Among these water masses, RSW shows higher $\delta^{13}C$ value (Naqvi and Fairbanks, 1996). Hence the positive excursion in $\delta^{18}O$ and $\delta^{13}C$ as recorded by *N. dutertrei* possibly indicates the presence of high salinity water mass at subsurface depth where *N. dutertrei* dwells. This inference is supported by two reasons:

Firstly, the positive excursion of $\delta^{18}O$ and $\delta^{13}C$ is confined to Holocene and starts to appear from ~11 kyr where the global sea level has almost attained present level (Fairbanks, 1992) (also evident from the $\delta^{18}O$ of *Gs. ruber* and *Gs. sacculifer*) thus

allowing outflow of RSW across the sill which otherwise restricted due to lowered sea level.

Secondly, the heavier $\delta^{18}O$ and $\delta^{13}C$ values of *N. dutertrei* coincide with the periods of enhanced summer monsoon precipitation which is deciphered from the variation in $\delta^{18}O$ value of *Gs. ruber* (see Fig 5.5 and text 5.6.2). This observation suggests that during the entire Holocene the presence of Red Sea water to the Indian west coast is controlled by the intensity of summer monsoon possibly through summer monsoon circulation. The observation of a strong control of summer monsoon circulation in the distribution of RSW to the Indian west coast (core site) is similar to the present day observation of Shankar et al., 2005.

5.6 Holocene changes in surface hydrography

The core collected from the northern part of eastern Arabian Sea (SK-172) and southeastern Arabian Sea (SK-177/11) falls with in the low salinity plume developed by the monsoonal runoff from *Sahyadri* (Sarkar et al., 2000b and Tiwari et al., 2005a). This freshwater influx tends to float on the surface thereby decreasing the $\delta^{18}O$ value of surface dwelling foraminifera (see Fig 5.1) to a considerable extent and below this depth its effect decreases resulting in subdued signals. Besides this, the $\delta^{18}O$ variation in foraminiferal calcite also depends on the ice-volume effect, SSS and SST of the ambient water. Among these, SST variation in the tropics for the last 10 kyr is 0.5^{0} C (Rostek et al., 1993) and there was no global ice-melting episode recorded during the last 10 kyr (Fairbanks, 1989, 1992). Thus, during the Holocene the contribution of SST variation and ice-melting effects to the $\delta^{18}O$ variation of foraminiferal calcite seems to

be insignificant. However the local effects like upwelling and fresh water influx, an indicator of summer monsoon, can contribute to the $\delta^{18}O$ of foraminiferal calcite. Upon considering all these facts, the palaeomonsoonal history is reconstructed from the core collected from eastern Arabian Sea.

5.6.1 Northern part of eastern Arabian Sea core SK-172

Among the various factors affecting $\delta^{18}O$ variation global component like ice-volume effect and SST changes are ruled out (see section 5.6). Moreover the contribution from upwelling is insignificant at the core site because the intensity of upwelling decreases from the south to the north (Shetye et al., 1994). Therefore the only factor that appears plausible is the surface runoff, which can bring significant change in the SSS of the eastern Arabian Sea as often observed during the present day southwest monsoon (Sarkar et al., 2000b and Tiwari et al., 2005a). These observations suggest that during the Holocene, the foraminiferal $\delta^{18}O$ variation as seen in Fig 5.6 fluctuates in response to the changing E-P budget. Based on this, various dry and wet spells (shown by bold and dashed arrow in Fig 5.6) have been identified and discussed in terms of variations in the strength of monsoon.

A} Wet period

During early the Holocene i.e. ~9 kyr, the wet episode owing to the enhancement of the SW monsoon is marked by the negative excursion in the surface to subsurface dwelling foraminifera i.e. *Gs. ruber*, *Gs. sacculifer* and *Gr. menardii*. Similarly mid

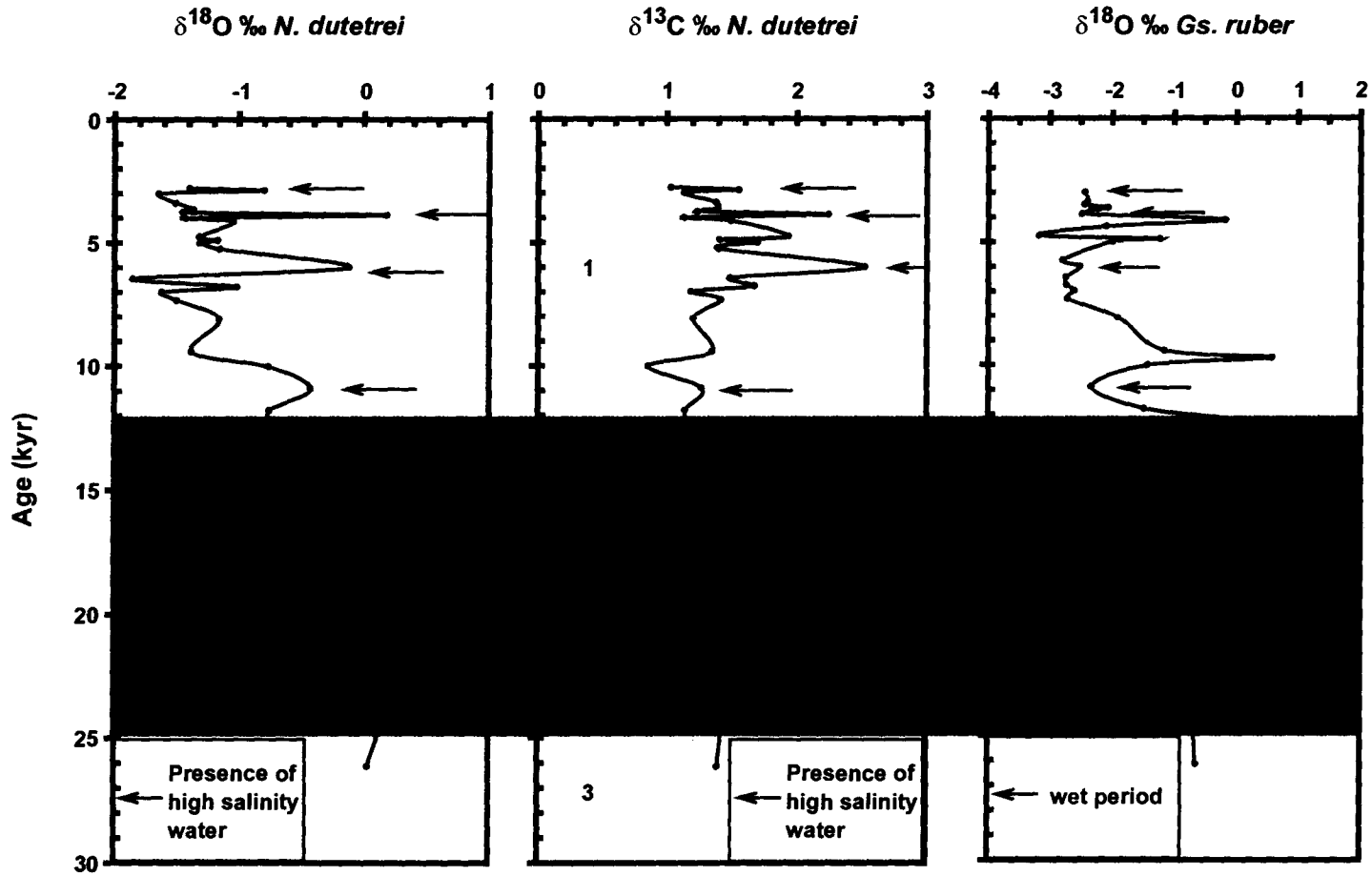

Fig 5.5. Variations in the $\delta^{18}O$ & $\delta^{13}C$ of *N. dutertrei* and the $\delta^{18}O$ variation of *Gs. ruber*. The positive excursion in $\delta^{18}O$ and $\delta^{13}C$ of *N. dutertrei* (as shown by bold arrows) indicates towards the presence of high salinity waters which coincide with the negative excursion in $\delta^{18}O$ of *Gs. ruber* (as shown by bold arrows). The numbers indicates isotopes stages and the shaded region represents glacial stage.

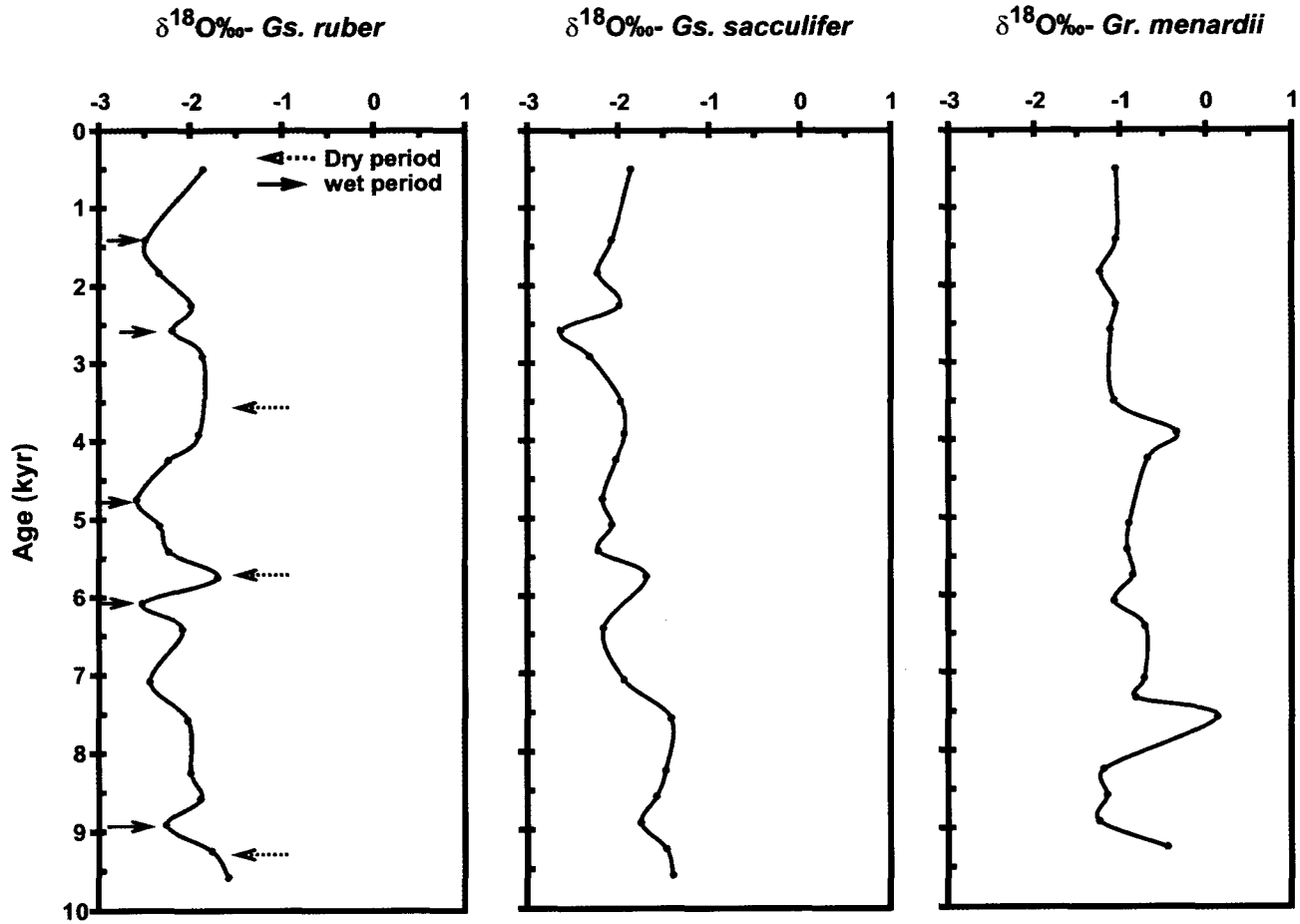

Fig 5.6 $\delta^{18}O$ variation of *Gs. ruber, Gs. sacculifer* and *Gs. menardii* for core SK-172. Note: Bold and dashed arrows represent wet and dry periods respectively.

Holocene i.e., at ~6 kyr, is marked by the negative excursion in $\delta^{18}O$ value of all the three species of foraminifera.

After a brief period of heavier $\delta^{18}O$ value, the lighter value at 4.7 kyr is observed in the $\delta^{18}O$ of *Gs. ruber* and *Gs. sacculifer* indicating the enhancement of summer monsoon precipitation. However, the signal is not strong enough to be picked up by relatively deeper dwelling *Gr. menardii*. Similarly, during late Holocene i.e., at 2.5 kyr and ~1.4 kyr, $\delta^{18}O$ values of *Gs. ruber* and *Gs. sacculifer* show two distinct episodes of enhancement in summer monsoon precipitation and its associated surface runoff.

B} Dry period

At 9.2 kyr, 5.7 kyr and ~4-3 kyr, $\delta^{18}O$ record of *Gs. ruber* and *Gs. sacculifer* shows heavier values. This is mainly attributed to the increase in the E-P budget (enhanced evaporation) due to the weakening of summer monsoon precipitation. Since evaporation is a surface phenomenon, the signal is very well reflected in surface dwelling species and subdued in deeper dwelling *Gr. menardii*.

The clay mineral records (continental proxies) as discussed in chapter 4 from the core SK-172 corroborates with the wet and dry periods as deciphered from the $\delta^{18}O$ variation of planktic foraminifera.

5.6.2 Southeastern Arabian Sea core SK-177/11

The temperature and salinity data of Levitus and Boyer (1994) and Levitus et al.

(1994) suggests that the present day southeastern Arabian Sea is characterized by weak upwelling system (Shetye, 1984) which starts with the onset of summer monsoonal winds. Apart from this, the southeastern Arabian Sea shows fluctuations in E-P budget due to summer monsoon precipitation (Sarkar et al., 2000 and the reference therein). Evidently, all these observations perhaps suggest that the hydrography of the southeastern Arabian Sea (core site) is primarily controlled by the summer monsoon, either through upwelling or monsoonal precipitation. Thus to reconstruct the palaeomonsoonal condition during Holocene, the technique of $\delta^{18}O$ variation along with the isotope gradient (discussed in section 5.3.2) is used and discussed in the following section.

A} Early Holocene

During the early Holocene i.e. from 10-~8 kyr, the $\delta^{18}O$ record of *Gs. ruber* and *Gs. sacculifer* shows a positive excursion whereas the deeper dwelling *N. dutertrei* remains unaffected (shaded region in Fig 5.7). The constructed isotopic gradient ($\Delta\delta^{18}O_{gradient}$) between the species of different depth habitat suggests stratification of the upper ocean with heaviest value for *Gs. ruber* indicating enhanced evaporation. Since evaporation is a surface phenomenon therefore it is very well recorded by surface dwelling *Gs. ruber* than the relatively deeper dwelling *Gs. sacculifer* and *Gr. menardii.*

B} Mid Holocene

During most of the period from 7.3-5 kyr, the $\delta^{18}O$ value of *Gs. ruber* and *Gs. sacculifer* shows lighter value (shaded region in Fig 5.7). During this period, the

$\Delta\delta^{18}O_{gradient}$ shows lightest value for *Gs. ruber* indicating decrease in E-P budget (salinity) due to enhancement in summer monsoon precipitation and its associated runoff. However the deeper dwelling *N. dutertrei*, does not show much variation except at 6 and 3.89 kyr where it shows abrupt enrichment in $\delta^{18}O$ value. The abrupt enrichment in $\delta^{18}O$ value is already dealt in section 5.5.

During the later part of mid Holocene (between 5 - ~ 4 kyr), the $\delta^{18}O$ variation of *Gs. ruber* shows short term abrupt oscillation with heavier values at 4.89 and 4.14 kyr and lighter values at 4.76 and 3.89 kyr (see Fig 5.7). The $\Delta\delta^{18}O_{gradient}$ at 4.89 and 4.14 kyr shows positive gradient (heavier value for the surface dwelling *Gs. ruber*). The positive gradient coupled with the heavier $\delta^{18}O$ values at 4.89 and 4.14 kyr suggests enhanced evaporation owing to the decrease in the intensity of summer monsoon. On the other hand the lighter value at 4.76 kyr and 3.89 kyr along with the negative gradient (lightest value for *Gs. ruber*) suggests decrease in E-P budget due to precipitation. However, the negative isotopic gradient at 3.89 kyr could be due to the combined effect of enhanced precipitation (reflected in $\delta^{18}O$ of *Gs. ruber* and *Gs. sacculifer*) as well as the presence of high salinity water mass at the thermocline depth which is reflected in the $\delta^{18}O$ of *N. dutertrei* (already discussed in section 5.5).

After a brief period of fluctuating condition, the $\delta^{18}O$ variation shows lighter value from 4-3 kyr. The $\Delta\delta^{18}O_{gradient}$ shows similar condition to those at 7.3-5 kyr suggesting decrease in E-P budget owing to the enhancement in summer monsoon precipitation and its associated surface runoff.

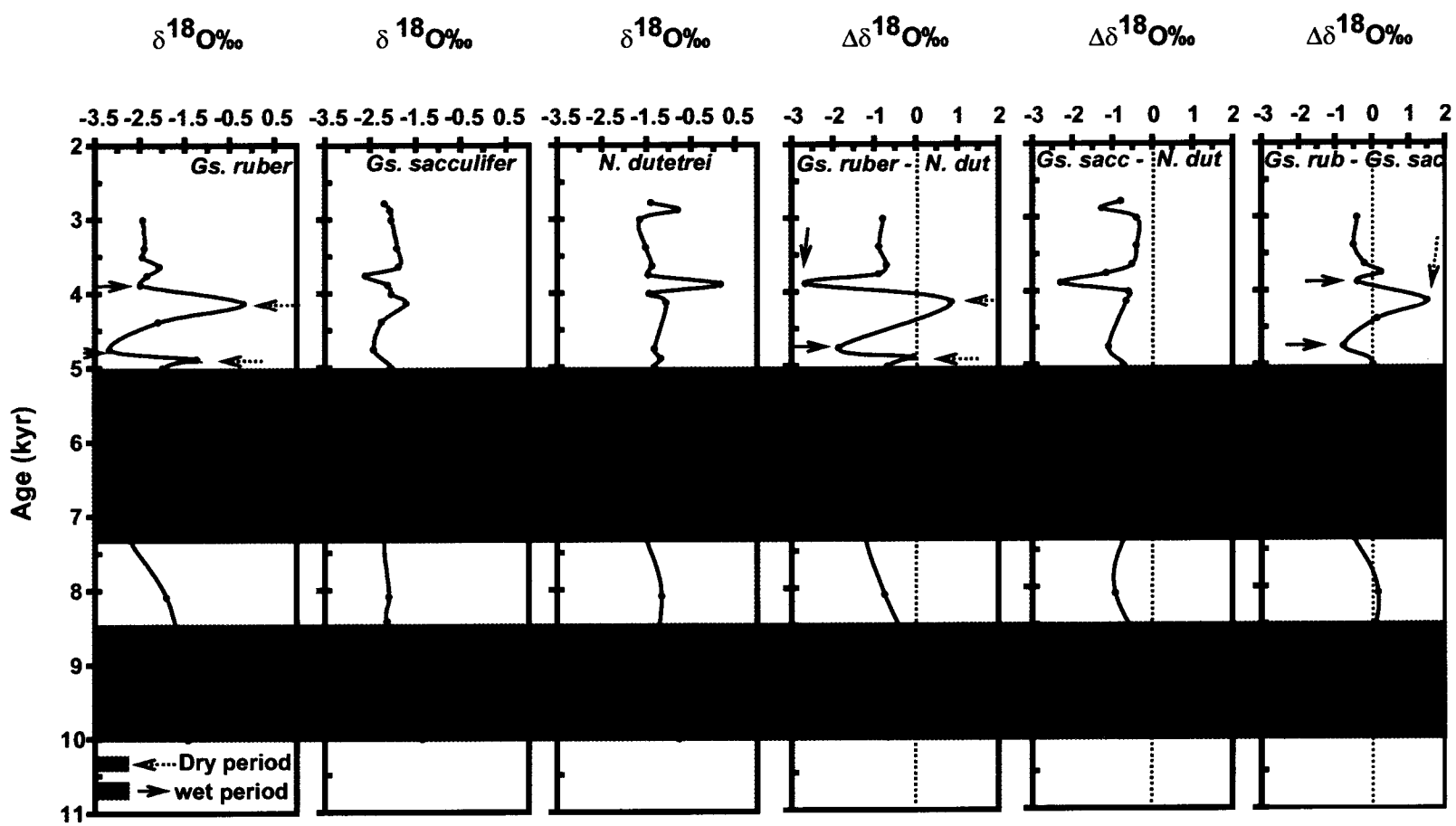

Fig 5.7 $\delta^{18}O$ variation in *Gs. ruber, Gs. sacculifer* and *N. dutertrei* along with the isotopic gradient ($\Delta\delta^{18}O$) for core SK-177/11. Bold and dashed arrows along with the shaded region represent wet and dry periods respectively.

5.6.3 Palaeomonsoonal condition during the Holocene

To investigate the coherency of palaeomonsoonal records of Holocene along the entire Arabian Sea, the records from western and eastern Arabian Sea are compared (see Fig 5.8). The eastern Arabian Sea records include the $\delta^{18}O$ variation of present study i.e., core SK-172, SK-177/11 ($\delta^{18}O$-*Gs. ruber*), SK-208 ($\delta^{18}O$-*Gs. sacculifer*) along with the record of Sarkar et al., 2000 (3268G5; $\delta^{18}O$-*Gs. sacculifer*); whereas the western Arabian Sea record includes core ODP 723A of Gupta et al., 2003 (%*Gs. bulloides*). Among these records the $\delta^{18}O$ variation of the cores SK-172, SK-177/11, SK-208 and 3268G5 reflects the strength of summer monsoon precipitation and its associated runoff (Sarkar et al., 2000b and the reference therein) and the core ODP 723A reflects the strength of summer monsoon wind.

During the early Holocene, the general trend of $\delta^{18}O$ variation shows enrichment (shown by shaded region in Fig 5.8) in all the cores of eastern Arabian Sea (SK-172, SK-177/11, SK-208, 3268G5). The $\delta^{18}O$ enrichment during this period indicates an increase in E-P budget due to the reduced intensity of SW monsoon. However, the upwelling records off Oman (Gupta et al., 2003), rainfall in the coastal mountain ranges of Oman (Fleitmann et al., 2003) show contrasting trends suggesting enhancement in SW monsoon during the early to mid Holocene. Moreover, from the core SK-177/11, a highly fluctuating period with abrupt dry and wet condition is reported between ~5- and ~4 kyr, which is not recorded by the core SK-172 and SK-208 due to its coarser resolution. These results of dry period during ~4 kyr are also corroborated from the continental records of Sukumar et al. (1993).

All these observations suggest a coherency between the records of Indian peninsula and marine records off *Sahyadri* whereas the upwelling records of western Arabian Sea shows an opposite trend. The spatial variability of monsoon in different basins of Arabian Sea suggests different monsoon domains having its own controlling factor (Staubwasser, 2006). They correlated the contrasting trend between eastern and western Arabian Sea with the "active" and "break" period of monsoon, akin to the present day. They also suggested that during early Holocene prolonged "break" period could have resulted in enhanced summer monsoon in western Arabian Sea.

5.7 Palaeoproductivity variation during glacial interglacial transition

Organic carbon in sediments is widely used as a proxy to decipher the palaeoproductivity and hence the intensity of summer/winter monsoon. Palaeoproductivity records from the eastern Arabian Sea invoke an argument that the organic carbon does not reflect the overhead productivity (Sarkar et al., 1993; Bhushan et al., 2001) rather it is also affected by the bottom water oxygen conditions, post depositional changes, texture and sedimentation rate. Moreover, terrestrial sources of organic carbon can also get mixed with the marine organic carbon (Pattan et al., 2003) and may lead to an erroneous interpretation. Therefore, for palaeoproductivity determination, it is better to use multiple proxies rather than a single, traditional proxy i.e., organic carbon. In view of this foraminiferal $\delta^{13}C$ can be used for palaeoproductivity determination because during high productivity, phytoplankton preferentially fix more ^{12}C than ^{13}C, leaving the sea water enriched in $\delta^{13}C$ (Kroopnick, 1985) which in turn is utilized by foraminifera. Thus, the higher organic productivity in the euphotic zone is likely to be reflected in the planktic foraminiferal calcite shells.

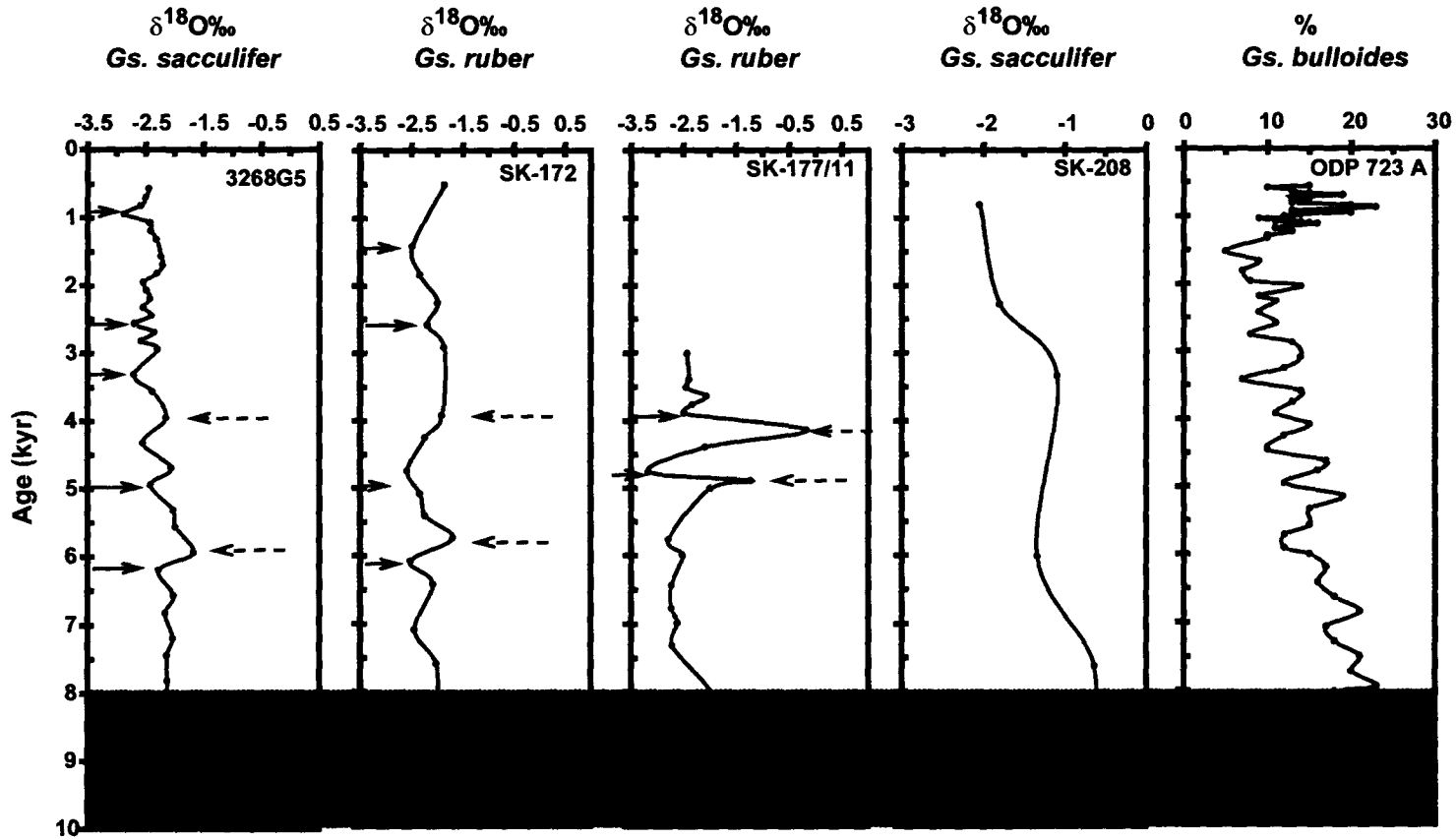

Fig 5.8 $\delta^{18}O$ variation as documented in SK-172, SK-177/11 (*Gs. ruber)*, SK-208 (*Gs. sacculifer)* of this study and *Gs. sacculifer* from the data of Sarkar et al., 2000 (3268G5) and Gupta et al., 2003 (ODP 723 A). Bold and dashed arrows represent wet and dry periods respectively. Note: the shaded region represents dry periods in 3268G5, SK-172, SK-177/11 and SK-208 whereas in Gupta et al., 2003 intense upwelling is recorded.

The oxidation of organic matter at deeper depth results in the depletion of $\delta^{13}C$ which through upwelling mixes with the surface water to alter the signal considerably (the net change in $\delta^{13}C$ of surface water depends on these two competing processes i.e. productivity and upwelling). Upon knowing the past variation of upwelling through $\delta^{18}O$ of foraminiferal calcite, productivity variation can be deciphered. Considering all these facts, two sediment cores collected from northern and southern part of eastern Arabian Sea (SK-208 and SK-177/11) were studied for palaeoproductivity using foraminiferal $\delta^{13}C$ and the results are compared with the traditional proxy i.e., organic carbon.

5.7.1. Central part of eastern Arabian Sea core SK-208

Planktic foraminiferal $\delta^{13}C$ of three different species viz *Gs. ruber*, *Gs. sacculifer* and *N. dutertrei* are shown in Fig 5.9. All the results are reported in ‰ with respect to V-PDB. It is evident from Fig 5.9 that the $\delta^{13}C$ value fluctuates between 2.5-1.7‰, 1.4-2.2‰ and 1.2-1.7‰ for *Gs. sacculifer*, *Gs. ruber* and *N. dutertrei* respectively. Based on these variations palaeoproductivity trend is deciphered and discussed.

A} The glacial period (MIS 2 and 4)

During glacial period 2 and 4, *Gs. ruber* and *Gs. sacculifer* shows positive excursion in $\delta^{13}C$ value whereas deeper dwelling *Gr. menardii* does not show any variation (see Fig 5.9.). The enrichment of $\delta^{13}C$ in surface dwelling foraminifera suggests increase in productivity. Since the productivity decreases with depth in the photic zone (maximum on sea surface) therefore it is very well reflected in surface

dwelling planktic foraminifers and subdued in deeper dwelling planktic foraminifera. The increase in productivity during glacial period matches with the downcore variation of organic carbon (discussed in chapter 4; section 4.5). These results of increase in productivity during glacials are also corroborated with the earlier studies of Prabhu et al. (2004), (2005).

B} The interglacial period (MIS 1, 3 and 5)

As compared to the glacial periods, surface dwelling *Gs. sacculifer* shows depletion in $\delta^{13}C$ values during interglacial periods whereas the *Gr. menardii* remains unaffected. This suggests decrease in surface productivity. On the contrary, organic carbon shows enrichment in this period which could be attributed to the preservation by finer siliciclastic sediments rather than productivity (discussed in Chapter 4; Section 4.5.2).

5.7.2. Southeastern Arabian Sea core SK-177/11

Core SK-177/11 is collected from southeastern Arabian Sea, a region of high productivity (Qasim, 1982; Bhattathiri et al., 1996) due to summer monsoon upwelling. The high productivity is very well reflected in the surface sediment of this region showing enrichment in organic carbon (Prakash Babu et al., 1999). Thus, to reconstruct palaeoproductivity of late Quaternary, $\delta^{13}C$ of foraminiferal calcite as shown in Fig 5.10 is discussed along with the organic carbon.

A} MIS 3

It is evident from Fig 5.10 that at ~26 kyr, $\delta^{13}C$ of *Gs. sacculifer* shows 2.2‰ almost comparable to that of Holocene. This period is also marked by the increase in calcium carbonate and decrease in organic carbon. Thus the enrichment in $\delta^{13}C$ of foraminiferal calcite coupled with increase in calcium carbonate suggests an increase in productivity probably due to the enhancement in summer monsoon intensity.

B} Glacial period (MIS 2)

During 16.4-16.2 kyr, 15.5-14.4 kyr and 12.3-11 kyr, $\delta^{13}C$ of *Gs. ruber* shows a large negative excursion (shown by bold arrow in Fig 5.10) of 0.6‰, 1.1‰ and 2.0‰ respectively. The negative excursion in $\delta^{13}C$ of Gs. *ruber* coincides with the period of lighter $\delta^{18}O$ i.e. enhanced summer monsoon precipitation (see Fig 5.10). The depletion in $\delta^{13}C$ is not recorded by deeper dwelling *Gs. sacculifer* and *N. dutertrei* except at 12.3- 11 kyr. The negative excursion of $\delta^{13}C$ and $\delta^{18}O$ as recorded by *Gs. ruber* possibly indicates the role of fresh water influx because the CO_2 which is dissolved in fresh water is depleted in $\delta^{13}C$ and $\delta^{18}O$ (Mulitza et al., 1999 and the references therein). *Gs. ruber* is a surface dweller therefore shows prominent signal than its deeper counterpart *Gs. sacculifer* and *N. dutertrei.* Hence in the precipitation dominated southeastern Arabian Sea, *Gs. ruber* cannot truly represent palaeoproductivity fluctuations.

However $\delta^{13}C$ of *Gs. sacculifer* shows decrease in productivity during glacial period which is very well corroborated by the organic carbon content (discussed in chapter 4; section 4.5.1). The reduced thermal gradient between land and ocean owing

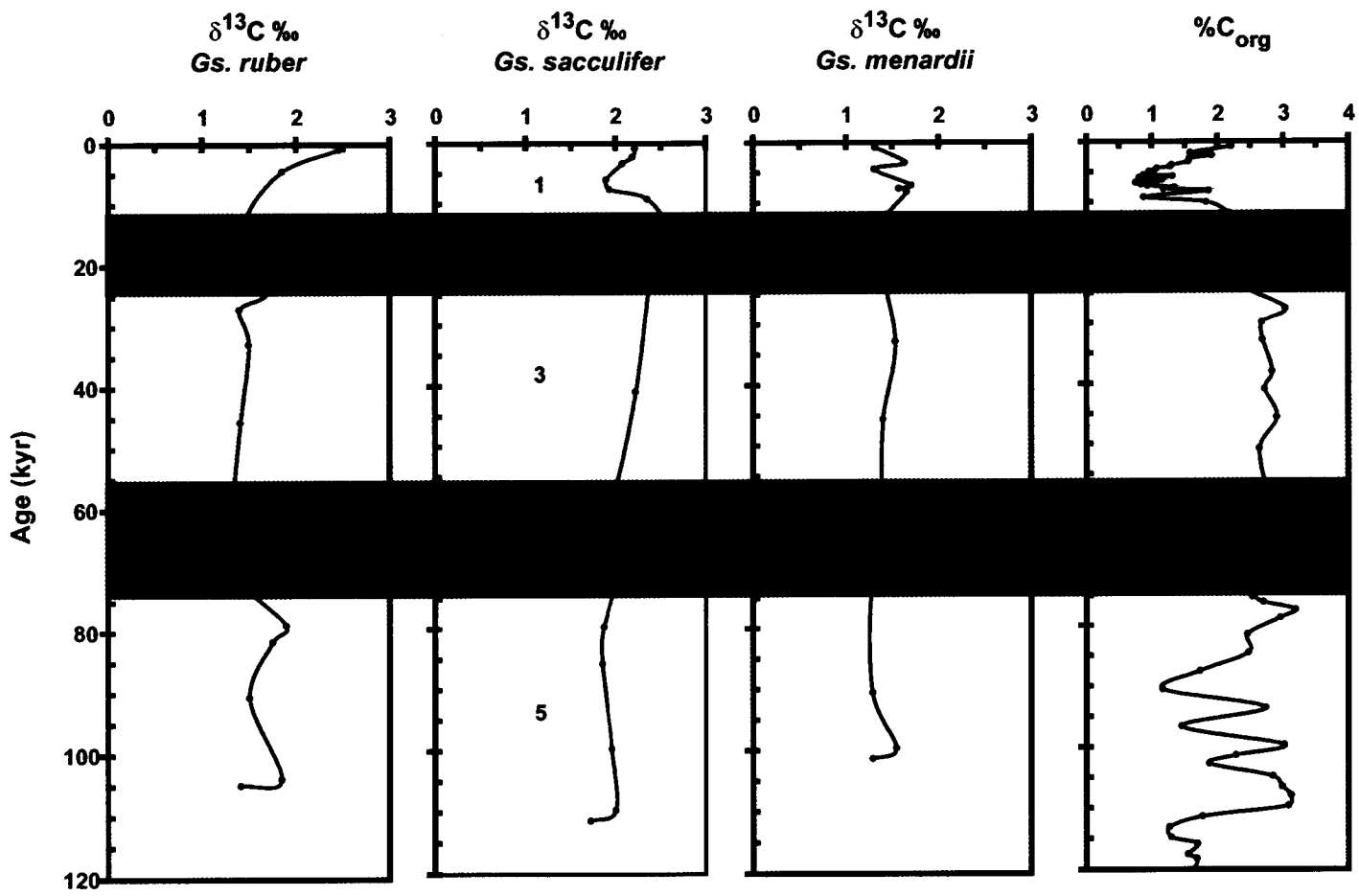

Fig 5.9. $\delta^{13}C$ variation in *Gs. ruber*, *Gs. sacculifer* and *Gr. menardii* along with the organic carbon content for core SK-208. The numbers indicates isotopes stages and the shaded region represents glacial period. Note: the trend of $\delta^{13}C$ and organic carbon is similar.

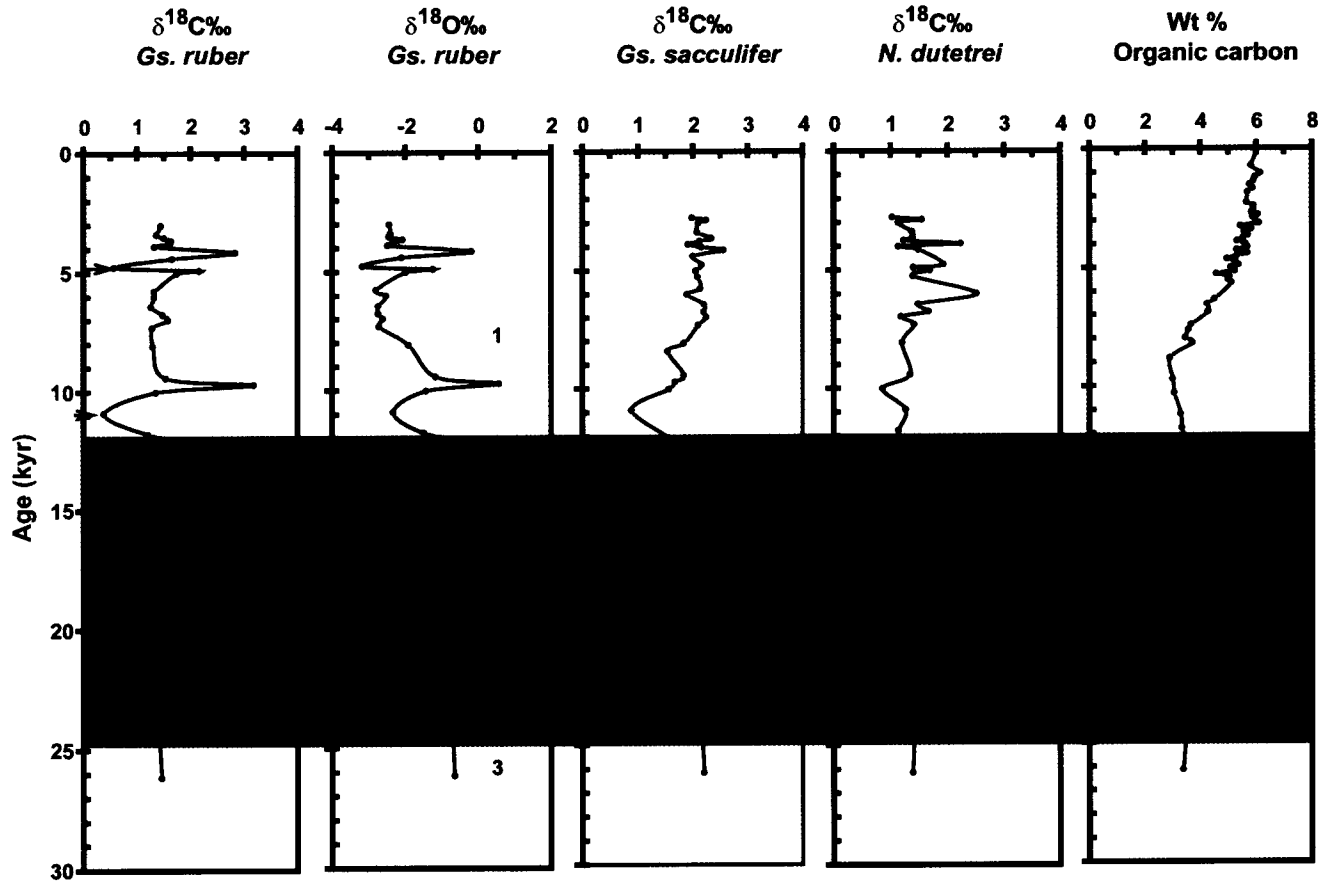

Fig 5.10 $\delta^{13}C$ variation in *Gs. ruber*, *Gs. sacculifer* and *N. dutertrei* for core SK-177/11. $\delta^{18}O$ variation in *Gs. ruber* along with the Wt% of organic carbon is also shown. The numbers indicates isotopes stages and the shaded region represents glacial period. Note: the trend of $\delta^{18}O$ and $\delta^{13}C$ in *Gs. ruber* is similar.

to the extensive snow cover over the Tibetan plateau could have resulted in the weakening of SW monsoonal wind and hence productivity. The results of decrease in monsoon induced productivity are consistent with the earlier report by Pattan et al., (2003).

C} Holocene period

During the entire Holocene the $\delta^{13}C$ of *Gs. ruber* shows constant value except at certain intervals where it fluctuates in accordance with the $\delta^{18}O$ (see Fig 5.10). This indicates that even in the Holocene $\delta^{13}C$ of *Gs. ruber* is affected by the freshwater input and cannot be considered for palaeoproductivity determination. Hence for palaeoproductivity determination, $\delta^{13}C$ of *Gs. sacculifer* is utilised. During early Holocene, $\delta^{13}C$ of *Gs. sacculifer* shows 1.5‰ whereas an enrichment of 2.2‰ is recorded during mid-late Holocene. Deeper dwelling *N. dutertrei* shows an average of 1.4‰ during the entire Holocene except at 6 kyr, 3.89 kyr and 2.88 kyr which are attributed to the sub surface intrusion of saline water probably of Red Sea origin (discussed separately in section 5.5). All these observations indicate that during early Holocene productivity has decreased while during mid-late Holocene productivity has increased. The increase in productivity is very well correlated by the records of organic carbon content (discussed in chapter 4; section 4.5.1). Thus, the correlation between $\delta^{13}C$ of *Gs. sacculifer* and organic carbon content (discussed in chapter 4; section 4.5.1) suggests surface overhead productivity to be the primary control for the deposition of organic carbon. These results of increase in surface productivity during mid-late Holocene match with the records of Thamban et al., (2001).

CHAPTER 6

CONCLUSION

6.1 Global Teleconnection of the Indian monsoon system

The most important aspect of palaeoclimatic research is to understand the cause of abrupt climate fluctuations and its teleconnection with the other parts of the globe. Pertaining to this various records exist which indicate a possible association of the Asian monsoon on millennial to centennial time scales with the high-latitude climate changes (Neff et al., 2001; Altabet et al., 2002; Gupta et al., 2003; Fleitmann et al., 2003; Naidu et al., 2006). Most of these records that suggest a teleconnection between tropical and extra tropical regimes are based on the studies from the western Arabian Sea or from the coast of western Arabian Sea. However, a few records are also available from the eastern Arabian Sea (e.g. Sarkar et al., 2000; Thamban et al., 2001; Tiwari et al., 2006). The present study makes an attempt to establish a teleconnection between Indian monsoon and the high latitude climate of the northern hemisphere by comparing SW monsoon fluctuation (represented by $\delta^{18}O$ record) of the eastern Arabian Sea with that of North Atlantic climate (represented by the $\delta^{18}O$ record of GISP2-Greenland ice core). The comparison of these records is shown in Fig 6.1.

Notwithstanding the differing resolution of the compared data, the SW monsoon shows fluctuation that can be correlated with the Greenland ice core (see Fig 6.1). From the fig 6.1 it may be evident that during ~15 kyr the enhanced SW monsoon precipitation recorded in the eastern Arabian Sea (SK-172 and SK-177/11) coincides with the warm period of North Atlantic also called as Dansgaard/Oeschger interstadials (D/O-1). On the other hand, the reduced precipitation during Younger Dryas in the eastern Arabian Sea coincides with the cold period of North Atlantic. The wet period which ushered towards the end of Younger Dryas also matches with the warmer period

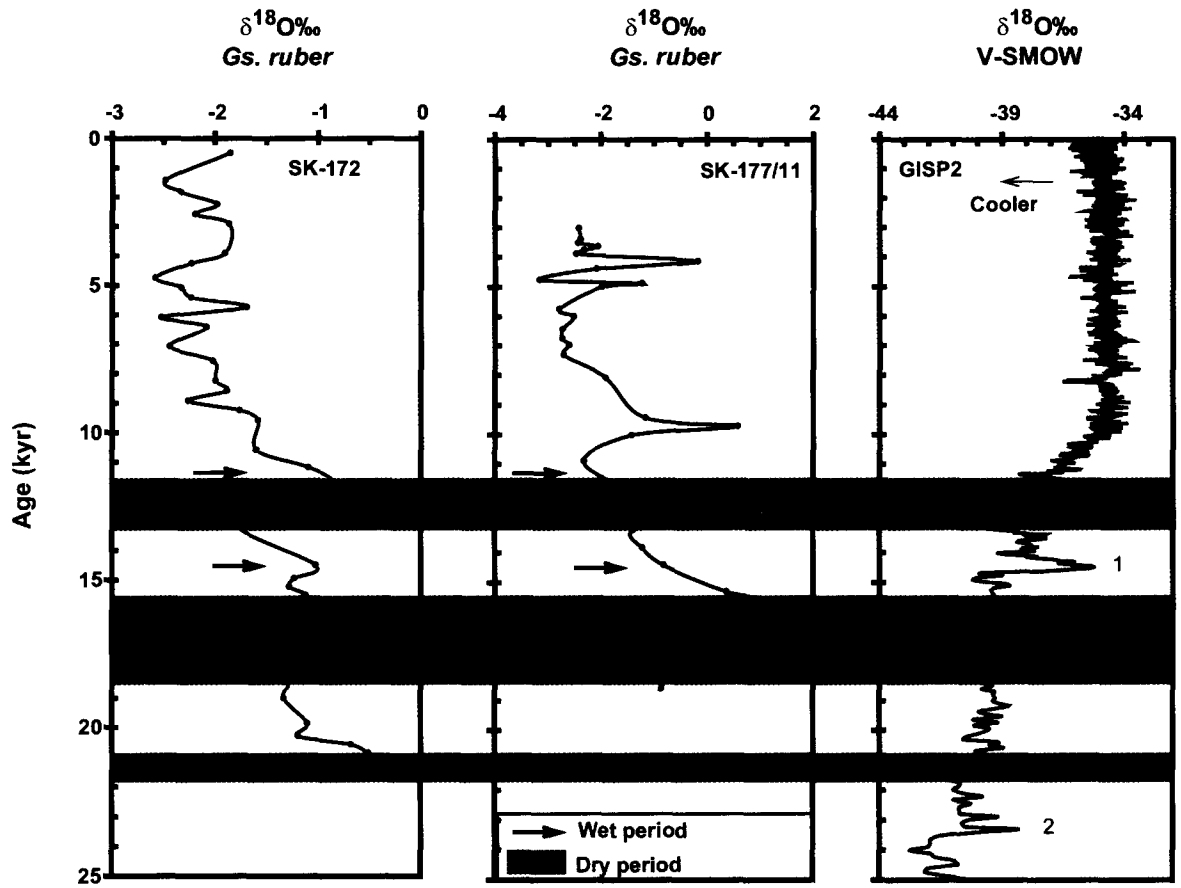

Fig 6.1. Comparison of $\delta^{18}O$ records of G. ruber (core SK-172 and SK-177/11) with the $\delta^{18}O$ records of GISP2 core. The numbers (1–2) in GISP2 core indicate Dansgaard/Oeschger interstadials (Dansgaard et al., 1993).

of North Atlantic. However, during Holocene such a correlation between eastern Arabian Sea and North Atlantic climate is not clearly evident and may need to be studied in greater detail. The reduced correlation between these two isolated regimes during Holocene was also reported by the equatorial records of Tiwari et al. (2006). However, during pre-Holocene, there exists a certain control of the North Atlantic climate over the Indian monsoon perhaps through atmospheric circulation.

6.2 Conclusion

The results of present work using a multiproxy approach are concluded in this chapter. The proxy records have been archived from the three sediment gravity cores collected across the length of eastern Arabian Sea, where SK-172 and SK-177/11 collected from the upper slope off Goa and Cochin and SK-208 collected from a topographic high off Karwar. The water depth ranges from 776 m to 383 m. The multiple proxies measured and evaluated include the organic carbon, calcium carbonate, clay minerals, oxygen & carbon isotopes and the sediment textural parameters. Based on the temporal variation of these proxies, the palaeoclimatic condition of the late Quaternary has been deciphered.

1. Sediment mixing specially the carbonates from different sources i.e., terrigeneous and/or relict sediments with the marine carbonates (i.e., foraminifers and cocolithosphores) is evident from the records of present study. The present study also suggests that the slope failure owing to sea level change and/or enhanced fluvial discharge to be the probable mechanism for the mixing of sediment from different sources.

2. In the present investigation, organic carbon and silisic fraction content of the cores mainly reflect the overhead surface productivity and terrigeneous input, respectively. Palaeoproductivity records from the northern part of eastern Arabian Sea (SK-208, SK-172) show an increase in productivity during glacial periods which is attributed to the intensification of NE monsoon and convective overturning. Whereas in southeastern Arabian Sea (SK-177/11), a decrease in productivity during glacial period is attributed to the weakening of upwelling/wind induced mixing due to the reduced strength of SW monsoon.

3. During MIS 3 (~26 kyr), the proxy records from the southeastern Arabian Sea (SK-177/11) show a decrease in organic carbon along with an increase in calcium carbonate. However $\delta^{13}C$, a palaeoproductivity indicator shows enrichment during this period suggesting increased productivity. Therefore, inspite of enhanced productivity; the low organic carbon during this period perhaps suggests poor preservation of organic carbon in the sediments.

4. During Holocene $CaCO_3$ from the southeastern Arabian Sea seems to be of marine origin i.e., free from dilution effect and can be correlated with the intensity of monsoon. Thus, increasing trend of $CaCO_3$ together with the increase in organic carbon and silisic fraction suggests intensification of southwest monsoon during Holocene.

5. Clay mineral records from the northern part of eastern Arabian Sea (SK-172) show enrichment of kaolinite during 14.8-14 kyr and MWP 1b indicating continental

humidity owing to the stronger SW monsoon. On the other hand, the depletion in kaolinite, K/I ratio during LGM and Younger Dryas suggests continental aridity.

6. The clay mineral record of sediment core collected from the Topographic high off Karwar (SK-208) demonstrates the dispersal of illite, the supply of which may have been regulated by the summer monsoon circulation. Based on the variation of illite, it is observed that the summer monsoon circulation was stronger during interglacial and weaker during glacials.

7. From illite distribution, it is suggested that during ~110 kyr the summer monsoon circulation was stronger than the present. During early Holocene the strength of summer monsoon circulation was weaker however, it became stronger in mid-late Holocene.

8. The present study of sea level and SST corrected $\delta^{18}O$ variation on foraminiferal calcite mainly reflects the regional E-P budget which seem to have been controlled by the intensity of summer monsoon precipitation. The magnitude of $\delta^{18}O$ variation (i.e. $\Delta\ \delta^{18}O$) suggests early deglacial strengthening of SW monsoon, the global melt water pulse 1a and 1b and Bølling-Allerød warming, accompanied by the enhanced summer monsoon precipitation in eastern Arabian Sea. The LGM and Younger Dryas period is characterized by the enhanced evaporation due to the reduced strength of SW monsoon.

9. During early Holocene $\delta^{18}O$ variation of surface dwelling foraminifera suggests enhanced evaporation owing to the weakening of SW monsoon whereas record

from Oman suggests stronger SW monsoon; thus showing the spatial variability as also seen in the present day monsoon.

10. The comparatively lighter values of foraminiferal $\delta^{18}O$ in southeastern Arabian Sea (core SK-177/11) compared to the northeastern part (core SK-172) suggest the influence of summer monsoon circulation in advecting the low salinity waters (monsoonal precipitation and/or runoff) more to the southeastern Arabian Sea.

11. During ~11, 6, 3.89 and 2.88 kyr, the $\delta^{18}O$ record of southeastern Arabian Sea shows the possible presence of high salinity water mass at the thermocline depth and it appears to be controlled by the summer monsoon circulation.

12. In the present study, $\delta^{13}C$ variation of surface dwelling *Gs. ruber* appears to be affected by the monsoon runoff (i.e. $\delta^{13}C$ of fresh water) and therefore was not considered as a proxy for palaeoproductivity determination especially in the precipitation dominated southeastern Arabian Sea.

13. In the northern part of eastern Arabian Sea productivity during glacial period (MIS 2, 4) increases due to the convective overturning and subsequent nutrient injection while in the southeastern Arabian Sea productivity decreases owing to the weakening of upwelling and SW monsoon.

14. During pre-Holocene the SW monsoonal fluctuations as recorded in the present study seem to have been controlled by the North Atlantic climate, perhaps suggesting a tropical –extra tropical connection.

6.3 Suggestions for future work

Multi proxy records from the present investigation using three sediment cores collected from the upper slope and topographic high of the eastern Arabian Sea revealed various geological, oceanographic and biogeochemical processes affecting the different component of sediments and its dispersal pattern. An attempt made to understand the unique association of these variables with the palaeoclimatic condition of the late Quaternary reports some interesting facts from the present study, which however need to be addressed for their better understanding on a regional scale. This includes:

1. The shelf and slope sediments of the northern part of eastern Arabian Sea comprise the relict carbonate deposits of biogenic origin and its disintegrated material. During the period of low sea level stand and/or enhanced fluvial strength during Holocene, the relict carbonates are reported to have mixed with the sediments of slope (Bhushan et al., 2001; and in the present study) or even in the deep ocean. Therefore a suitable technique has to be employed for the identification of these transported carbonate and the mixed modeling studies should be initiated for the quantification of these carbonates.

2. The clay mineral assemblage from the slope and topographic high are reported to contain the admixtures of Indus province with the Deccan province in the north and gneissic province in the south (Rao and Rao, 1995). Since these provinces have distinct geological origin/regime, a suitable geochemical proxy may be identified to quantify the contribution of the source.

3. From the variation of carbon and oxygen isotopes of surface dwelling *Gs. ruber*, $\delta^{13}C$ seems to be affected by the fresh water influx along with the $\delta^{18}O$. Therefore the spatial and temporal (monsoon and pre-monsoon) distribution of carbon isotope ($\delta^{13}C$) of sea water should be studied along with the oxygen isotopic composition.

4. During MIS 3, palaeoproductivity record from the southeastern Arabian Sea shows enrichment in $\delta^{13}C$ and $CaCO_3$. In variance to this, the organic carbon shows depletion probably due to the poor preservation of organic carbon. Therefore in this region especially during this period, the study of redox sensitive elements like Cr, V and Mn is recommended as it could better reflect the prevailed Oxygen Minimum Zone (OMZ) condition.

5. The high salinity water mass identified at the subsurface depth of southeastern Arabian Sea should be studied in detail by using oxygen and carbon isotopes of benthic foraminifera which may provide a better understanding of the prevailed conditions .

6. The mechanism suggesting tropical – extra tropical connection need to be probed in detail by using global climate models.

REFERENCES

1. Agnihotri, R. (2001) Chemical and isotopic studies of sediments from the Arabian Sea and Bay of Bengal. Unpublished Ph.D. thesis, M. L. S. University, Udaipur.

2. Agnihotri, R., Dutta, K., Bhushan, R., Somayajulu, B. L. K. (2002) Evidence for solar forcing on the Indian monsoon during the last millennium. *Earth Planet. Sci. Lett.*, **198**, 521–527.

3. Agnihotri, R., Sarin, M. M., Somayajulu, B. L. K., Jull, A. J. T., Burr, G. S. (2003) Late Quaternary biogenic productivity and organic carbon deposition in the eastern Arabian Sea. *Palaeogeogr. Palaeclimatol. Palaeoecol.*, **197,** 43-60.

4. Alley, R.B and Mc Ayeal (1994) Ice-rafted debris associated with binge/purge oscillations of the Laurentide Ice Sheet. *Palaeoceanography*, **9(4)**, 503-512. 10.1029/94PA01008.

5. Altabet, M. A., Higginson, M. J., Murray, D. W. (2002) The effect of millennial-scale changes in Arabian Sea denitrification on atmospheric CO2. *Nature*, 415, 159-162.

6. Anderson, D. M., Overpeck, J. T., Gupta, A. K. (2002) Increase in the Asian SW monsoon over the four centuries. *Science*, **297**, 596-599.

7. Anderson, D. M. and Prell, W. L. (1993) A 300 Kyr record of upwelling off Oman during the late Quaternary: evidence of the Asian Southwest Monsoon. *Palaeoceanography*, **8**, 193-208.

8. Andruleit, H., Von Rad, U., Bruns, A., Ittekkot, V. (2000) Cocolithophore from sediment traps in the northeastern Arabian Sea off Pakistan. *Mar. Micropal.*, **38**, 285-308.

9. Anil Kumar, A., Rao, V. P., Patil, S. K., Kessarkar, P. M., Thamban, M. (2005) Rock magnetic records of the sediments of the eastern Arabian Sea: Evidence for late Quaternary climate change. *Mar. Geol.*, **220**, 59-82.

10. Banakar, V. K., Oba, T., Chodankar, A. R., Kuramoto, T., Yamamoto, M., Minagawa, M. (2005) Monsoon related changes in the sea surface productivity and water column denitrification in the Eastern Arabian Sea during last glacial cycle. *Mar. Geol.*, **219**, 99-108.

11. Bard, E., Hamelin, B., Arnold, M., Montaggioni, L., Cabioch, G., Faure, G., Rougerie, F. (1996a) Deglacial sea-level record from Tahiti corals and the timing of global meltwater discharge. *Nature*, **382**, 241–244.

12. Bard, E., Jouannic, C., Hamelin, B., Pirazzoli, P., Arnold, M., Faure, G., Sumosusastro, P., Syaefuddin (1996b) Pleistocene sea level and tectonic uplift based on dating of corals from Sumba Island, Indonesia. *Geophysical Res. Lett.*, **23**, 1473-1476.

13. Bard, E. (1998) Geophysical and Geochemical implications of the radiocarbon calibration. *Geochem. Cosmochem. Acta.*, **62 (12),** 2025-2038.

14. Bard, E., Raisbeck, G., Yiou, F., Jouzel, J. (2000) Solar irradiance during the last 1200 years based on cosmogenic nuclides. *Tellus*, **52B**, 585-992.

15. Barnes, H. (1959) Apparatus and methods in Oceanography. (London: Allan and Unwin) pp 341.

16. Beal, L. M., Chereskin, T. K., Bryden, H. L., F.eld, A. (2003) Variability of water properties, heat and salt fluxes in the Arabian Sea, between the onset and wane of the 1995 southwest monsoon. *Deep-Sea Res. II*, **50,** 2049–2075.

17. Beaufort, L., Lancelot, Y., Camberlin, P., Cayre, O., Vincent, E., Bassinot, F., Labeyrie, L. (1997) Insolation cycles as a major control of the equatorial Indian Ocean primary production. *Science*, **278**, 1451–1454.

18. Bhattathiri, P.M.A., Pant, A., Sawant, S., Gauns, M., Matondkar, S.G.P., Mohanraju, R. (1996) Phytoplankton production and chlorophyll distribution in the eastern and central Arabian Sea in 1994–1995. *Curr. Sci.*, 71 (11), 857–862.

19. Bhushan, R., Dutta, K., Somayajulu, B. L. K. (2001) Concentrations and burial fluxes of organic and inorganic carbon on the eastern margins of the Arabian Sea. *Mar. Geol.*, **178**, 95-112.

20. Biscaye, P. E. (1965) Mineralogy and sedimentation of recent deep sea clays in the Atlantic Ocean and adjacent seas and Oceans, *Bull. Geol. Soc. Am.*, **76**, 803-832.

21. Bond, G., Broecker, W., Johnsen, S., Mc Manus, J., Labeyrie, L., Jouzel, J., Bonani, G. (1993) Correlations between climate records from North Atlantic sediments and Greenland ice. *Nature*, **365**, 143-147.

22. Bond, G., Showers, W., Cheseby, M., Lotti, R., Almasi, P., deMenocal, P., Cullen, H., Hajdas, I., Bonani, G. (1997) A pervasive millennial-scale cycle in North Atlantic Holocene and glacial climates. *Science*, **278**, 1257-1266.

23. Bond, G., Kromer, B., Beer, J., Muscheler, R., Evans, M. N., Showers, W., Hoffmann, S., Lotti-Bond, R., Hajdas, I., Bonani, G. (2001) Persistent solar influence on North Atlantic climate during the Holocene. *Science*, **294**, 2130-2136.

24. Bouvier-Soumagnac, Y., Duplessy, J. C. (1985) Carbon and oxygen isotopic composition of planktonic foraminifera from laboratory culture, plankton tows and recent sediment: implications for them reconstruction of paleoclimatic

conditions and of the global carbon cycle. *Jour. Foraminiferal Res.*, **15**, 302–320.

25. Broecker, W. S., Denton, G. H., (1990) What drives glacial cycles? *Scientific American*, **262**, 42-50.

26. Broecker, W. S., (1997) Thermohaline circulation, the Achilles heel of our climate system: Will man-made CO_2 upset the current balance? *Science*, **278**, 1582-1588.

27. Broecker, W. S., (2003) Does the trigger for abrupt climate change reside in the ocean or in the atmosphere? *Science*, **300**, 1519-1522.

28. Bruce, J. G., Johnson, D. R., Kindle, J. C. (1994) Evidence for Eddy formation in the Eastern Arabian Sea during the North East monsoon. *Jour. Geophys. Res.*, **99**, 7651-7664.

29. Burns, S. J., Fleitmann, D., Matter, A., Neff, U., Mangini, A. (2001) Speleothems evidence from Oman for continental pluvial events during interglacial periods. *Science*, **29 (7)**, 623-626.

30. Burns, S. J., D. Fleitmann, Mudelsee, M., Neff, U., Matter, A., Mangini, A. (2002) A 780-year annually resolved record of Indian Ocean monsoon precipitation from a speleothem from south Oman, *Jour. Geophys. Res. Atmos.*, ***107*(D20)**.

31. Burns, S. J., Fleitmann, D., Matter, A., Kramers, J., Al-Subbary, A. (2003) Indian Ocean climate and an absolute chronology over Dansgaard/Oeschger Events 9 to 13. *Science*, **301**, 1365-1367.

32. Calvert, S. E., Pedersen, T. F., Naidu, P. D., von Stackelberg, U. (1995) On the organic carbon maximum on the continental slope of the eastern Arabian Sea. *Jour. Mar. Res.*, **53**, 269–296.

33. Cane, M. A. (1998) A role for the tropical Pacific. *Science*, **282**, 59-61.

34. Carpenter, G. (1981) Coincident slump/clatherate complexes on the U.S. Atlantic continental slope. *Geo-marine Lett.*, **1**, 29-32.

35. Carroll, D. (1970) Clay Minerals: A Guide to their X-ray Identification. *Geol. Soc. Am., Spec. Pap.* 77- 80 pp.

36. Cayre, O and Bard, E. (1999) Planktonic foraminiferal and alkenone records of the last deglaciation from the eastern Arabian Sea. *Quat. Res.*, **52** 337-342.

37. Chamely, H. (1989) *Clay sedimentology*. Springer-Verlag, Germany, pp 623

38. Chauhan, O. S and Almeida, F. (1993) Influence on Holocene Sea level, regional tectonics, and fluvial gravity and slope currents induced sediments on the regional geomorphology of the continental slope off Northwestern India. *Mar Geol.*, **112**, 313-328.

39. Chauhan, O. S., Gujar, A. R. (1996) Surficial clay mineral distribution on the southwestern continental margin of India: Evidence of input from the Bay of Bengal. *Cont. Shelf. Res.*, **16**, 321-333.

40. Chodankar, A. R., Banakar, V. K., Oba, T. (2005) Past 100 kyr surface salinity-gradient response in the Eastern Arabian Sea to the summer monsoon variation recorded by $\delta^{18}O$ of *G. sacculifer*. *Glob. Planet. Change*, **47**, 135-142.

41. Clemens, S., Prell, W. L., Murray, D., Shimmield, G. B., Weedon, G. (1991) Forcing mechanisms of the Indian Ocean monsoon. *Nature*, **353**, 720-725.

42. Cowis, G. L., Calvert, S. E., Pederson, T. F., Von Rad, U. (1996) International symposium on Geology and Geophysics of the Indian Ocean. National Institute of Oceanography, Goa, pp. 64-65 (abs).

43. Craig, H. (1957) Isotopic standards for carbon and oxygen and correction factors for mass spectrometric analysis of carbon dioxide. *Geochem. Cosmochem. Acta*, **12**, 133-149.

44. Curry, W. B., Ostermann, D. R., Guptha, M. V. S., Ittekkot, V. (1992) Foraminiferal production and monsoonal upwelling in the Arabian Sea: evidence from sediment traps. In: Summerhays, C. P., Prell, W. L., Emeis, K. C. (Eds.), Upwelling Systems: Evolution since the Early Miocene. *Geol. Soc. Spec. Publ.*, **64**, 93-106.

45. Dannenmann, S., Linsley, B. K., Oppo, D. W., Rosenthal, Y., Beaufort, L. (2003) East Asian monsoon forcing of suborbital variability in the Sulu Sea during Marine Isotope Stage 3: Link to Northern Hemisphere climate. Geochem. Geophys Geosys., **4**, 1001, doi:10.1029/2002GC000390.

46. Dansgaard, W., Johnsen, S. J., Clausen, H. P., Dahl-Jensen, D., Gundestrup, N. S., et al. (1993) Evidence for general instability of past climate from a 250-Kyrs ice core record. *Nature*, **364**, 218-220.

47. Dean, W. E., Gardner, J. V., Piper, D. Z. (1997) Inorganic geochemical indicators of glacial-interglacial changes in productivity and anoxia on the California continental margin. *Geochem. Cosmochem. Acta*, **61**, 4507-4518.

48. Dilli, K. and Pant, R. K. (1994) Clay minerals as indicators of the provenance and paleoclimatic record of the Kashmir loess. *Jour. Geol. Soc. India*, **44**, 563-574.

49. Doyle, L. J., Cleary, W. J., Pilkey, O. H. (1968) Mica: its use in determining shelf-depositional regimes. *Mar. Geol.*, **6**, 381-389.

50. Duplessy, J. C. (1982) Glacial to interglacial contrast in the Northern Indian Ocean. *Nature*, **295**, 494-498.

51. El Wakeel, S. K. and Riley, J. P. (1957) Determination of organic matter in marine muds, *J. Con. Int. Expl. Mer.*, **22**, 180-183.

52. Emeis, K. C., Anderson, D. M., Doose, H., Kroon, D., Schulz- Bull, D. (1995) Sea-surface temperatures and the history of monsoon upwelling in the northwest Arabian Sea during the last 500,000 years. *Quat. Res.* **43**, 355-361.

53. Emiliani, E. (1955) Pleistocene temperatures. *Jour. of Geology*, **63**, 538– 578.

54. Fairbanks, R. G., Sverdlove, M., Free, R., Wiebe, P. H., Bé, A. W. H. (1982) Vertical distribution and isotopic fractionation of living planktonic foraminifera from the Panama basin. *Nature*, **298**, 841-844.

55. Fairbanks, R., Wiebe, P. H., and Bé, A. (1980) Vertical distribution and isotopic composition of living planktonic foraminifera in the Western North Atlantic. *Science*, **207**, 61-63.

56. Fairbanks, R. G. (1989) A 17000 year glacio-eustatic sea level record: influence of glacial melting on the younger dryas event and the deep-ocean circulation. *Nature*, **342**, 637-642.

57. Fairbanks, R.G. (1992) Barbados sea level and TH/ U ^{14}C calibration. In: IGBP PAGES/ World Data Center-A for paleoclimatology Data Contribution series No. 92-020. NOAA/ NGDC Paleoclimatology program, Boulder Co.

58. Fleitmann, D., Burns, S. J., Mudelsee, M., Neff, U., Kramers, J., Mangini, A., Matter, A. (2003) Holocene forcing of the Indian monsoon recorded in a stalagmite from Southern Oman. *Science*, **300**, 1737-1739.

59. Folk, R. L. (1968) Petrology of Sedimentry rocks. Hemphills, Austin. p 177.

60. Gamsakhurdiya, G. R., Meschanov, S. L., Shapiro, G. K. (1991) Seasonal variations in the distribution of Red Sea waters in the northwestern Indian Ocean. *Oceanology*, **31**, 32-37.

61. Ganeshram, R. S., Calvert, S. E., Pedersen, T. F., Cowie, G. A. (1999) Factors controlling the burial of organic carbon in laminated and bioturbated sediments off NW Mexico: Implications for hydrocarbon preservation. *Geochem. Cosmochem. Acta*, **63**, 1723-1734.

62. Ganssen, G., Sarnthein, M. (1983) Stable-isotope composition of foraminifers: the surface and bottom water record of coastal upwelling. In: Suess, E., Thiede, J. (Eds.), Coastal upwelling its sediment record. Plenum, New York, pp. 99–121.

63. Gingele, F. X. (1996) Holocene climatic optimum in Southwest Africa-evidence from the marine clay mineral record. *Palaeogeogr. Palaeoclimatol. Palaeoecol.*, **122**, 77-87.

64. Gupta, A. K., Anderson, D. M. and Overpeck, J. T. (2003) Abrupt changes in the Asian southwest monsoon during the Holocene and their links to the North Atlantic Ocean. *Nature*, **421**, 354-356.

65. Guptha, M. V. S., Rahul Mohan and Muralinath, A. S. (2002) Slumping on the Western continental margin of India. *Geo Acta*, **1**, 45-48.

66. Haake, B., Ittekkot, V., Rixen, T., Ramaswamy, V., Nair, R. R., Curry, W. B. (1993) Seasonality and interannual variability of particle fluxes to the deep Arabian Sea. *Deep-Sea Res.*, **40**, 1323-1344.

67. Hashimi, N. H., Nigam, R., Nair, R. R., and Rajagopalan, G. (1995) Holocene sea level fluctuations on western India continental margin: An update. *Jour. Geol. Soc. India*, **46**, 157–162.

68. Hendy, I. L., and Kennett, J. P. (2003) Tropical forcing of North Pacific intermediate water distribution during Late Quaternary rapid climate change? *Quat. Sci. Rev.*, **22**, 673-689.

69. Hoerling, M. P., Hurrell, J. W., Taiyi Xu (2001) Tropical Origins for Recent North Atlantic Climate Change. *Science*, **292 no. 5514**, pp. 90–92 DOI: 10.1126/science.1058582.

70. http://www.newmediastudio.org/DataDiscovery/Hurr_ED_Center/Stages_of_Hurricane_Dev/ITCZ/ITCZ.html.

71. http://pubs.usgs.gov/openfile/of01-041/htmldocs/xrpd.htm.

72. http://pubs.usgs.gov/openfile/of01-041/htmldocs/xrpd.htm.

73. Hussain, N and Guptha, M. V. S. (1985) Ooids in a deep sea core from the western continental margin of India. Indian. *Jour. of Mar. Sci.*, **14**, 123-126.

74. Imbrie, J., Hays, J. D., Martinson, D. G., McIntyre, A., Mix, A. C., Morley, J. J., Pisias, N. G., Prell, W. L., Shackleton, N. J. (1984) The orbital theory of Pleistocene climate: support from a revised chronology of the marine $\delta^{18}O$ record. In: Berger, A. L., Imbrie, J., Hays, J., Kukla, G., Saltzman, B. (Eds.), Milankovitch and Climate, Part I. D. Reidel, Dordrecht, pp. 269–305.

75. Imbrie, J., Boyle, E. A., Clemens, S. C., Duffy, A., Howard, W. R., Kulka, G., Kutzbach, J., Martinson, D. G., McIntyre, A., Mix, A. C., Molfino, B., Morley, J. J., Peterson, L. C., Pisias, N. G., Prell, W. L., Raymo, M. E., Shackleton, N. J., Toggweiler, J. R. (1992) On the structure and origin of major glaciation cycles. 1. Linear responses to Milankovitch forcing. *Palaeoceanography*, **7 (6)**, 701-738.

76. Kessarkar, P. M., Rao, V. P., Ahmad, S. M., Anil Babu, G. (2003) Clay mineral and Sr- Nd isotope of the sediments along the western margin of India and their implication for the sediment provenance, *Mar. Geol.*, **202**, 55-69.

77. Kroon, D., Ganssen, G. (1989) Northern Indian Ocean upwelling cells and the stable isotopic composition of living planktonic foraminifers. *Deep-Sea Res.*, **36**, 1219–1236.

78. Kroopnick, P. M. (1985) The distribution of $\delta^{13}C$ of ΣCO_2 in the world oceans. *Deep Sea Res.*, **32**, 57-84.

79. Kumar, S. P., Prasad, T. G. (1996) Winter cooling in the northern Arabian Sea. *Curr. Sci.*, (JGOFS-India Sp. Section), **71**, 834–841.

80. Lea, D. W., Pak, D. K., Peterson, L. C. and Hughen, K. A. (2003) Synchroneity of tropical and high-latitude Atlantic temperatures over the last glacial termination. *Science*, **301**, 1361-1364.

81. Levitus, S., Boyer, T. P. (1994) In: World Ocean Atlas Vol. 4: Temperature NOAA Atlas NESDIS 4. US Department of Commerce, Washington DC.

82. Levitus, S., Burgett, R., Boyer, T. P. (1994) In: World Ocean Atlas Vol. 3: Salinity NOAA Atlas NESDIS 3. US Department of Commerce, Washington DC.

83. Luckge, A., Rolinski, A. D., Khan, A. A., Schulz, H and von Rad, U. (2001) Monsoonal variability in the northeastern Arabian Sea during the past 5000 years: geochemical evidence from laminated sediments. *Palaeogeogr. Palaeoclimatol. Palaeoecol.*, **167**, 273–286.

84. Madhupratap, M., Kumar, S. P., Bhattathiri, P. M. A., Kumar, R. D., Raghukumar, S., Nair, K. K. C., Ramaiah, N. (1996) Mechanism of the biological response to winter cooling in the northeastern Arabian Sea. *Nature*, **384**, 549– 552.

85. Merh, S. S. (1995) Geology of Gujarat. *Geol. Soc. of India.*, Bangalore, India, p. 222.

86. Milankovitch, M. M. (1941) *Canon of Insolation and the Ice Age Problem.* Königlich Serbische Academie, Belgrade. English translation by the Israel Program for Scientific Translations, United States Department of Commerce and the National Science Foundation, Washington D.C.

87. Mulitza, S., Wolff, T., Pätzold, J., Hale, W., Wefer, G. (1998) Temperature sensitivity of planktonic foraminifera and its influence on the oxygen isotope record. *Mar. Mircopal.*, **33**, 223–240.

88. Mulitza, S., Arz, H., Mucke, Kemle-von., Moos, C., Niebler, H. –S., Pätzold, J. and Segl, M. (1999) The South Atlantic carbon isotope record of planktic foraminifera. In: Fischer, G., Wefer, G. (eds.), Use of proxies in palaeoceanography: Examples from South Atlantic. Springer-Verlag, pp 427-445.

89. Naidu, P. D. (1991) Glacial to interglacial contrasts in the calcium carbonate content and influence of Indus discharge in two eastern Arabian Sea cores. *Palaeogeogr. Palaeoclimatol. Palaeoecol.*, **86**, 255-263.

90. Naidu P. D, Prakash Babu C., Rat Ch. M. (1992) The upwelling record in the sediments of the western continental margin of India. *Deep-Sea Res.*, **39**, 715-723.

91. Naidu, P. D. (1998) Driving forces of Indian summer monsoon on Milankovitch and sub-milankovitch time scales: A review. *Jour. Geol. Soc. India*, **52,** 257-272.

92. Naidu, P. D., Malmgreen, B. A. (1999) Quaternary carbonate record from the equatorial Indian Ocean and its relationship with productivity changes. *Mar. Geol.*, **161**, 49-62.

93. Naidu, P. D and Nobuaki Niitsuma (2003) Carbon and oxygen isotope time series records of planktonic and benthic foraminifera from the Arabian Sea: implications on upwelling processes. *Palaeogeogr. Palaeoclimatol. Palaeoecol.*, **202**, 85-95.

94. Naidu, P. D. (2004) Isotopic evidences of past upwelling intensity in the Arabian Sea. *Glob. Planet. Change*, **40**, 285–293.

95. Nair, R. R., Ittekkot, V., Manganini, S. J., Ramaswamy, V., Haake, B., Degens, E. T., Desai, B. N., Honjo, S. (1989) Increased particle flux to the deep ocean related to monsoons, *Nature*, **338**, 749-751.

96. Naqvi, S.W.A. (1987). Some aspects of oxygen deficient conditions and denitrification of the Arabian Sea. *Jour. Mar. Res.*, **45**, 1049-1072.

97. Naqvi, W. A., Fairbanks, R. G. (1996) A 27,000 year record of Red Sea outflow: Implications for timing of post-glacial monsoon intensification. *Geophys. Res. Lett.*, **23**, 1501-1504.

98. Neff, U., Burns, S. J., Mangini, A., Mudelsee, M., Fleitmann, D., Matter, A. (2001) Strong coherence between solar variability and the monsoon in Oman between 9 and 6 kyr ago. *Nature*, **411**, 290-293.

99. Niitsuma, N., Oba, T., Okada, M. (1991) Oxygen and carbon isotope stratigraphy at Site 723, Oman Margin. *Proc. ODP Sci. Results*, **117**, 321-341.

100. Nyberg, J., Malmgren, B. A., Kuijpers, A and Winter, A. (2002) A centennial-scale variability of tropical North Atlantic surface hydrography during the late Holocene. *Palaeogeog. Palaeoclimatol. Palaeoecol.*, **183**, 25–41.

101. Overpeck, J., Anderson, S., Trumbore, S., Prell, W. (1996) The south-west monsoon over the last 18,000 yrs. *Clim. Dyn.*, **12**, 213-225.

102. Pandarinath, K., Verma, S. P., and Yadava, M. G. (2004) Dating of Sediment layers and sediment accumulation studies along the western continental margin of India: A review. *Internl. Geol. Rev.*, **46**, 939-956.

103. Pandarinath, K., Prasad, S., Deshpande R. D and Gupta, S. K. (1999) Late Quaternary sediments from Nal Sarovar, Gujarat, India: distribution and provenance. *Proc. Indian Acad. Sci. (Earth Planet Sci.)*, **108**, 107-116.

104. Pant, R. K. (1993) Spread of loess and March of desert in western India. *Curr. Sci.*, **64**, 841-847.

105. Paropkari A L, Rao, Ch. M and Murthy, P. S. N. (1987) Environmental controls on the distribution of organic matter in the recent sediments of the western continental margin of India. In: Petroleum geochemistry and exploration in Afro-Asian Region (eds) R. K. Kumar, P. Dwivedi, V. Banerjie and V. Gupta (Balkema: Rotterdam) p 347-361.

106. Paropkari, A. L., Prakash Babu, C and Mascarenhas, A. (1992) A critical evaluation of the depositional parameters controlling the variability of organic carbon in Arabian Sea. *Mar. Geol.*, **107**, 213-226.

107. Paropkari, A. L., Prakash Babu, C and Mascarenhas, A. (1993) New evidence for enhanced preservation of organic carbon in contact with oxygen minimum zone on the western continental slope of India. *Mar. Geol.*, **111**, 7-13.

108. Pattan, J. N., Masuzawa, T., Naidu, P. D., Parthiban, G., Yamamoto, M. (2003) Productivity fluctuation in the southeastern Arabian Sea during the last 140 ka. *Palaeogeogr. Palaeclimatol. Palaeoecol.*, **193**, 575-590.

109. Pedersen, T. F., Calvert, S. E. (1990) Anoxia vs. productivity: what controls the formation of organic carbon rich sediments and sedimentary rocks? *Am. Assoc. Pet. Geol.*, **74**, 454–466.

110. Peeters, F. (2000) The distribution and stable isotope composition of living planktic foraminifera in relation to seasonal changes in the Arabian Sea. Ph. D. thesis, Free University, Amsterdam, The Netherlands, p. 184.

111. Petschick, R., Kuhn, G., Gingele, F. (1996) Clay mineral distribution in surface sediments of the South Atlantic: sources, transport and relation to oceanography. *Mar. Geol.*, **130**, 203-229.

112. Prabhu, C. N., Shankar, R., Anupama, K., Taieb, M., Bonnefille, R., Vidal, L., Prasad, S., (2004) A 200-ka pollen and oxygen isotopic record from two sediment cores from the eastern Arabian Sea. *Palaeogeogr. Palaeoclimatol. Palaeoecol.*, **214 (4)**, 309–321.

113. Prabhu, C. N. and Shankar, R. (2005) Palaeoproductivity of the eastern Arabian Sea during the past 200 ka: A multi-proxy investigation. *Deep-Sea Res. II*, **52**, 1994–2002.

114. Prakash Babu, C., Brumsack, H.-J., Schnetger, B. (1999) Distribution of organic carbon in surface sediments along the eastern Arabian Sea: A revisit. *Mar. Geol.*, **162**, 91–103.

115. Prakash Babu, C., Brumsack, H.-J., Schnetger, B., Böttcher, M. E. (2002) Barium as a productivity proxy in continental margin sediments: a study from the eastern Arabian Sea. *Mar. Geol.*, **184**, 189–206.

116. Prell, W. L., Marvil, R. E and Luther, M. E. (1990) Variability in the upwelling field in the northwestern Indian Ocean; Part 2: Data-Model comparison at 9,000 years B. P. *Palaeoceanography*, **5**, 447-457.

117. Prell, W. L., Murray, D. W., Clemens, S. C., Anderson, D. M. (1992) Evolution and variability of the Indian Ocean summer monsoon: evidence from the western Arabian Sea drilling program. *Geophysical Monograph,* **70,** 447-469.

118. Qasim, S. Z. (1977) Biological productivity of the Indian Ocean. *Indian Jour. Mar. Sci.*, **6**, 122-137.

119. Qasim, S. Z. (1982) Oceanography of the Northern Arabian Sea. *Deep Sea Res.*, **29**, 1041-1068.

120. Ramesh, R. and M. Tiwari (2005) Significance of stable oxygen ($\delta^{18}O$) and carbon ($\delta^{13}C$) isotopic compositions of individual foraminifera (O. universa) in a sediment core from the Eastern Arabian Sea. In Micropaleontology: Application in Stratigraphy and Paleoceanography, (ed.) Sinha, D. K., Narosa, New Delhi, pp. 309– 329.

121. Ramswamy, V., Nair, R. R. (1994) Fluxes of material in the Arabian Sea and Bay of Bengal sediment trap studies. *Proc. Indian Acad. Sci (Earth Planet. Sci.)*, **103**, 189-210.

122. Rao, K. L. (1979) India's Water Wealth: It's Assessment, Uses and Projections. Orient Longman Limited, New Delhi.

123. Rao, P. S., Rao, Ch. M., and Reddy, N. P. C. (1988) Pyritized ooids from the Arabian Sea basin. *Deep Sea Res.*, **35**, 1215-1221.

124. Rao, P. S. (1989) Ooids turbidites from the Central Western Continental Margin of India. *Geo-Marine Lett.*, **9**, 85-90.

125. Rao, V. P. (1991) Clay mineral distribution in the continental and slope off Saurashtra, west coast of India. *Indian Jour. Mar. Sci.*, **20**, 1-6.

126. Rao, V. P. and B. R. Rao (1995) Provenance and distribution of clay minerals in the sediments of the western continental shelf and slope of India. *Cont. Shelf. Res.*, **15**, 1757-1771.

127. Rao, V. P., Rao, Ch. M., Thamban, M., Natarajan, R., and Rao, B. R. (1995) Origin and significance of high grade phosphorite in a sediment core from the continental slope off Goa, India. *Curr. Sci.*, **69**, 1017–1022.

128. Rao, V. P. and Wagle, B. G. (1997) Geomorphology and surficial geology of the western continental shelf and slope of India: A review. *Curr. Sci.*, **73 (4),** 330-350.

129. Rao, V. P., Rajagopalan, G., Vora, K. H. and Almeida, F. (2003) Late Quaternary sea level and environmental changes from relic carbonate deposits of the western margin of India. *Proc. Indain Acad. Sci. (Earth planet. Sci.)*, **112 (1),** 1-25.

130. Reichert, G. J., Dulk, M. D., Visser, H. J., van der Weijden, C. H. and Zachariasse, W. J. (1997) A 225 Kyr record of dust supply, paleoproductivity and the oxygen minimum zone from the Murray ridge (northern Arabian Sea). *Palaeogeogr. Palaeclimatol. Palaeoecol.*, **134,** 149-169.

131. Reichart, G. J., Schenau, S. J., de Lange, G. J., Zachariasse, W. J. (2002) Synchroneity of oxygen minimum zone intensity on the Oman and Pakistan Margins at sub-Milankovitch time scales. *Mar. Geol.*, **185**, 403–415.

132. Rixen, T., Ittekkot, B., Gaye, B. H., Schafer, P. (2000) The influence of the SW monsoon on the deep-sea organic carbon cycle in the Holocene. *Deep-Sea Res. II*, **47**, 2629-2651.

133. Rohling, E. J., Fenton, M., Jorrison, F. J., Bertrand, P., Ganssen, G and Caulet, J. P. (1998) Magnitude of the sea-level lowstand for the past 500, 00 years. *Nature*, **394**, 162-165.

134. Rohling, E. J., and Cooke, S. (2002) Stable isotopes in foraminiferal carbonate. In: Gupta, B. K. (ed.), Modern Foraminifera. Dordrecht/Boston/London. pp. 239-258.

135. Rosenthal, Y., Oppo, D. W. and Linsley, B. K. (2003) The amplitude and phasing of climate change during the last deglaciation in the Sulu Sea, western equatorial Pacific. *Geophys. Res. Lett.*, **30**, 1428, doi:10.1029/2002GL016612.

136. Rostek, F., Ruhland, G., Bassinot, F. C., Muller, P. J., Labeyrie, L. D., Lancelot, Y. and Bard, E. (1993) Reconstructing sea surface temperature and salinity using $\delta^{18}O$ and alkenone records. *Nature*, **364**, 319-321.

137. Rostek, F., Bard, E., Beufort, L., Sonzogni, C., Ganssen, G. (1997) Sea surface temperature and productivity records for the past 240 kyrs in the Arabian Sea. *Deep-Sea Res.*, **44(6-7)**, 1461-1480.

138. Sachs, J. P. and Lehman, S. J. (1999) Subtropical North Atlantic Temperatures 60,00 to 30,000 years ago. *Science*, **286**, 756-759.

139. Sarkar, A., Bhattacharya, A. (1992) Glacial to interglacial isotopic changes in planktonic and benthic foraminifera from the western Arabian Sea. In: Desai, B. N. (Ed.), Oceanography of the Indian Ocean. Oxford & IBH Publishing, New Delhi, pp. 447–455.

140. Sarkar, A., Ramesh, R., Bhattacharya, S. K. and Rajagopalan, G. (1990) Oxygen isotope evidence for a stronger winter monsoon current during the last glaciation. *Nature*, **343**, 549– 551.

141. Sarkar, A., Bhattacharya, S. K., Sarin, M. M. (1993) Geochemical evidence for anoxic deep water in the Arabian Sea during the last glaciation. *Geochem. Cosmochem. Acta*, **57**, 1009-1016.

142. Sarkar, A., Ramesh, R., Bhattacharya, S. K. and Price, N. B. (2000a) Palaeomonsoonal and palaeoproductivity records of $\delta^{18}O$, $\delta^{13}C$ and $CaCO_3$ variations in the northern Indian Ocean sediments. *Proc. Indian Acad. Sci. (Earth Planet Sci.)*, **109**, 157-169.

143. Sarkar, A., Ramesh, R., Somayajulu, B. L. K., Agnihotri, R., Jull, A. J. T. and Burr, G. S. (2000b) High resolution Holocene monsoon record from the eastern Arabian Sea. *Earth Planet. Sci. Lett.*, **177 (3-4),** 209-218.

144. Schott, F., Swallow, J. C. and Fieux, M. (1990) The Somali Current at the Equator: Annual cycle of currents and transports in the upper 1000m and connection to neighbouring latitudes. *Deep-Sea Res.*, **37**, 1825-1848.

145. Schulz, H., von Rad, U. and Erlenkeuser, H. (1998) Correlation between Arabian Sea and Greenland climate oscillations of the past 110,000 years. *Nature*, **393**, 54-57.

146. Schulte, S., Rostek, F., Bard, E., Rullkotter, J., Marchal, O. (1999) Variations of oxygen-minimum and primary productivity recorded in sediments of the Arabian Sea. *Earth Planet. Sci. Lett.*, **173**, 205-221.

147. Setty, M. G. A. P. (1972) A description of sediment cores from the Arabian Sea. *Proc. Internl. Geol. Cong.*, **8**, 109-111.

148. Shackleton, N. J. (1967), Oxygen isotope analyses and Pleistocene temperatures reassessed, *Nature*, **215**, 15-17.

149. Shackleton, N. J., Opdyke, N. D. (1973) Oxygen isotopes and paleomagnetic stratigraphy of equatorial Pacific core V28-238: oxygen isotope temperatures and ice-volume on a 105-year and 106-year scale. *Quat. Res.*, **3**, 39– 55.

150. Shackleton, N. J (1974) Attainment of isotopic equilibrium between ocean water and the benthic foraminifera genus *uvigerina*: isotopic changes in the

ocean during the last glacial. *CNRS, Colloques Internationals*, **219**, 203-209.

151. Shackleton, N. J (1987) Oxygen isotopes, ice volume and sea-level. *Quat. Sci. Rev.*, **6**, 183-190.

152. Shackleton, N. J. (2000) A 100,000 year ice-age cycle identified and found to lag temperature, carbon-dioxide, and orbital eccentricity. *Science*, **289**, 1897–1902.

153. Shankar, D., Vinayachandran, P. N. and Unnikrishnan, A. S. (2002) The monsoon currents in the north Indian Ocean. *Prog. Oceanogr.*, **52,** 63–120.

154. Shankar, D., Shenoi, S. S. C., Nayak, R. K., Vinayachandran, P. N., Nampoothiri, G., Almeida, A. M., Michael, G. S., Ramesh Kumar, M. R., Sundar, D. and Sreejith, O. P. (2005) Hydrography of the eastern Arabian Sea during summer monsoon 2002. *Jour. Earth Syst. Sci.*, **114 (5)**, 459–474

155. Shankar, R and Manjunatha, B. (1995) *Jour. Geol. Soc. India*, **45**, 689-694.

156. Shenoi, S. S. C., Shankar, D., Michael, G. S., Kurian, J., Varma, K. K., Ramesh Kumar, M. R., Almeida, A. M., Unnikrishnan, A. S., Fernandes, W., Barreto, N., Gnanaseelan, C., Mathew, R., Praju, K. V., Mahale, V. (2005) Hydrography and water masses in the southeastern Arabian Sea during March–June 2003. *Jour. Earth Syst. Sci.*, **114 (5),** 475-491.

157. Shetye, S. R. (1984) Seasonal variablity of the temperature field off the southwest coast of India. *Proc. Indian Acad. Sci. (Earth Planet. Sci.)*, **93 (4)**, 399–411.

158. Shetye, S. R., Gouveia, A. D., Shenoi, S. S. C., Michael, G. S., Sundar, D., Almeida, A. M., Santanam, M. (1990) Hydrography and circulation off the west coast of India during the southwest monsoon. *Jour. Mar. Res.*, **48**, 359-378.

159. Shetye, S. R., Gouveia, A. D., Shenoi, S. S. C., Michael, G. S., Sundar, D., Almeida, A. M., Santanam, K. (1991) The coastal current off western India during the northeast monsoon. *Deep-Sea Res.*, **38**, 1517– 1529.

160. Shetye, S. R., Gouveia, A. D., Shenoi, S. S. C. (1994) Circulation and water masses of the Arabian Sea. *Proc. Indian Acad. Sci. (Earth Planet Sci.)*, **103**, 107-123.

161. Singer, A. (1984) The palaeoclimatic interpretation of clay minerals in sediments- a review. *Earth Sci. Rev.*, **21**, 251-293.

162. Singh, A. D., Kroon, D and Ganeshram, R. S. (2006) Millennial scale variations in productivity and OMZ intensity in the eastern Arabian Sea. *Jour. Geol. Soc. of India.*, **68**, 369-377.

163. Sirocko, F. and Lange, H. (1991) Clay mineral accumulation rates in the Arabian Sea during the late Quaternary. *Mar. Geol.*, **97**, 105-119.

164. Sirocko, F., Sarnthein, M., Erlenkeuser, H., Lange, H., Arnold, M., Duplessy, J. C. (1993) Century-scale events in monsoonal climate over the past 24,000 years. *Nature*, **364**, 322-324.

165. Sirocko, F., Garbe-Schonberg, D., Mc Intyre, A. and Molfino, B. (1996) Teleconnections between the subtropical monsoons and high-latitude climates during the last deglaciation. *Science*, **272**, 526-529.

166. Sirocko, F., Dieter, Garbe-Schonberg., Devey, C. (2000) Processes controlling trace element geochemistry of Arabian Sea sediments during the last 25,000 years. *Glob. Planet. Change*, **26**, 217-303.

167. Sonzogni, C., Bard, E., Rostek, F. (1998) Tropical sea surface temperatures during the last glacial period: a view based on alkenones in Indian Ocean sediments. *Quat. Sci. Rev.*, **17**, 1185-1201.

168. Staubwasser, M. (2006) An overview of Holocene South Asian monsoon records-Monsoon domains and regional contrasts. *Jour. Geol. Soc. of India.*, **68**, 433-446.

169. Steens, T. N. F., Ganssen, G., Kroon, D. (1992) Oxygen and carbon isotopes in planktonic foraminifera as indicators of upwelling intensity and upwelling-induced high productivity in sediments from the northwestern Arabian Sea. In: Summerhays, C. P., et al. (Ed.), Upwelling Systems. Evolution since the Early Miocene. *Geol. Soc. Special Publication*, **64**, pp. 107– 119.

170. Stuiver, M., et al (1998) INTCAL 98 radiocarbon age calibration, 24,000-0 cal BP. *Radiocarbon*, **40,** 1041-1083.

171. Subramanya, K. R. (1996) Active intraplate deformation in South India. *Tectonophysics*, **262**, 231-241.

172. Sukumar, R., Ramesh, R., Pant, R. K., Rajagopalan, G. (1993) A $\delta^{13}C$ record of the late Quaternary climate change from tropical peats in southern India. *Nature*, **364**, 703-706.

173. Tchernia, P. (1980) Descriptive Regional Oceanography. 2nd edition Pergamon, Tarrytown, N.Y. pp 253.

174. Thamban, M., Rao, V. P. C., Schneider, R. R. and Grootes, P. M. (2001) Glacial to Holocene fluctuations in hydrography and productivity along the southwestern continental margin of India. *Palaeogeogr. Palaeclimatol. Palaeoecol.*, **165,** 113-127.

175. Thamban, M., Rao, V. P., Raju, S. V. (1997) Controls on organic carbon distribution in the sediment cores from the eastern Arabian Sea. *Geo-Mar. Lett.*, **17**, 20-27.

176. Thamban, M., Rao, V. P., Schneider, R. R., Grootes, P. M. (2001) Glacial to Holocene fluctuation in hydrography and productivity along the southwestern continental margin of India. *Palaeogeogr. Palaeoclimatol. Palaeoecol.*, **165**, 113-127.

177. Thamban, M., Rao, V. P., Schneider, R. R. (2002) Reconstruction of Late Quaternary monsoon oscillations based on clay mineral proxies using sediment cores from the western margin of India. *Mar. Geol.*, **186**, 527-539.

178. Tiwari, M., Ramesh, R., Somayajulu, B. L. K., Jull, A. J. T. and Burr, G. S. (2005a) Solar control of southwest monsoon on centennial timescales. *Curr., Sci.*, **89**, 1583-1588.

179. Tiwari, M., Ramesh, R., Somayajulu, B. L. K., Jull, A. J. T. and Burr, G. S. (2005b) Early deglacial (~19-17 ka) strengthening of the northeast monsoon. *Geophys. Res. Lett.*, **32**, L19712, doi:10.1029/2005GL024070.

180. Tiwari, M., Ramesh, R., Yadava, M. G., Somayajulu, B. L. K., Jull, A. J. T. and Burr, G. S. (2006a) Is there a persistent control of monsoon winds by precipitation during late Holocene? *Geochem. Geophys. Geosyst.*, 7, Q03001, doi:10.1029/2005GC001095.

181. Tiwari, M., Ramesh, R., Somayajulu, B. L. K., Jull, A. J. T. and Burr, G. S. (2006b) Paleomonsoon precipitation deduced from sediment core from the equatorial Indian Ocean. *Geo-Mar. Lett.*, ***26*(1)**, 23-30, doi:10.1007/s00367-005-0012-0.

182. Tiwari, M., Ramesh, R., Bhushan, R., Somayajulu, B. L. K., Jull, A. J. T., Burr, G. S. (2006c) Paleoproductivity variations in the equatorial Arabian sea: Implications for east African and Indian summer rainfalls and the El Niño frequency. *Radiocarbon*, **48 (1)**, 17-29.

183. Van Campo, E., Duplessy, J. C. and Rossignol-Strick, M. (1982) Climatic conditions deduced from a 150,000 yr oxygen isotope-pollen record from the Arabian Sea. *Nature*, **296,** 56-59.

184. Van Campo, E. (1986) Monsoon fluctuation in two 20,000 yr B.P. oxygen-isotope/pollen records of southwest India. *Quat. Res.*, **26,** 376-388.

185. Velinga-Chiang., Visser, K., Thunell, R. and Stott, L. (2003) Magnitude and timing of temperature change in the Indo-Pacific warm pool during deglaciation. *Nature*, **421**, 152-155.

186. Verma, K., Rajeevan, M., Rahul Mohan, Sudhakar, M., and Pandey, P.C., Paleoclimatic conditions during the late Quaternary period: A study of marine sediments off Goa. Abstract presented at the XIX Indian colloquium on Micropaleontology and Stratigraphy & Symposium on Recent Developments in Indian Ocean Paleoceanography and Paleoclimate, Banaras Hindu University, Varanasi, 2003.

187. Verma, K and Sudhakar, M. (2006) Evidence of reworking and resuspension of carbonates during the Last Glacial Maximum and early deglacial period along the South West coast of India. *Jour. Earth Sys. Sci.*, **115** (6), 695-702.

188. Von Rad, U., Schaaf, M., Michels, K. H., Schulz, H., Berger, W. H., Sirocko, F. (1999a) A 5000-yr record of climate change in varved sediments from the Oxygen Minimum Zone off Pakistan, Northeastern Arabian Sea. *Quat. Res.*, **51,** 39–53.

189. Von Rad, V., Schulz, H., Riech, V., Den-Dulk, M., Berner, V., Sirocko, F. (1999b) Multiple monsoon controlled breakdown of oxygen minimum conditions during the past 30,000 years documented in laminated sediments off Pakistan. *Paleogeogr. Paleoclimatol. Paleoecol.*, **152**, 129– 161.

190. Vora, K. H., Wagle, B. G, Veeraya, M., Almeida, F., Karisiddaiah, S. M. (1996) 1300 km long Late Pleistocene-Holocene shelf edge barrier reef system along the western continental shelf of India: occurrences and significance. *Mar. Geol.*, **134**, 145-162.

191. Wagle, B. G, Vora, K. H., Karisiddiah, S. M, Veeraya, M., Almeida, F. (1994) Holocene submarine terraces on the continental shelf in India: verification for sea level changes. *Mar. Geol.*, **117**, 207-225.

192. Wang, L., Sarnthein, M., Erlenkeuser, H., Grimalt, J., Grootes, P., Heilig, S., Ivanova, E., Kienast, M., Pelejero, C., Pflaumann, U. (1999) East Asian monsoon climate during the Late Pleistocene: high resolution sediment records from the South China Sea. *Mar. Geol.*, **156**, 245–284.

193. Wang, Y. J., Cheng, H., Edwards, R. L., An, Z. S., Wu, J. Y., Shen, C.-C., Dorale, J. A. (2001) A high-resolution absolute-dated late Pleistocene monsoon record from Hulu Cave, China. *Science*, **294**, 2345-2348.

194. Wang, P., Clemens, S. C., Beaufort, L., Branconnot, P., Ganssen, G. M., Jian, Z., Kershaw, P., Sarnthein, M. (2005) Evolution and variability of the Asian monsoon system: State of the art and outstanding issues. *Quat. Sci. Rev.*, **24**, 595-629.

195. Webster, P. J., Palmer, T., Yanai, M., Tomas, R., Magana, V., Shukla, J. and Yasunari, A. (1998) Monsoons: Processes, predictability, and the prospects for prediction. *Jour. Geophys. Res.*, **103**, 14,451–14,510.

196. Wefer, G., Berger, W. H. (1991) Isotope paleontology: growth and composition of extant calcareous species. *Mar. Geol.*, **100**, 207–248.

197. Wyrtki, K. (1971) Oceanographic Atlas of the International Indian Ocean Expedition; Washington D C, National Science Foundation. p 531.

198. Wyrkti, K., (1973) Physical oceanography of the Indian Ocean. In: Zeitzschel, B. (Ed.), The Biology of the Indian Ocean. Springer, Berlin, pp. 18-36.

199. Yadav, D. N. (1996) Manganese mobilization from the Western Continental margin of India. *Curr. Sci.*, **71**, 900-905.

200. Yadava, M. G., and Ramesh, R. (1999) "Speleothems- Useful proxies for Past Monsoon Rainfall". *Jour. Sci. & Ind. Res.*, **58**, 339-348.

201. Zonneveld, K. A. F., Gannssen, G., Troelstra, S., Versteegh, G. J. M and Visscher, H. (1997) Mechanisms forcing abrupt fluctuations of the Indian Ocean summer monsoon during the last deglaciation. *Quat. Sci. Rev.*, **16**, 187-201.

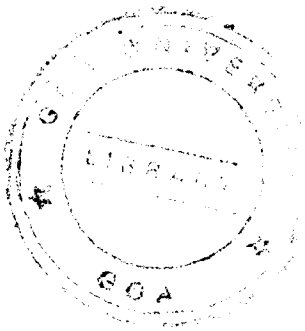

List of Publications (Published, Communicated)

1. **Verma, K** and Sudhakar, M. (2006) Evidence of reworking and resuspension of carbonates during the Last Glacial Maximum and early deglacial period along the South West coast of India. *Jour. Earth Sys. Sci.*, **115 (6)**, 695-702.

2. **Verma, K.,** Sudhakar, M., Tiwari, M., Yadava, M. G., and Ramesh, R. Identification of sediment-mixing events by bulk-carbonate ^{14}C dating and $\delta^{18}O$ analysis. **Communicated to Current Science (Ref number: P946).**

3. **Verma, K** and Sudhakar, M. Tropical extratropical connection evident from the $\delta^{18}O$ record of sediment cores from the eastern Arabian Sea. **Communicated to Journal of Coastal Research (Ref number: 07-0989)**

4. **Verma, K** and Sudhakar, M. Variation in summer monsoon circulation for the last ~120 kyr along the eastern Arabian Sea **(Communicated to Geo-Marine Letters).**

List of abstracts presented in Seminar/ Symposia

1. **Verma, K.**, Rajeevan, M., Rahul Mohan, Sudhakar, M., Pandey, P. C., (2003) **Paleoclimatic conditions during the Late Quaternary period: A study of marine sediments off Goa**. XIX Indian Colloquium on Micropaleontology and stratigraphy "Symposium on recent developments in Indian Ocean paleoceanography and palaeoclimate", BHU, Varanasi 9-11 Oct 2003.

2. **Verma, K.**, Sudhakar, M., Tiwari, M., Yadava, M. G., Ramesh, R. (2007) **Inconsistency between the conventional radiocarbon and $\delta^{18}O$ derived chronology: A case study from the sediments off Goa**. Geosphere-Biosphere Workshop on "High resolution monsoon reconstruction since the Last Glacial Maximum (~20000 yrs)", Cochin University, Cochin 20-21 July 2007.

3. **Verma, K** and Sudhakar, M. (2007) **Tropical extra tropical connection evident from the $\delta^{18}O$ record of sediment cores from the eastern Arabian Sea.** International seminar on "Crustal evolution, Sedimentry processes and Metallogeny", S. D. M. College, Dharwar, 29-30 November 2007.

National Centre for Antarctic and Ocean Research, Headland Sada

Vasco - da - Gama, Goa - 403 804